

# **Cardiovascular Reviews**

Editors-in-Chief

**Bo Eklöf**

*University of Lund, Sweden*

**Yan Song**

*The First Affiliated Hospital of Zhengzhou University, China*

BIO-BYWORD SCIENTIFIC PUBLISHING PTY LTD

(619 649 400)

Level 10

50 Clarence Street

SYDNEY NSW 2000

Copyright © 2025. Bio-Byword Scientific Publishing Pty Ltd.

Complimentary Copy



## Cardiovascular Reviews

### Focus and Scope

*Cardiovascular Reviews* publishes peer-reviewed research articles across basic, translational, and clinical cardiovascular medicine. The journal aims to enhance insight into cardiovascular disease mechanisms and the prospects for innovation. The Journal covers all topics within cardiology and cardiovascular biology with an emphasis on studies that challenge the status quo of treatments, at the molecular, sub-cellular, cellular, organ, and organism level, and of clinical proof-of-concept and translational studies and practices in cardiovascular care or facilitate the translation of scientific advances into the clinic as new therapies or diagnostic tools. Manuscripts are expected to provide a significant contribution to the field with relevance for cardiovascular biology and diseases.

### About Publisher

Bio-Byword Scientific Publishing is a fast-growing, peer-reviewed and open access journal publisher, which is located in Sydney, Australia. As a dependable and credible corporation, it promotes and serves a broad range of subject areas for the benefit of humanity. By informing and educating a global community of scholars, practitioners, researchers and students, it endeavors to be the world's leading independent academic and professional publisher. To realize it, it keeps creative and innovative to meet the range of the authors' needs and publish the best of their work.

By cooperating with University of Sydney, University of New South Wales and other world-famous universities, Bio-Byword Scientific Publishing has established a huge publishing system based on hundreds of academic programs, and with a variety of journals in the subjects of medicine, construction, education and electronics.

### Publisher Headquarter

BIO-BYWORD SCIENTIFIC PUBLISHING PTY LTD

Level 10

50 Clarence Street

Sydney NSW 2000

Website: [www.bbwpublisher.com](http://www.bbwpublisher.com)

Email: [info@bbwpublisher.com](mailto:info@bbwpublisher.com)



## Table of Contents

- 1 A Discussion on ROC Curve: Exploring the Predictive Value of P-Selectin and PTX3 Levels in Patients with Nonvalvular Atrial Fibrillation Complicated with Ischemic Stroke**  
*Qinhao Duanmu*
- 8 The Impact of Combined Application of Bisoprolol and Rivaroxaban on Cardiac Function in Patients with Coronary Heart Disease**  
*Ziyue Wu*
- 14 Analysis of Sensitivity and Accuracy of Transthoracic Echocardiography Right Heart Contrast Combined with Transcranial Doppler Bubble Test in the Diagnosis of Patent Foramen Ovale**  
*Jianmei Chen, Dai Zhang, Dongdong Ji, Shuhua Wang, Qiushuang Wang*
- 21 The Impact of Early Initiation of Intensive Lipid-Lowering Therapy on Lipid Target Achievement and Major Adverse Cardiovascular Events in Patients with Acute Coronary Syndrome Undergoing Percutaneous Coronary Intervention**  
*Yue Kan, Yongfu Zhao, Hong Gao, Shihao Zhao, Jiaxu Liu, Zhanxiu Zhang*
- 29 The Clinical Effect of Xuesaitong in the Treatment of Coronary Heart Disease and its Influence on the Hemorheology of Patients**  
*Dejia Hu, Jihai Fan, Wei Gui, Zhen Li, Peng Zhao, Xianlei Deng, Chenran Guo, Lingui Xu*
- 35 Clinical Application of PCSK9 Inhibitor in Tumor Therapy**  
*Wenjie Lu, Lusha E*
- 42 Prediction of Rapidly Progressing Coronary Plaques Using a 3D Convolutional Neural Network Model Based on Coronary CT Angiography**  
*Wentao Zhang, Bingcang Huang, Weiping Lu, Ying Wang, Guangjie Sun, Jiahong Xu, Zhiru Ge*
- 52 Exploration of the Relationship Between Aldehyde Dehydrogenase 2 Gene Polymorphisms and Venous Thromboembolism in Critically Ill Patients**  
*Chunlei Xia, Wentao Zhang, Kun Zhang, Zhao Lin, Siyu Xu*

**60 Clinical Diagnostic Value of Serum Low-Density Lipoprotein Cholesterol Combined with Carotid Artery Ultrasound Parameters in Patients with Coronary Heart Disease**

*Hongping Lu, Qilong Chen*

# A Discussion on ROC Curve: Exploring the Predictive Value of P-Selectin and PTX3 Levels in Patients with Nonvalvular Atrial Fibrillation Complicated with Ischemic Stroke

Qinhao Duanmu\*

Department of Neurology, Emergency General Hospital, Ministry of Emergency Management, No. 29, Xiba Henan Li, Xiangheyuan Street, Chaoyang District, Beijing 1000028, China

\*Corresponding author: Qin Haoduanmu, 764334476@qq.com

**Copyright:** © 2025 Author(s). This is an open-access article distributed under the terms of the Creative Commons Attribution License (CC BY 4.0), permitting distribution and reproduction in any medium, provided the original work is cited.

**Abstract:** *Objective:* To explore the predictive value of P-Selectin and Pentraxin 3 (PTX3) levels in patients with nonvalvular atrial fibrillation (NVAF) complicated with ischemic stroke using ROC curve analysis. *Methods:* Selected 48 patients with NVAF and ischemic stroke admitted to the hospital from June 2018 to December 2020 as the occurrence group, and 50 patients with NVAF without ischemic stroke during the same period as the nonoccurrence group. Clinical data of the two groups were collected. Serum CD62P and PTX3 levels were detected and compared between the two groups. Logistic regression analysis was used to analyze the risk factors for ischemic stroke in patients with NVAF, and the receiver operating characteristic curve (ROC) was used to evaluate the predictive value of serum CD62P and PTX3 levels for ischemic stroke in patients with NVAF. *Results:* The age, left atrial diameter (LAD), CHA2DS2VASc score, and serum CD62P and PTX3 levels of patients in the occurrence group were higher than those in the nonoccurrence group ( $P < 0.05$ ). Logistic regression analysis showed that serum CD62P and PTX3 levels, CHA2DS2VASc score, LAD, and age were risk factors for ischemic stroke in patients with NVAF ( $P < 0.05$ ). ROC analysis showed that the sensitivity, specificity, accuracy, and area under the curve (AUC) of serum CD62P and PTX3 in predicting ischemic stroke in NVAF patients were 80.72%/83.54%, 77.31%/74.29%, 79.35%/81.41%, and 0.769/0.787, respectively. The sensitivity, specificity, accuracy, and AUC of the combined prediction of the two were 90.36%, 68.75%, 87.91%, and 0.854, respectively. *Conclusion:* The abnormal increase in serum CD62P and PTX3 levels is related to NVAF patients complicated with ischemic stroke, and serum CD62P and PTX3 are risk factors for ischemic stroke in NVAF patients. The combination of the two has high clinical value in predicting ischemic stroke in NVAF patients.

**Keywords:** Nonvalvular atrial fibrillation; Ischemic stroke; P-Selectin; Pentraxin 3; Predictive value

**Online publication:** December 31, 2025

## 1. Introduction

Nonvalvular atrial fibrillation (NVAF) is a prevalent cardiac arrhythmia associated with a heightened risk of ischemic stroke<sup>[1]</sup>. Although clinical scoring systems such as CHA<sub>2</sub>DS<sub>2</sub>-VASc are widely used, their predictive accuracy remains suboptimal<sup>[2]</sup>. Emerging evidence suggests that biomarkers involved in thrombosis and inflammation, such as P-selectin (CD62P) and pentraxin 3 (PTX3), may enhance risk stratification<sup>[3,4]</sup>. This study investigates the predictive value of serum CD62P and PTX3 levels in NVAF patients with ischemic stroke using ROC curve analysis.

## 2. Materials and methods

### 2.1. General materials

From June 2018 to December 2020, 48 patients with NVAF and ischemic stroke admitted to the hospital were selected as the occurrence group, and 50 patients with NVAF without ischemic stroke during the same period were selected as the nonoccurrence group. The clinical data of the two groups were collected.

Inclusion criteria: (1) Based on the diagnostic criteria revised at the 6th National Cerebrovascular Disease Academic Conference, and confirmed by 24-hour Holter monitoring, echocardiography, cranial MRI, and CT as NVAF or NVAF with ischemic stroke; (2) Patients in the occurrence group had their first episode of ischemic stroke, with the time from onset to hospitalization less than 24 hours; (3) Age between 18 and 80 years old; (4) Good compliance and signed informed consent.

Exclusion criteria: (1) Patients with intracranial hemorrhage or bleeding in the gastrointestinal or urinary system within the past 6 months; (2) Patients who had taken antibiotics or anticoagulant drugs within the past week; (3) Patients with rheumatic heart disease or artificial valve replacement; (4) Patients with severe liver and kidney dysfunction; (5) Patients with malignant tumors

### 2.2. Methods

#### 2.2.1. Data collection

The clinical medical records of all patients were collected, including gender, age, body mass index (BMI), drinking history, smoking history, history of hypertension, diabetes, coronary heart disease, heart failure, duration of NVAF, left atrial diameter (LAD), left atrial diameter index (LADi), drug use (warfarin, aspirin,  $\beta$ blockers, calcium channel blockers), and CHA<sub>2</sub>DS<sub>2</sub>-VASc score for thrombotic risk in atrial fibrillation. LAD was measured as the anteroposterior diameter of the left atrium. LADi was calculated as the mean left atrial diameter divided by body surface area. Body surface area (m<sup>2</sup>) was calculated as  $0.0061 \times \text{height (cm)} + 0.0128 \times \text{weight (kg)} - 0.1529$ .

#### 2.2.2. Detection of serum CD62P and PTX3 levels

On the morning following admission, 4 mL of fasting venous blood was collected from all patients, placed in ethylenediaminetetraacetic acid anticoagulant tubes, and centrifuged at 3500 rpm for 10 minutes. The supernatant was collected and stored at 80 °C for later use. Enzyme-linked immunosorbent assay (ELISA) (reagent kits purchased from Shanghai Enzyme-linked Biotechnology Co., Ltd.) was used to detect serum CD62P and PTX3 levels.

### 2.3. Statistical methods

SPSS 23.0 statistical software was used for data analysis. Measurement data were expressed as mean  $\pm$  standard

deviation (SD) and analyzed using *t*-tests. Count data were expressed as cases (%). Logistic regression analysis was used to calculate the relative risk factors, odds ratios (OR), and 95% confidence intervals (CI) for ischemic stroke in patients with NVAf. The receiver operating characteristic curve (ROC) was used to evaluate the predictive ability of serum CD62P and PTX3 levels for ischemic stroke in patients with NVAf, and the area under the curve (AUC) was calculated.  $P < 0.05$  was considered statistically significant.

### 3. Results

#### 3.1. Comparison of clinical data between the two groups

The age, LAD, CHA2DS2VASc score, and serum CD62P and PTX3 levels of patients in the occurrence group were higher than those in the nonoccurrence group ( $P < 0.05$ ). There were no significant differences between the two groups in gender, BMI, drinking history, smoking history, history of hypertension, diabetes, coronary heart disease, heart failure, duration of NVAf, LADi, or the use of warfarin, aspirin,  $\beta$ blockers, and calcium channel blockers ( $P > 0.05$ ). See **Table 1**.

**Table 1.** Comparison of clinical data between the two groups [mean  $\pm$  SD, n (%)]

Item	Occurrence group (n = 48)	Non-occurrence group (n = 50)	t/ $\chi^2$ value	p value
Gender (Male)	32 (66.67)	29 (58.00)	0.783	0.376
Age (years old)	62.85 $\pm$ 6.34	59.14 $\pm$ 5.62	3.068	0.003
BMI (kg/m <sup>2</sup> )	23.04 $\pm$ 2.37	22.61 $\pm$ 1.89	0.995	0.322
Drinking History	33 (68.75)	26 (52.00)	2.868	0.09
Smoking History	31 (64.58)	24 (48.00)	2.735	0.098
Hypertension History	35 (72.92)	31 (62.00)	1.327	0.249
Diabetes History	16 (33.33)	12 (24.00)	1.045	0.307
Coronary Heart Disease History	25 (52.08)	19 (38.00)	1.963	0.161
Heart Failure History	15 (31.25)	8 (16.00)	3.171	0.075
Duration of NVAf (years)	1.05 $\pm$ 0.33	0.97 $\pm$ 0.21	1.438	0.154
LAD (mm)	41.53 $\pm$ 4.28	37.26 $\pm$ 3.09	5.68	< 0.001
LADi (mm/m <sup>2</sup> )	26.15 $\pm$ 3.28	24.97 $\pm$ 2.89	1.892	0.062
Drug Use				
Warfarin	13 (27.08)	11 (22.00)	0.342	0.559
Aspirin	30 (62.50)	27 (54.00)	0.727	0.394
$\beta$ -Blockers	29 (60.42)	28 (56.00)	0.196	0.658
Calcium Channel Blockers	19 (39.58)	16 (32.00)	0.613	0.434
CHA2DS2-VASc Score	3.12 $\pm$ 0.67	1.96 $\pm$ 0.41	10.385	< 0.001
CD62P (ng/mL)	18.93 $\pm$ 3.95	11.68 $\pm$ 2.74	10.593	< 0.001
PTX3 (ng/mL)	9.42 $\pm$ 1.46	5.89 $\pm$ 1.02	13.921	< 0.001

### 3.2. Logistic regression analysis of risk factors for ischemic stroke in patients with NVAf

Possible risk factors for ischemic stroke in patients with NVAf were used as independent variables (X), and whether ischemic stroke occurred as the dependent variable (Y). The related factors were assigned values, with ischemic stroke occurrence coded as 1 and nonoccurrence as 0. Logistic regression analysis was performed. Logistic regression analysis showed that serum CD62P and PTX3 levels, CHA2DS2-VASc score, LAD, and age were risk factors for ischemic stroke in patients with NVAf ( $P < 0.05$ ). See **Table 2** and **Table 3**.

**Table 2.** Variable assignment for logistic regression analysis

Variable	Variable Name	Assignment Method
Ischemic Stroke	Y	0 for non-occurrence, 1 for occurrence
PTX3	X1	Continuous Variable
CD62P	X2	Continuous Variable
CHA2DS2-VASc Score	X3	Continuous Variable
LAD	X4	Continuous Variable
Age	X5	Continuous Variable

**Table 3.** Logistic regression analysis of risk factors for ischemic stroke in patients with NVAf

Independent variable	$\beta$	SE	Wald	<i>P</i> -value	OR	95% CI
PTX3	1.223	0.276	19.635	< 0.001	3.397	1.541–5.416
CD62P	1.146	0.287	15.944	< 0.001	3.146	1.335–4.912
CHA2DS2-VASc Score	0.975	0.299	10.633	< 0.001	2.651	1.225–4.077
LAD	0.681	0.308	4.889	0.025	1.976	1.027–3.289
Age	0.594	0.317	3.511	0.037	1.811	1.004–2.868

### 3.3. ROC analysis of the predictive value of CD62P and PTX3 for ischemic stroke in patients with NVAf

The results of ROC analysis showed that the combination of CD62P and PTX3 had higher sensitivity and accuracy in predicting ischemic stroke in patients with NVAf than either marker alone. See **Table 4**.

**Table 4.** ROC analysis of the predictive value of CD62P and PTX3 levels for ischemic stroke in patients with NVAf

Indicator	Optimal cut-off point	Sensitivity	Specificity	Accuracy	AUC	95% CI
CD62P	16.21 ng/mL	80.72%	77.31%	79.35%	0.769	0.665–0.928
PTX3	8.05 ng/mL	83.54%	74.29%	81.41%	0.787	0.675–0.947
Combined	–	90.36%	68.75%	87.91%	0.854	0.716–0.963

## 4. Discussion

Nonvalvular atrial fibrillation (NVAf) represents a prevalent supraventricular tachyarrhythmia, marked by disorganized atrial electrical activation and loss of effective atrial mechanical contraction<sup>[1]</sup>. The incidence of

NVAF escalates with advancing age, exceeding 10% in individuals older than 70 years old <sup>[2]</sup>. This condition predisposes to thrombus formation, primarily through stasis in the left atrial appendage, culminating in embolic events such as ischemic stroke—a principal cause of morbidity and mortality in this patient cohort <sup>[2,5]</sup>. Consequently, identifying robust biomarkers for stratifying stroke risk is of paramount clinical importance.

P-selectin (CD62P), a cell adhesion molecule expressed on activated platelets and endothelial cells, is pivotal in mediating leukocyte-platelet aggregates and endothelial interactions <sup>[3,4,6]</sup>. Its release promotes a prothrombotic state by facilitating monocyte tissue factor expression and enhancing fibrin deposition <sup>[4,7]</sup>. Elevated soluble CD62P levels have been correlated with atrial thrombogenesis and ischemic stroke risk among NVAF patients, underscoring its potential utility as a predictive biomarker <sup>[7]</sup>.

Pentraxin 3 (PTX3), an acute-phase inflammatory protein belonging to the long pentraxin family, is rapidly upregulated in response to vascular injury and inflammation <sup>[8,9]</sup>. PTX3 exhibits distinct structural and functional characteristics from the short pentraxin CRP, including localized production at inflammation sites and greater responsiveness to specific cardiovascular insults <sup>[10–12]</sup>. Elevated circulating PTX3 has been implicated in the pathogenesis of atherosclerosis, acute coronary syndromes, and ischemic stroke, reflecting its role in innate immunity and vascular inflammation <sup>[11–13]</sup>.

Established clinical factors for stroke risk in NVAF include advanced age, female sex, and elevated CHA<sub>2</sub>DS<sub>2</sub>-VASc score <sup>[14,15]</sup>. Furthermore, left atrial dilation, quantified by LAD, serves as an indicator of atrial remodeling and stasis, and has been identified as an independent risk factor for thromboembolism <sup>[16]</sup>.

The present study corroborates these findings, demonstrating significantly elevated serum CD62P and PTX3 levels in NVAF patients with ischemic stroke compared to those without. Furthermore, age, LAD, and CHA<sub>2</sub>DS<sub>2</sub>-VASc score were also significantly higher in the stroke group. Multivariable logistic regression analysis confirmed that each of these variables, including CD62P and PTX3, represents an independent risk factor for ischemic stroke <sup>[17,18]</sup>.

ROC curve analysis demonstrated that both CD62P and PTX3 possess significant predictive capability for ischemic stroke, with AUC values of 0.769 and 0.787, respectively. Notably, the combination of these biomarkers yielded a superior AUC of 0.854, indicating enhanced discriminatory power over either marker alone. These observations suggest that CD62P and PTX3 contribute complementary pathophysiological information related to thrombotic and inflammatory pathways, respectively.

In conclusion, the integration of CD62P and PTX3 into existing risk stratification models may improve the identification of NVAF patients at high risk for ischemic stroke, thereby enabling more targeted and effective prophylactic therapy <sup>[19–21]</sup>.

## 5. Conclusion

In summary, serum CD62P and PTX3 levels are elevated in NVAF patients with ischemic stroke, and both are risk factors for ischemic stroke in NVAF patients. Their combination has high predictive value for ischemic stroke in NVAF patients.

## Funding

Study on the Impact of FT0 Gene Polymorphism on the Effect of Exercise-Induced Weight Loss in Individuals from Different Ethnic Groups and Its Molecular Regulatory Mechanism (Project No.: 2020MS03015)



## Disclosure statement

The author declares no conflict of interest.

## References

- [1] Zhu C, Li C, 2018, Analysis of Some Clinical Characteristics of Nonvalvular Atrial Fibrillation Patients With Ischemic Stroke. *Chinese Journal of Clinical Neuroscience*, 26(1): 38–42.
- [2] Alkhouli M, Friedman P, 2019, Ischemic Stroke Risk in Patients With Nonvalvular Atrial Fibrillation: JACC Review Topic of the Week. *J Am Coll Cardiol*, 74(24): 3050–3065.
- [3] Alkhouli M, Noseworthy P, Rihal C, et al., 2018, Stroke Prevention in Nonvalvular Atrial Fibrillation: A Stakeholder Perspective. *J Am Coll Cardiol*, 71(24): 2790–2801.
- [4] Grobler C, Maphumulo S, Grobbelaar L, Bredenkamp J, Laubscher G, Lourens P, Steenkamp J, Kell D, Pretorius E, 2020, Covid-19: The Rollercoaster of Fibrin(ogen), D-Dimer, Von Willebrand Factor, P-Selectin and Their Interactions With Endothelial Cells, Platelets and Erythrocytes. *Int J Mol Sci*, 21(14): 5168.
- [5] Jing Y, Hu Y, Li H, et al., 2018, Assessment of Thrombotic Risk in Atrial Fibrillation With Ultrasound Molecular Imaging of P-Selectin. *Thromb Haemost*, 118(2): 388–400.
- [6] Li Y, Yang Y, Zhang T, et al., 2020, A Study on the Relationship Between Pentraxin 3 and Carotid Stenosis in Patients With Ischemic Stroke. *Chinese Journal of Stroke*, 15(5): 72–76.
- [7] Wang W, Wang X, 2004, Proceedings of the 6th National Cerebrovascular Disease Academic Conference. *Chinese Journal of Neurology*, 37(4): 346–348.
- [8] Cho D, Choi J, Choi J, et al., 2021, Impact of Carotid Atherosclerosis in CHA2DS2-VASc-Based Risk Score on Predicting Ischemic Stroke in Patients With Atrial Fibrillation. *Korean J Intern Med*, 36(2): 342–351.
- [9] Kim J, Lee Y, Kang K, et al., 2021, Comparative Occurrence of Ischemic Stroke With the Rhythm Versus Rate Control Strategy in a National Prospective Cohort of Atrial Fibrillation. *Korean J Intern Med*, 36(1): 114–123.
- [10] Zhu M, Wang M, Ma X, et al., 2018, The Value of Left Atrial Strain and Strain Rate in Predicting Left Atrial Appendage Stasis in Patients With Nonvalvular Atrial Fibrillation. *Cardiol J*, 25(1): 87–96.
- [11] Shen L, Yang T, Xia K, et al., 2020, P-Selectin (CD62P) and Soluble TREM-Like Transcript-1 (sTLT-1) Are Associated With Coronary Artery Disease: A Case Control Study. *BMC Cardiovasc Disord*, 20(1): 387.
- [12] Perkins L, Anderson C, Novelli E, 2019, Targeting P-Selectin Adhesion Molecule in Molecular Imaging: P-Selectin Expression as a Valuable Imaging Biomarker of Inflammation in Cardiovascular Disease. *J Nucl Med*, 60(12): 1691–1697.
- [13] Wysokinski W, Cohoon K, Melduni R, Mazur M, Ammash N, Munger T, Konik E, McLeod T, Gosk-Bierska I, McBane R, 2018, Association Between P-Selectin Levels and Left Atrial Blood Stasis in Patients With Nonvalvular Atrial Fibrillation. *Thromb Res*, 172(2): 48.
- [14] Wang W, Liu H, Li H, et al., 2020, Application Value of Inflammatory Factor Levels and Platelet Function Testing in the Treatment of Progressive Cerebral Infarction. *Thrombosis and Hemostasis*, 26(6): 62–64.
- [15] Tuttolomondo A, Pinto A, 2020, Serum Pentraxin 3 as a Clinical Biomarker of Branch Atheromatous Disease: A Marker of Brain Ischemia or an Atherothrombosis Marker? *Eur J Neurol*, 27(7): 1100–1101.
- [16] Zhu Y, Wang X, Wang W, et al., 2018, Expression and Influence of Pentraxin-3, HbA1c and ApoA1/ApoB in Serum of Patients With Acute Myocardial Infarction Combined With Type 2 Diabetes Mellitus. *Exp Ther Med*, 15(5): 4395–4399.
- [17] Zhang Y, Hu H, Liu C, et al., 2021, Serum Pentraxin 3 as a Biomarker for Prognosis of Acute Minor Stroke Due to



Large Artery Atherosclerosis. *Brain Behav*, 11(1): e01956.

- [18] Kontny F, Andersen T, Ueland T, et al., 2020, Pentraxin-3 vs C-Reactive Protein and Other Prognostic Biomarkers in Acute Coronary Syndrome: A Substudy of the Platelet Inhibition and Patients Outcomes (PLATO) Trial. *Eur Heart J Acute Cardiovasc Care*, 9(4): 313–322.
- [19] Wang D, Yu H, Feng K, 2019, Clinical Characteristics Analysis of Elderly Patients With Nonvalvular Atrial Fibrillation Combined With Acute Ischemic Stroke. *Chinese Journal of Geriatric Cardiology and Cerebrovascular Disease*, 21(11): 1129–1132.
- [20] Cui J, Yin L, 2019, Assessment Value of CHA2DS2-VASc Score for Prognosis of Patients With Nonvalvular Atrial Fibrillation and Ischemic Stroke. *Journal of Dalian Medical University*, 41(3): 214–219.
- [21] Wang X, Zhang Y, Zhao W, et al., 2018, Application of Left Atrial Diameter and Left Atrial Diameter Index in the Diagnosis of Nonvalvular Atrial Fibrillation Complicated With Ischemic Stroke. *Shandong Medical Journal*, 58(23): 63–66.

**Publisher's note**

Bio-Byword Scientific Publishing remains neutral with regard to jurisdictional claims in published maps and institutional affiliations.

# The Impact of Combined Application of Bisoprolol and Rivaroxaban on Cardiac Function in Patients with Coronary Heart Disease

Ziyue Wu

Department of Cardiology, The First Affiliated Hospital of Soochow University, Suzhou 215006, Jiangsu, China

*\*Author to whom correspondence should be addressed.*

**Copyright:** © 2025 Author(s). This is an open-access article distributed under the terms of the Creative Commons Attribution License (CC BY 4.0), permitting distribution and reproduction in any medium, provided the original work is cited.

**Abstract:** *Objective:* To investigate the impact of the combined application of bisoprolol and rivaroxaban on cardiac function in patients with coronary heart disease. *Methods:* This study employed a retrospective design, including 90 patients diagnosed with coronary heart disease and treated in our hospital from January 2022 to June 2024. The patients were divided into a combination group (receiving both bisoprolol and rivaroxaban,  $n = 44$ ) and a control group (receiving bisoprolol alone,  $n = 46$ ) based on their medication regimen. Baseline data, cardiac ultrasound indicators (left ventricular ejection fraction, left ventricular end-diastolic diameter), serum N-terminal pro-B-type natriuretic peptide (NT-proBNP) levels, 6-minute walk test distance, and the occurrence of major adverse cardiovascular events were collected through the electronic medical record system. *Results:* After treatment, the left ventricular ejection fraction in the combination group was significantly higher than that in the control group ( $P < 0.05$ ), and the left ventricular end-diastolic diameter in the combination group was significantly lower than that in the control group ( $P < 0.05$ ). The combination group had a significantly lower NT-proBNP level compared to the control group ( $P < 0.05$ ). The 6-minute walk test distance in the combination group was significantly higher than that in the control group ( $P < 0.05$ ). No significant statistical difference was observed in the occurrence of major adverse cardiovascular events between the two groups ( $P > 0.05$ ). *Conclusion:* The combined treatment of bisoprolol and rivaroxaban for patients with coronary heart disease can better improve cardiac function and enhance exercise tolerance in patients.

**Keywords:** Coronary heart disease; Bisoprolol; Rivaroxaban; Cardiac function

**Online publication:** December 31, 2025

## 1. Introduction

Coronary heart disease is a common condition in the cardiovascular department, often caused by coronary artery stenosis or obstruction leading to ischemia and hypoxia of myocardial tissue. Its main symptoms include chest pain, fatigue, palpitations, and shortness of breath. In severe cases, it can result in sudden death in patients,

posing a threat to life safety <sup>[1]</sup>. Drug therapy is a commonly used treatment plan for coronary heart disease and serves as the foundation for controlling the condition. However, how to administer medications is a key research focus in clinical practice <sup>[2]</sup>. Bisoprolol is frequently used for lowering blood pressure and improving cardiac blood supply <sup>[3]</sup>. Rivaroxaban is primarily used for anticoagulant therapy, exerting a direct inhibitory effect on coagulation factor Xa to achieve antithrombotic effects. There is a lack of clinical research on the combined application of bisoprolol and rivaroxaban. Therefore, this study selected 90 patients with coronary heart disease as subjects to analyze the therapeutic effects of combined medication.

## 2. Materials and methods

### 2.1. General information

This study was a retrospective analysis involving 90 subjects who were diagnosed with coronary heart disease and received hospitalization treatment in our hospital from January 2022 to June 2024. Based on their medication regimens, they were divided into a combined group (n = 44) and a control group (n = 46).

The details of combined group are as listed:

- (1) Gender: 28 males and 16 females;
- (2) Age: Ranging from 40 to 78 years old, with an average age of  $(59.37 \pm 5.42)$  years;
- (3) Disease duration: Ranging from 1 to 8 years, with an average duration of  $(4.78 \pm 1.21)$  years;
- (4) Disease types: 18 cases of angina pectoris, 16 cases of myocardial infarction, and 10 cases of ischemic cardiomyopathy;
- (5) Body mass index: Ranging from 19.12 to 28.65 kg/m<sup>2</sup>, with an average of  $(23.88 \pm 1.23)$  kg/m<sup>2</sup>.

The details of control group are as listed:

- (1) Gender: 26 males and 18 females;
- (2) Age: Ranging from 42 to 77 years old, with an average age of  $(59.90 \pm 5.56)$  years;
- (3) Disease duration: Ranging from 1 to 7 years, with an average duration of  $(4.35 \pm 1.06)$  years;
- (4) Disease types: 20 cases of angina pectoris, 15 cases of myocardial infarction, and 11 cases of ischemic cardiomyopathy;
- (5) Body mass index: Ranging from 19.00 to 28.23 kg/m<sup>2</sup>, with an average of  $(23.61 \pm 1.08)$  kg/m<sup>2</sup>.

There were no significant differences in general data between the two groups ( $P > 0.05$ ).

The inclusion criteria are as follows:

- (1) Meeting the diagnostic criteria for coronary heart disease outlined in the “Guidelines for Primary Care Diagnosis and Treatment of Stable Coronary Artery Disease (2020)” <sup>[4]</sup>;
- (2) Confirmed diagnosis via electrocardiogram, cardiac ultrasound, coronary angiography, etc.;
- (3) All patients having indications for medication;
- (4) Informed consent for participation in the study.

The exclusion criteria are as follows:

- (1) Severe organ dysfunction;
- (2) Concomitant other serious organic diseases;
- (3) Concomitant mental abnormalities;
- (4) Concomitant immune disorders;
- (5) Failure to take medication as prescribed.

## 2.2. Methods

All included patients received various conventional treatments such as cardiac strengthening, blood pressure reduction, and diuresis. The control group was treated solely with bisoprolol. Bisoprolol tablets (manufactured by Chengdu Yuandong Biopharmaceutical Co., Ltd., packaging specification: 5mg\*18 tablets, National Medical Products Administration Approval Number H20083008) were administered orally once daily at a dose of 5mg for 4 weeks. If the patient's condition improved and the drug was tolerated, the dosage was increased to 7.5mg once daily. Observation continued for another 4 weeks, and if the patient's tolerance remained good, the dosage was further increased to 10mg once daily, which was maintained for treatment. Patients were treated for a total of 12 weeks. The combination group received rivaroxaban in addition to the aforementioned treatment. Rivaroxaban tablets (manufactured by CSPC Ouyi Pharmaceutical Co., Ltd., specification and dosage form: 10mg, National Medical Products Administration Approval Number H20203077) were administered orally once daily at a dose of 15mg for 12 weeks.

## 2.3. Observation indicators

The observation indicators are as outlined:

- (1) Cardiac ultrasound indicators, including left ventricular ejection fraction and left ventricular end-diastolic diameter, were measured via cardiac color Doppler ultrasound;
- (2) Serum N-terminal pro-B-type natriuretic peptide (NT-proBNP) levels were measured by collecting 3mL of fasting elbow venous blood, which was then processed routinely and analyzed using a biochemical immunoanalyzer;
- (3) For the 6-minute walk test distance, prepare a straight path and record the longest distance walked by the patient in 6 minutes. Running or jogging is prohibited. Conduct the test three times consecutively and record the average value;
- (4) Occurrence of major adverse cardiovascular events, including bleeding, acute myocardial infarction, recurrent angina, and arrhythmia.

## 2.4. Statistical methods

Data were compared using SPSS 27.0 software. Continuous variables were tested for normality using the Shapiro-Wilk test and expressed as mean  $\pm$  standard deviation (SD), with t-tests performed. Categorical variables were expressed as frequencies (percentages), and chi-square ( $\chi^2$ ) tests were conducted. A *P*-value of less than 0.05 was considered statistically significant.

## 3. Results

### 3.1. Comparison of cardiac ultrasound indicators between the two groups

As shown in **Table 1**, after 12 weeks of treatment, the combined treatment group exhibited a higher left ventricular ejection fraction ( $P < 0.05$ ) and a lower left ventricular end-diastolic diameter ( $P < 0.05$ ) compared to the control group.

**Table 1.** Cardiac ultrasound indicators in the two groups (mean  $\pm$  SD)

Group	n	LVEF (%)		LVEDD (mm)	
		Pre-treatment	12 weeks post-treatment	Pre-treatment	12 weeks post-treatment
Combination group	44	40.17 $\pm$ 4.32	52.38 $\pm$ 4.98 <sup>a</sup>	61.87 $\pm$ 3.67	53.02 $\pm$ 3.05 <sup>a</sup>
Control group	46	40.56 $\pm$ 4.58	47.27 $\pm$ 4.82 <sup>a</sup>	61.32 $\pm$ 3.50	56.87 $\pm$ 3.27 <sup>a</sup>
t		0.415	4.947	0.728	5.770
P		0.679	< 0.001	0.469	< 0.001

**Note:** Compared with the same group before treatment, <sup>a</sup> $P < 0.05$ .

### 3.2. Comparison of NT-proBNP and 6-minute walk test distance between the two groups

As shown in **Table 2**, at 12 weeks post-treatment, the combination therapy group demonstrated significantly lower NT-proBNP levels and a greater 6-minute walk distance compared to the control group (both  $P < 0.05$ ).

**Table 2.** NT-proBNP and 6-minute walk test distance in the two groups (mean  $\pm$  SD)

Group	n	NT-proBNP (pg/mL)		6-minute walk distance (m)	
		Pre-treatment	12 weeks post-treatment	Pre-treatment	12 weeks post-treatment
Combination group	44	569.87 $\pm$ 45.83	320.18 $\pm$ 32.17 <sup>a</sup>	308.23 $\pm$ 35.67	512.56 $\pm$ 49.67 <sup>a</sup>
Control group	46	575.92 $\pm$ 46.71	379.45 $\pm$ 36.78 <sup>a</sup>	315.28 $\pm$ 36.82	428.67 $\pm$ 45.32 <sup>a</sup>
t		0.620	8.123	0.922	8.376
P		0.537	< 0.001	0.359	< 0.001

**Note:** Compared with the same group before treatment, <sup>a</sup> $P < 0.05$ .

### 3.3. Comparison of the incidence of major adverse cardiovascular events between the two groups

As shown in **Table 3**, within 12 weeks of treatment, there was no statistically significant difference in the incidence of major adverse cardiovascular events between the two groups ( $P > 0.05$ ).

**Table 3.** Incidence of major adverse cardiovascular events in the two groups (n/%)

Group	Combination group	Control group	$\chi^2$	P
n	44	46	0.623	0.430
Bleeding	0 (0.00)	1 (2.17)		
Acute myocardial infarction	0 (0.00)	1 (2.17)		
Recurrent angina	1 (2.27)	1 (2.17)		
Arrhythmia	1 (2.27)	1 (2.17)		
Incidence of Major Adverse Cardiovascular Events (MACE)	2 (4.55)	4 (8.70)		

## 4. Discussion

Coronary heart disease (CHD) is a highly prevalent cardiovascular disease with extremely high morbidity,

disability, and mortality rates <sup>[5]</sup>. With the increasing number of elderly individuals in China, socioeconomic development, and changes in dietary and lifestyle habits, the prevalence of chronic diseases such as CHD has risen. Clinical studies have indicated that abnormal lipid metabolism leads to the extensive deposition of lipids in the intimal layer of the coronary arteries, triggering coronary atherosclerosis and stenosis or occlusion of the vascular lumen <sup>[6]</sup>. This is the primary cause of impaired cardiac blood flow and the development of CHD. If the disease is not diagnosed early and its progression is not promptly controlled, it can lead to various issues such as angina pectoris, shortness of breath, palpitations, and chest pain, ultimately threatening the patient's life safety.

CHD is primarily treated with medications, among which bisoprolol is commonly used. It can antagonize  $\beta_1$  adrenergic receptors with high selectivity and is applied in the treatment of various cardiovascular diseases <sup>[7]</sup>. When used in the treatment of CHD, it can promote rapid vasodilation, lower blood pressure levels, improve myocardial function, and alleviate symptoms such as chest pain and palpitations. However, some studies have found that most patients with CHD have complex conditions and are of advanced age <sup>[8]</sup>. While bisoprolol alone can exert certain effects, it cannot meet the treatment needs and is difficult to rapidly achieve the expected goals. Therefore, it is necessary to combine it with other medications to enhance efficacy and promptly control symptoms and the disease progression. In the past, anticoagulant therapy was often combined with warfarin to improve efficacy, but warfarin has safety concerns and a higher risk of bleeding, thus limiting its clinical application. Rivaroxaban, a novel anticoagulant drug available in oral form, exhibits stable anticoagulant effects compared to warfarin and is less likely to induce bleeding issues, hence its widespread clinical use <sup>[9]</sup>. As an anti-Xa factor agent, rivaroxaban has a drug half-life of up to 7–11 hours. It achieves anticoagulation by selectively inhibiting coagulation factor Xa, typically reaching peak plasma concentration 4 hours after oral administration. During treatment, continuous monitoring of coagulation function is not required, and there is no risk of bleeding, allowing it to play a significant role in preventing thrombus formation.

In this study, compared with the control group, the combination therapy group demonstrated more significant improvements in cardiac ultrasound parameters, NT-proBNP levels, and 6-minute walk test distance ( $P < 0.05$ ). Bisoprolol can inhibit  $\beta_1$  adrenergic receptors, thereby slowing heart rate, ventricular conduction, and myocardial contraction, as well as lowering blood pressure. This effectively controls heart rate and reduces myocardial oxygen consumption. Rivaroxaban can inhibit the activity of coagulation factor Xa, interfere with normal platelet activation, affect the binding of coagulation proteins, achieve effective anticoagulation, prevent thrombus formation, reduce platelet aggregation, inhibit platelet activation, alleviate blood coagulation, ensure continuous vascular patency, prevent abnormal cardiac pumping, and protect cardiac function. Rivaroxaban offers outstanding efficacy and extremely high safety, with a stable anticoagulation process and pharmacokinetics. Therefore, it can prevent adverse reactions and events while ensuring therapeutic efficacy, leading to better patient tolerance <sup>[10]</sup>. Combined medication can enhance therapeutic effects and better improve cardiac function and exercise tolerance. In this study, the incidence of major adverse cardiovascular events was comparable between the two groups, suggesting that combined medication can stabilize therapeutic effects and prevent various adverse events.

## 5. Conclusion

In summary, the combined application of bisoprolol and rivaroxaban in patients with coronary heart disease can effectively improve cardiac function, NT-proBNP levels, and exercise tolerance, ensuring treatment safety and warranting clinical promotion. However, this study has certain limitations, including a short observation period and a lack of indicators such as thrombus formation factors, vascular endothelial function, and coagulation



function. Therefore, it is unable to comprehensively analyze the value of combined medication. Clinical studies should extend the observation period and enrich observation indicators based on the current situation to analyze the value of combined medication treatment from multiple aspects.

## Disclosure statement

The author declares no conflict of interest.

## References

- [1] Shen J, Wang D, Wang Z, et al., 2025, The Efficacy of Trimetazidine Combined with Clopidogrel in Treating Patients with Coronary Heart Disease and Angina Pectoris and its Impact on the Expression of cTnI, CK-MB, and NT-proBNP. *Chinese Journal of Hospital Pharmacy*, 25(7): 835–838.
- [2] Zhao T, Ren Y, Cheng T, 2025, The Impact of Hyperbaric Oxygen Combined with Atorvastatin Treatment on Vascular Endothelial Function, Coagulation Function, and Inflammatory Response in patients with Coronary Heart Disease After PCI. *Chinese Journal of Nautical Medicine and Hyperbaric Medicine*, 32(3): 271–276.
- [3] Lin Z, Tu Y, Teng Z, et al., 2024, A Randomized Controlled Study on the Treatment of Cardiac Dysfunction after Percutaneous Coronary Intervention in Patients with Coronary Heart Disease using Kuanxiong Aerosol. *Chinese Journal of Integrated Traditional and Western Medicine*, 44(12): 1431–1436.
- [4] Chinese Medical Association, Journal Office of Chinese Medical Association, General Practice Branch of Chinese Medical Association, et al., 2021, Guidelines for Primary Care of Stable Coronary Artery Disease (2020). *Chinese Journal of General Practitioners*, 20(3): 265–273.
- [5] Zhang Y, Nie Y, 2023, A Comparative Study on the Impact of Bisoprolol Fumarate and Freeze-Dried Recombinant Human Brain Natriuretic Peptide on Cardiac Function Recovery in Patients with Coronary Heart Disease Undergoing PCI. *Journal of Health Medicine Research and Practice*, 20(4): 21–24.
- [6] Zhang H, Zhang H, Xu X, et al., 2023, Clinical Study on the Treatment of Stable Angina Pectoris with Yinzhao Xinmai Dripping Pills Combined with Bisoprolol. *Modern Drugs & Clinical Practices*, 38(3): 630–634.
- [7] Liang H, Li Z, Chen X, et al., 2025, Clinical Observation on the Treatment of Coronary Heart Disease Complicated with Paroxysmal Atrial Fibrillation (Syndrome of Phlegm-Fire Disturbing the Heart) with Modified Huanglian Wendan Decoction Combined with Rivaroxaban. *Journal of Emergency in Traditional Chinese Medicine*, 34(6): 1046–1050.
- [8] Ma L, Shi R, He J, et al., 2025, Efficacy of Different Doses of Rivaroxaban Combined with Rosuvastatin in Patients with Atrial Fibrillation Complicated with Coronary Heart Disease. *Chinese Journal of Drug Application and Monitoring*, 22(5): 934–937.
- [9] Liu Y, Li Y, Zhou T, et al., 2025, Analysis of the Efficacy and Safety of Clopidogrel Combined with Rivaroxaban and Aspirin in Elderly Patients with Coronary Heart Disease Complicated with Gastrointestinal Diseases. *Journal of Clinical Military Medicine*, 53(8): 785–790.
- [10] Shang Z, Xu Y, 2024, Therapeutic Effect of Rivaroxaban Combined with Indobufen on Patients with Atrial Fibrillation Complicated with Coronary Heart Disease. *Journal of Cardiovascular Rehabilitation Medicine*, 33(6): 674–678.

### Publisher's note

Bio-Byword Scientific Publishing remains neutral with regard to jurisdictional claims in published maps and institutional affiliations.

# Analysis of Sensitivity and Accuracy of Transthoracic Echocardiography Right Heart Contrast Combined with Transcranial Doppler Bubble Test in the Diagnosis of Patent Foramen Ovale

Jianmei Chen, Dai Zhang, Dongdong Ji, Shuhua Wang, Qiushuang Wang\*

The Fourth Medical Center of the PLA General Hospital, Beijing 100048, China

\*Author to whom correspondence should be addressed.

**Copyright:** © 2025 Author(s). This is an open-access article distributed under the terms of the Creative Commons Attribution License (CC BY 4.0), permitting distribution and reproduction in any medium, provided the original work is cited.

**Abstract:** *Objective:* To analyze the diagnostic value of transthoracic right heart contrast echocardiography (c-TTE) combined with transcranial color-coded Doppler (c-TCCD) in patent foramen ovale (PFO). *Methods:* A total of 180 suspected PFO patients admitted from October 2023 to October 2025 were selected and evenly divided using a random number table. The observation group underwent c-TTE combined with c-TCCD for diagnosis, while the reference group underwent c-TTE alone. The diagnostic effects of the two groups were compared. *Results:* The detection rates of PFO in the observation group under both resting state and Valsalva maneuver were higher than those in the reference group ( $p < 0.05$ ). Apart from the aperture size and thickness of the secondary septum, there were differences in other anatomical indicators between the two groups ( $p < 0.05$ ). The detection rate of grade III shunt in the observation group was higher than that in the reference group ( $p < 0.05$ ). Using the diagnostic results of transesophageal echocardiography (TEE) as the gold standard, the sensitivity and accuracy of the observation group were higher than those of the reference group, while the missed diagnosis rate was lower than that of the reference group ( $p < 0.05$ ). *Conclusion:* The diagnosis of c-TTE combined with c-TCCD can effectively detect PFO, fully assess changes in the cardiac anatomical structure of patients, and determine shunt conditions, demonstrating high diagnostic efficacy.

**Keywords:** Contrast transthoracic echocardiography; Transcranial doppler cerebral bubble study; Patent foramen ovale; Sensitivity; Accuracy

**Online publication:** December 31, 2025

## 1. Introduction

Patent foramen ovale (PFO) is a relatively common congenital heart disease, characterized by a structural abnormality in which the physiological channel (foramen ovale) that exists during fetal development fails to close completely by the age of three after birth. The underlying cause of this condition is developmental abnormalities<sup>[1]</sup>.



The gold standard for diagnosing this disease is transesophageal echocardiography (TEE), which can accurately assess the closure status of the foramen ovale in patients and thereby comprehensively evaluate the condition. However, this diagnostic procedure is invasive, causing significant discomfort to patients and resulting in poor compliance, thus presenting certain limitations. Contrast transthoracic echocardiography (c-TTE) is a non-invasive and safe diagnostic technique that can be performed repeatedly and demonstrates high diagnostic sensitivity. When combined with contrast transcranial Doppler cerebral bubble study (c-TCCD), it can qualitatively diagnose the disease and utilize the grading of right-to-left shunt (RLS) to semi-quantitatively assess the severity of the disease<sup>[2]</sup>.

Furthermore, the operational method of c-TCCD is simple, non-invasive, and highly accurate, enabling it to achieve a high level of patient cooperation and thus demonstrating excellent diagnostic efficiency. Based on this, this study selected 180 suspected PFO patients to evaluate the diagnostic role of c-TTE combined with c-TCCD.

## **2. Materials and methods**

### **2.1. General information**

A total of 180 patients suspected of having patent foramen ovale (PFO) who were admitted and diagnosed between October 2023 and October 2025 were selected. These patients were evenly divided into two groups using a random number table: the observation group (90 cases), comprising 49 males and 41 females, aged between 19 and 57 years with a mean age of  $(36.52 \pm 2.74)$  years; and the reference group (90 cases), comprising 48 males and 42 females, aged between 20 and 59 years with a mean age of  $(36.73 \pm 2.65)$  years. Comparisons of the data between the two groups yielded a *p*-value greater than 0.05.

#### **2.1.1. Inclusion criteria**

Preliminary diagnosis of PFO; meeting the indications for examination; able to fully tolerate the examination procedure; normal liver and kidney function; complete basic information; informed consent and agreement to participate in the study.

#### **2.1.2. Exclusion criteria**

Presence of severe somatic diseases; concurrent cardiomyopathy; presence of psychiatric disorders; moderate to severe pulmonary hypertension; presence of cerebrovascular malformations; concurrent severe arrhythmia or valvular heart disease; inability to perform the Valsalva maneuver; withdrawal from the study midway.

### **2.2. Methods**

The reference group underwent c-TTE diagnosis: Color Doppler ultrasound was used, with the S5-1 probe selected, and the specific frequency range was between 2 and 5 MHz. The patient was positioned in the left lateral decubitus position. First, two-dimensional ultrasound scanning was performed to comprehensively observe the cardiac chambers and assess the specific sizes of each chamber as well as the intracardiac structures. Determine whether there is shunting between the ventricles and between the atria, and check for any gaps between the foramen ovale valve and the observed secondary septum.

Then, perform color Doppler flow imaging to evaluate the trans-septal shunting flow. After puncturing the left upper extremity vein, inject a certain amount of normal saline. The patient is required to perform the Valsalva maneuver, after which right heart opacification will be observed. Three cardiac cycles are monitored to identify the characteristics of the shunting.

The observation group underwent diagnosis using c-TTE combined with c-TCCD. The diagnostic method for c-TTE is the same as described above. The operational procedure for c-TCCD is as follows: Select transcranial Doppler ultrasound and set the probe frequency at 2 MHz. Instruct the patient to maintain a supine position. Establish a venous access in one elbow vein, connect a three-way stopcock, with one end connected to a syringe containing 10 ml of normal saline. Install embolus detection equipment and monitor the middle cerebral artery using dual-depth and single-channel mode, with a depth of 50–60 mm. In the patient's resting state, inject an appropriate amount of normal saline through the elbow vein and observe the microbubble signals that appear within 10 seconds.

The diagnostic method for TEE is as follows: Select color Doppler ultrasound with a probe model of X7-2t and set its frequency at 2–7 MHz. Instruct the patient to take dyclonine hydrochloride capsules orally, followed by local anesthesia. The patient should lie in a left lateral position. Place the probe in the middle to lower segment of the esophagus, with the section at the level of the double atria, and scan for any obvious gaps between the secondary and primary septa.

## 2.3. Observation indicators

### (1) Detection rate of PFO

Observe the detection rate of PFO under resting state and Valsalva maneuver.

### (2) Anatomical indicators

Observe indicators such as aperture size, thickness of the secondary septum, length of the Eustachian valve, tunnel length, shunt angle, and mobility of the primary septum.

### (3) Shunt grading

Refer to the “Chinese Expert Consensus on Prophylactic Closure of Patent Foramen Ovale”. The specific grading is defined as follows: No right-to-left shunt (RLS) is observed, and no microbubbles/frame images are detected in the left cardiac chamber, recorded as Grade 0; A small amount of RLS is observed, with 1–10 microbubbles/frame images detected in the left cardiac chamber, recorded as Grade I; A moderate amount of RLS is observed, with 11–30 microbubbles/frame images recorded as Grade II; A large amount of RLS is observed, with more than 30 microbubbles/frame images recorded as Grade III.

### (4) Diagnostic efficacy positive c-TTE

The presence of three or more microbubbles in the left atrium; Positive c-TCCD: Refer to the “Venice Conference Recommended Criteria (1999)” to evaluate specific data on microembolic signals. If no microembolic signals are detected, it is recorded as Grade I; If microembolic signals are present, with a quantity of 1–10, it is recorded as Grade II; If microembolic signals are visible, with a specific quantity of 11–25, it is recorded as Grade III; If the number of microembolic signals detected exceeds 25 and appears as a curtain-like pattern, it is recorded as Grade IV. A grade of  $\geq$  II is considered positive. A positive TEE result indicates the presence of RLS or right-to-left shunt (LRS) in the primary and secondary septum. Using TEE diagnostic results as the gold standard, sensitivity = number of true positives / (number of true positives + number of false negatives); accuracy = (number of true positives + number of true negatives) / total number of cases in this group; specificity = number of true negatives / (number of true negatives + number of false positives); missed diagnosis rate = number of false negatives / (number of true positives + number of false negatives); misdiagnosis rate = number of false positives / (number of false positives + number of true negatives).

## 2.4. Statistical analysis

Data were processed using SPSS 28.0 software. Measurement values were compared using *t*-tests, and count values were compared using chi-square ( $\chi^2$ ) tests. Statistical significance was defined as  $p < 0.05$ .

## 3. Results

### 3.1. Comparison of PFO detection rates between the two groups

The detection rates of PFO in the observation group were higher than those in the reference group under both resting state and Valsalva maneuver conditions ( $p < 0.05$ ) (refer **Table 1**).

**Table 1.** Comparison of PFO detection rates between the two groups [n/%]

Group	n	Resting state	Valsalva maneuver
Observation group	90	59 (65.56)	71 (78.89)
Reference group	90	45 (50.00)	59 (65.56)
$\chi^2$		4.464	3.988
p		0.035	0.046

### 3.2. Comparison of anatomical indicators between the two groups

Apart from aperture size and secondary septal thickness, there were differences in other anatomical indicators between the two groups ( $p < 0.05$ ) (refer **Table 2**).

**Table 2.** Comparison of anatomical indicators between the two groups ( $\bar{x} \pm s$ )

Group	n	Defect size (mm)	Septum secundum thickness (mm)	Eustachian valve length (mm)	Tunnel length (mm)	Shunt angle (°)	Septum primum mobility (mm)
Observation group	90	2.75 ± 0.49	6.69 ± 1.78	7.66 ± 1.59	9.75 ± 1.64	6.98 ± 1.77	11.72 ± 2.59
Reference group	90	2.81 ± 0.52	6.58 ± 1.80	5.92 ± 1.43	4.98 ± 1.98	15.53 ± 2.64	6.87 ± 1.57
t		0.797	0.412	7.719	17.601	25.520	15.192
p		0.427	0.681	0.000	0.000	0.000	0.000

### 3.3. Comparison of shunt grades between the two groups

The detection rate of Grade III shunts in the observation group was higher than that in the reference group ( $p < 0.05$ ) (refer **Table 3**).

**Table 3.** Comparison of shunt grades between the two groups [n/%]

Group	n	Grade 0	Grade I	Grade II	Grade III
Observation group	90	4 (4.44)	8 (8.89)	13 (14.44)	65 (72.22)
Reference group	90	11 (12.22)	17 (18.89)	22 (24.44)	40 (44.44)
$\chi^2$		3.564	3.763	2.873	14.286
p		0.059	0.052	0.090	0.000

### 3.4. Comparison of diagnostic efficacy between the two groups

Using the diagnostic results from TEE as the gold standard, the diagnostic outcomes of the two groups are presented in **Table 4**. The observation group demonstrated higher sensitivity and accuracy, along with a lower missed diagnosis rate compared to the reference group ( $p < 0.05$ ), as shown in **Table 5**.

**Table 4.** Analysis of diagnostic results in the two groups

Diagnostic method		Gold standard		Total
		Positive	Negative	
Observation group	Positive	68	3	71
	Negative	2	17	19
Reference group	Positive	55	4	59
	Negative	15	16	31

**Table 5.** Comparison of diagnostic efficacy between the two groups [n/%]

Group	Sensitivity	Accuracy	Specificity	Missed diagnosis rate	False positive rate
Observation group	97.14 (68/70)	94.44 (85/90)	85.00 (17/20)	2.86 (2/70)	15.00 (3/20)
Reference group	78.57 (55/70)	78.89 (71/90)	80.00 (16/20)	21.43 (15/70)	20.00 (4/20)
$\chi^2$	11.315	9.423	0.173	11.315	0.173
p	0.001	0.002	0.677	0.001	0.677

## 4. Discussion

PFO is a primary type of congenital heart disease that does not cause biventricular shunting and does not affect the hemodynamics of myocardial tissue, resulting in a relatively high rate of missed or incorrect diagnoses<sup>[3]</sup>. The long-term presence of this condition increases the risk of stroke and is considered a risk factor for various cardiovascular and cerebrovascular diseases. It is also associated with symptoms such as migraines and angina pectoris. Therefore, early diagnosis of the disease is essential to fully assess its severity and to implement appropriate treatment measures.

Transesophageal echocardiography (TEE) serves as the gold standard for diagnosing this disease, capable of assessing atrial size and structural changes, reflecting the pathological conditions of cardiac valves, and observing the blood flow status in cardiac arteries and veins to facilitate differential diagnosis<sup>[4]</sup>. However, due to its invasive nature and the generally moderate tolerance of patients during the examination, TEE is difficult to be widely applied. Transthoracic echocardiography (TTE) is a commonly used diagnostic method for this disease.

However, it is susceptible to interference from gas factors and excessive obesity, making it difficult to clearly display the images of the atrial septal biatrial section. To enhance disease differentiation ability, it is necessary to increase the probe pressure during enhanced scanning and adjust the color gain mode<sup>[5]</sup>. Nevertheless, its detection effectiveness for lesions with small internal diameters and low-velocity blood flow remains limited. In comparison, contrast-enhanced transthoracic echocardiography (c-TTE) offers a more scientifically robust diagnosis. It utilizes microbubble signals to evaluate right-to-left shunt (RLS) conditions, boasting the advantages of being non-invasive and convenient. On the basis of evaluating cardiac function and structure, it can assess the

flow state of microbubbles using right heart contrast echocardiography, thereby determining the severity of the disease <sup>[6]</sup>. Contrast-enhanced transcranial color-coded duplex sonography (c-TCCD) can place microspheres into the right atrium under the guidance of an esophageal ultrasound catheter. After injecting a contrast agent, it evaluates the distribution trajectory of microbubbles during cardiac pulsation to assess the shunt between the left and right atria. As microspheres pass through the left atrium, blood flow velocity increases; conversely, when they do not pass through, blood flow velocity slows down. Based on this, the presence or absence of a patent foramen ovale (PFO) can be determined.

The combined diagnosis of these two methods can leverage their respective strengths, thus offering high diagnostic feasibility <sup>[7]</sup>. The results showed that the detection rate of PFO in the observation group was higher than that in the reference group during both resting state and Valsalva maneuver; the length of the Eustachian valve, tunnel length, and mobility of the primary septum in the observation group were greater than those in the reference group, while the shunt angle was smaller in the observation group; the detection rate of grade III shunt in the observation group was higher than that in the reference group; taking the diagnostic results of TEE as the gold standard, the sensitivity and accuracy of the observation group were higher than those of the reference group, while the missed diagnosis rate was lower in the observation group ( $p < 0.05$ ). The reasons for the analysis are as follows: c-TTE can utilize acoustic contrast agents to evaluate the number of microbubbles in the left and right atria, allowing for a comprehensive observation of shunt volume. However, it has limited temporal windows for a single diagnosis, only observing the blood flow status of the middle cerebral artery, making it difficult to accurately detect microbubble signals, which may lead to missed diagnoses <sup>[8,9]</sup>.

Additionally, due to its average image quality, it is challenging to clearly visualize subtle emboli, resulting in a relatively high false-positive rate. Combining c-TCCD can enhance quantitative resolution and provide dual detection of the middle cerebral artery to observe the distribution of tiny bubbles. During the Valsalva maneuver, this diagnostic approach can bring microbubbles to their peak, enabling clear observation of disease conditions and improving diagnostic accuracy <sup>[10]</sup>. The combination of the two can effectively evaluate changes in cardiac anatomical structures, accurately measure the mobility and size of cardiac structures, and semi-quantitatively grade the number of microbubbles to accurately assess disease severity, thus demonstrating excellent diagnostic efficacy.

## 5. Conclusion

In conclusion, the combination of c-TTE and c-TCCD demonstrates superior diagnostic performance for PFO, enabling a comprehensive assessment of disease conditions and providing scientific guidance for subsequent treatment.

## Disclosure statement

The author declares no conflict of interest.

## References

- [1] Zhou J, Guo T, Kong C, 2025, Application of Transthoracic Echocardiography Right Heart Contrast Combined with Transcranial Doppler Bubble Test in the Diagnosis of Patent Foramen Ovale. *Smart Healthcare*, 11(1): 7–9 + 13.
- [2] Liu L, Weng Q, Chang R, et al., 2023, Diagnostic Value of Transthoracic Right Heart Contrast Echocardiography



Combined with Transesophageal Echocardiography and Transcranial Doppler Bubble Test for Patent Foramen Ovale. *Chinese Journal of Integrative Medicine on Cardio-Cerebrovascular Disease*, 21(10): 1900–1903.

- [3] Shao X, Qin W, 2025, Research on the Application Value of Transthoracic Right Heart Contrast Echocardiography Combined with c-TCD in the Diagnosis of Patent Foramen Ovale. *Heilongjiang Medicine and Pharmacy*, 48(10): 147–149.
- [4] Dong Q, Bu H, Cai D, et al., 2025, Diagnostic Value of Contrast Echocardiography in Young Patients with Transient Ischemic Attack Combined with Right-to-Left Shunt Due to Patent Foramen Ovale. *Chinese Journal of Clinical Medical Imaging*, 36(1): 34–37.
- [5] Li S, 2024, Clinical Application Value of c-TTE Combined with TCD Bubble Test Versus TEE in Patients with Migraine Complicated by Patent Foramen Ovale. *Medicine, Diet and Health*, 22(1): 154–156 + 159.
- [6] Liu J, Liu J, Xue P, et al., 2025, Clinical Value of Transthoracic Echocardiography Combined with Right Heart Acoustic Contrast in Evaluating Right-to-Left Shunt Through Patent Foramen Ovale in Patients with Cryptogenic Stroke. *Journal of Clinical and Experimental Medicine*, 24(6): 667–670.
- [7] Du Y, Wang X, Gao B, 2025, Comparative Analysis of the Diagnostic Efficacy of Painless Transesophageal Two-Dimensional or Three-Dimensional Echocardiography Combined with Transthoracic Right Heart Acoustic Contrast for Patent Foramen Ovale in Adults. *Journal of Medical Imaging*, 35(9): 52–55.
- [8] Peng S, Huang Y, Zhu H, 2025, Application Value of Transthoracic Echocardiography Combined with Right Heart Acoustic Contrast in Evaluating Right-to-Left Shunt Through Patent Foramen Ovale. *China Modern Medicine Journal*, 27(6): 83–88.
- [9] Song B, Ni W, Ma B, et al., 2025, Value of Transthoracic Echocardiography and Right Heart Acoustic Contrast in Diagnosing Patent Foramen Ovale in Patients with Cryptogenic Stroke. *Prevention and Treatment of Cardio-Cerebrovascular Diseases*, 25(7): 48–51.
- [10] Han Q, Yu Q, Chen S, 2025, Value of Right Heart Acoustic Contrast Combined with Transthoracic Echocardiography in Evaluating Left Atrial Function After Closure of Patent Foramen Ovale. *Sichuan Journal of Anatomy*, 33(4): 25–27.

**Publisher's note**

Bio-Byword Scientific Publishing remains neutral with regard to jurisdictional claims in published maps and institutional affiliations.

# The Impact of Early Initiation of Intensive Lipid-Lowering Therapy on Lipid Target Achievement and Major Adverse Cardiovascular Events in Patients with Acute Coronary Syndrome Undergoing Percutaneous Coronary Intervention

Yue Kan, Yongfu Zhao, Hong Gao, Shihao Zhao, Jiaxu Liu, Zhanxiu Zhang\*

The Second People's Hospital of Huludao City, Huludao 125000, Liaoning, China

*\*Author to whom correspondence should be addressed.*

**Copyright:** © 2025 Author(s). This is an open-access article distributed under the terms of the Creative Commons Attribution License (CC BY 4.0), permitting distribution and reproduction in any medium, provided the original work is cited.

**Abstract:** *Objective:* This study primarily investigates the impact of early initiation of intensive lipid-lowering therapy on lipid target achievement rates and the incidence of major adverse cardiovascular events (MACE) in patients with acute coronary syndrome (ACS) undergoing percutaneous coronary intervention (PCI). *Methods:* A total of 100 patients with ACS who underwent PCI in our hospital were selected as the study subjects. They were randomly divided into a control group (treated with statin combined with ezetimibe,  $n = 41$ ), study group 1 (initiated with statin combined with a PCSK9 inhibitor immediately after surgery,  $n = 32$ ), and study group 2 (received routine oral statin and initiated with a combined PCSK9 inhibitor before discharge,  $n = 27$ ). The safety of treatment, lipid target achievement, and differences in the incidence of cardiovascular adverse events were compared and analyzed among the three groups. *Results:* The treatment regimen in study group 1 demonstrated the optimal effect in improving liver and kidney function and lipid indicators, followed by study group 2, while the control group showed relatively weaker efficacy, with statistically significant differences ( $P < 0.05$ ). The overall incidence of cardiovascular adverse events was 25.00% in the control group, 5.00% in study group 1, and 15.00% in study group 2, with statistically significant differences between the groups ( $P < 0.05$ ), with study group 1 having the lowest incidence. *Conclusion:* Early intensive lipid-lowering therapy can significantly improve lipid target achievement rates and reduce the risk of MACE in patients with ACS undergoing PCI, with good safety and significant clinical implications.

**Keywords:** Early; Intensive lipid-lowering; Patients with acute coronary syndrome undergoing PCI; Lipids; Major adverse cardiovascular events

**Online publication:** December 31, 2025

# 1. Introduction

Acute coronary syndrome (ACS), one of the most critical clinical types among cardiovascular diseases, has a pathogenesis closely related to atherosclerotic plaque rupture and thrombosis, with dyslipidemia serving as the core driver of atherosclerosis progression <sup>[1]</sup>. Although percutaneous coronary intervention (PCI) can rapidly restore blood flow, residual postoperative inflammatory responses, endothelial dysfunction, and plaque instability may still lead to major adverse cardiac events (MACE), including reinfarction, revascularization, stroke, and even cardiovascular death <sup>[2]</sup>. In recent years, evidence from evidence-based medicine has indicated that intensive lipid-lowering therapy can delay the progression of atherosclerosis, stabilize plaques, and improve endothelial function by significantly reducing lipid levels, thereby reducing the risk of MACE <sup>[3,4]</sup>. However, there is still controversy regarding the optimal timing, intensity, and long-term prognostic impact of early initiation of intensive lipid-lowering therapy (such as the use of high-intensity statins combined with PCSK9 inhibitors within 24 hours) in patients with ACS after PCI.

Some studies suggest that early intensive intervention can more rapidly achieve lipid targets (e.g., LDL-C < 1.4 mmol/L or a  $\geq 50\%$  reduction from baseline) and reduce the release of inflammatory factors. However, others argue that overly aggressive lipid-lowering may increase the risk of liver enzyme abnormalities or myopathy, and the benefit-risk ratio in different populations (e.g., elderly individuals, those with comorbid diabetes, or chronic kidney disease) requires further stratified evaluation <sup>[5]</sup>. Additionally, current guidelines on lipid-lowering strategies during the perioperative period of PCI are still based on the overall ACS population and lack individualized approaches tailored to the dynamic changes in lipid metabolism under surgical stress <sup>[6]</sup>.

Therefore, exploring the short-term and long-term effects of early intensive lipid-lowering therapy on lipid target attainment rates, treatment safety, and MACE events in patients with ACS undergoing PCI will not only help clarify the optimal treatment time window and drug combinations but also provide evidence-based support for developing precise lipid-lowering strategies, ultimately improving clinical outcomes in this high-risk population. This study aims to systematically evaluate the efficacy and safety of early intensive lipid-lowering therapy through prospective cohort analysis to fill the evidence gap between current guidelines and clinical practice.

# 2. Research subjects and methods

## 2.1. Research subjects

A total of 100 patients with ACS who underwent PCI at our hospital were selected as research subjects, including 55 male and 45 female patients.

Inclusion criteria are as follows:

- (1) Meeting the criteria outlined in the “Guidelines for Rapid Emergency Diagnosis and Treatment of Acute Coronary Syndrome”;
- (2) Meeting the indications for PCI surgery, with coronary angiography revealing at least one coronary artery lesion with a stenosis degree > 70%;
- (3) Aged between 18 and 79 years, regardless of gender;
- (4) Diagnosed with acute coronary syndrome, including patients with acute ST-segment elevation myocardial infarction and acute non-ST-segment elevation myocardial infarction;
- (5) Adhering to ethical principles and having signed an informed consent form.

Exclusion criteria are as follows:

- (1) Patients who have received lipid-lowering therapy in the past 6 months;



- (2) Those with other heart diseases or severe cardiac dysfunction with a left ventricular ejection fraction less than 30%;
- (3) Patients with creatine kinase levels exceeding five times the normal range or unexplained CK elevation or those who cannot tolerate lipid-lowering therapy;
- (4) Patients with concurrent malignant tumors, immune system diseases such as rheumatoid connective tissue disorders;
- (5) Those with impaired liver and kidney function [blood urea nitrogen (BUN)  $\geq$  10.71 mmol/L (30 mg/dL) or creatinine (Cr)  $\geq$  176 mmol/L (2.0 mg/dL)], obstructive jaundice, active liver disease, chronic hepatitis, aspartate aminotransferase (AST) or ALT levels three times or more the upper limit of normal, or hyperbilirubinemia;
- (6) Patients currently taking medications that may interact with the study drugs (such as immunosuppressants), as well as medications that, when combined with statins, may increase the risk of rhabdomyolysis;
- (7) Patients allergic to any statin or those with contraindications to ezetimibe use.

## **2.2 Methods**

### **2.2.1. Experimental grouping**

The 100 patients included in the study were divided into three groups: control group (statin combined with ezetimibe treatment, n = 41), study group 1 (immediate initiation of statin combined with PCSK9 inhibitor post-surgery, n = 32), and study group 2 (routine oral statin with initiation of combined PCSK9 inhibitor before hospital discharge, n = 27).

The control group was treated with a combination of statins and ezetimibe: oral administration of 20 mg atorvastatin tablets (Lipitor, Lepu Pharmaceutical Technology Co., Ltd.) every night, combined with 10 mg ezetimibe tablets (Ezetrol, Merck & Co., Inc.), for a continuous treatment period of 6 months.

Group 1 initiated statin therapy combined with a PCSK9 inhibitor immediately after surgery: oral administration of 20 mg atorvastatin tablets (Lipitor, Lepu Pharmaceutical Technology Co., Ltd.) every night, combined with subcutaneous injection of evolocumab injection immediately after surgery, administered every 2 weeks at a dose of 140 mg per injection, for a continuous treatment period of 6 months.

Group 2 received conventional oral statin therapy and initiated combination therapy with a PCSK9 inhibitor before discharge: oral administration of 20 mg atorvastatin tablets (Lipitor, Lepu Pharmaceutical Technology Co., Ltd.) every night, with subcutaneous injection of evolocumab injection initiated before discharge, administered every 2 weeks at a dose of 140 mg per injection, for a continuous treatment period of 6 months.

### **2.2.2. Safety assessment analysis of treatment in the three groups of patients**

The safety of treatment in the three groups of patients was assessed before treatment, as well as 1 month, 3 months, and 6 months after treatment. This included indicators of liver damage: Alanine aminotransferase (ALT), Aspartate aminotransferase (AST), Total bilirubin (TBIL), Direct bilirubin (DBIL), and Indirect bilirubin (IBIL); and indicators of kidney damage: Urea nitrogen (BUN), Creatinine (CR), Uric acid (UA), and Creatine kinase isozyme (CK-MB). Among these, CK-MB was measured using a dry-type immunofluorescence method with a fluorescence immunoassay analyzer.

### **2.2.3. Analysis of blood lipid levels reaching standard in the three groups of patients**

All three groups of patients maintained a fasting state for at least 12 hours, and 3 mL of forearm cubital vein blood

was collected for blood biochemical testing using a Siemens Atellica device, record the changes in Apolipoprotein A (ApoA), Total Cholesterol (TC), Triglyceride (TG), High-Density Lipoprotein Cholesterol (HDL-C), Low-Density Lipoprotein Cholesterol (LDL-C), Lipoprotein(a) [Lp(a)], and Apolipoprotein B (ApoB) before treatment, and at 1 month, 3 months, and 6 months after treatment.

## 2.2.4. Incidence of cardiovascular adverse events in three groups of patients

During the follow-up period, the occurrence of cardiovascular adverse events (acute myocardial infarction, heart failure, death, and rehospitalization) was documented for all three patient groups, and incidence rates were determined.

## 2.3. Statistical analysis

All data in this study were processed using SPSS 20.0 statistical analysis software (IBM, USA). Measurement data were expressed as “mean  $\pm$  standard deviation” (mean  $\pm$  SD), and comparisons between groups were performed using independent sample t-tests. Enumeration data were expressed as percentages (%), and comparisons between groups were performed using  $\chi^2$  analysis. A *P*-value  $< 0.05$  indicated a statistically significant difference.

## 3. Results

### 3.1. Analysis of therapeutic efficacy in three groups of patients

There were no significant differences in liver and kidney damage indicators (ALT, AST, TBIL, DBIL, IBIL, BUN, CR, UA, CK-MB) among the three groups of patients before treatment ( $P > 0.05$ ). At 1 month, 3 months, and 6 months after treatment, all indicators significantly improved, with significant differences between groups ( $P < 0.05$ ). Among them, study group 1 showed the greatest improvement in liver and kidney indicators. The therapeutic efficacy of study group 2 was between that of the control group and study group 1, but some indicators (such as TBIL, DBIL, BUN, CR) were still significantly better than those in the control group ( $P < 0.05$ ). That is, the treatment regimen of study group 1 demonstrated the most optimal effect in improving liver and kidney function and myocardial injury, followed by study group 2, while the control group showed relatively weaker efficacy. (Table 1)

**Table 1.** Analysis of therapeutic efficacy in three patient groups (mean  $\pm$  SD)

Grouping	Control group (n = 41)	Study group 1 (n = 32)	Study group 2 (n = 27)	t/ $\chi^2$ value	<i>P</i> value
Before treatment					
Liver damage indicators					
ALT (U/L)	40.88 $\pm$ 3.09	40.40 $\pm$ 3.56	42.75 $\pm$ 1.46	0.469	0.789
AST (U/L)	144.75 $\pm$ 15.62	27.60 $\pm$ 5.41	63.50 $\pm$ 3.07	2.642	0.769
TBIL ( $\mu$ mol/L)	20.60 $\pm$ 1.25	12.33 $\pm$ 3.58	19.07 $\pm$ 1.08	0.859	0.436
DBIL ( $\mu$ mol/L)	6.71 $\pm$ 0.22	3.60 $\pm$ 0.61	6.55 $\pm$ 0.76	0.483	0.126
IBIL ( $\mu$ mol/L)	14.12 $\pm$ 1.06	8.62 $\pm$ 0.38	12.27 $\pm$ 0.23	0.268	0.700
Kidney damage indicators					
BUN (mg/dL)	52.98 $\pm$ 1.12	52.57 $\pm$ 1.78	52.21 $\pm$ 3.92	0.119	0.257
CR (mg/dL)	70.99 $\pm$ 15.23	67.30 $\pm$ 2.71	59.60 $\pm$ 8.87	2.650	0.160
UA (mg/dL)	313.25 $\pm$ 52.93	337.60 $\pm$ 16.36	361.50 $\pm$ 16.54	1.593	0.226
CK-MB (ng/mL)	24.37 $\pm$ 1.01	35.27 $\pm$ 0.37	26.85 $\pm$ 3.93	0.894	0.390

**Table 1 (Continued)**

Grouping	Control group (n = 41)	Study group 1 (n = 32)	Study group 2 (n = 27)	t/ $\chi^2$ value	P value
1 month post-treatment					
Liver damage indicators					
ALT (U/L)	32.01 $\pm$ 2.51	29.67 $\pm$ 0.21	33.62 $\pm$ 1.49	8.047	0.001
AST (U/L)	26.47 $\pm$ 1.21	23.19 $\pm$ 1.19	24.10 $\pm$ 1.02	3.283	0.002
TBIL ( $\mu$ mol/L)	12.81 $\pm$ 5.01	15.53 $\pm$ 5.15	13.01 $\pm$ 5.04	2.115	0.042
DBIL ( $\mu$ mol/L)	13.58 $\pm$ 4.74	6.28 $\pm$ 2.26	5.19 $\pm$ 1.90	3.786	0.047
IBIL ( $\mu$ mol/L)	8.01 $\pm$ 3.24	9.22 $\pm$ 3.32	7.82 $\pm$ 3.35	5.482	0.026
Kidney damage indicators					
BUN (mg/dL)	38.91 $\pm$ 0.37	26.53 $\pm$ 0.27	33.45 $\pm$ 9.98	13.267	0.007
CR ( $\mu$ mol/L)	89.21 $\pm$ 10.99	78.56 $\pm$ 18.39	71.05 $\pm$ 12.03	4.528	0.014
UA ( $\mu$ mol/L)	333.91 $\pm$ 15.24	352.22 $\pm$ 16.55	321.43 $\pm$ 17.70	5.097	0.025
CK-MB (ng/mL)	12.68 $\pm$ 1.32	10.49 $\pm$ 1.90	11.46 $\pm$ 6.52	10.434	0.001
3 months post-treatment					
Liver damage indicators					
ALT (U/L)	42.80 $\pm$ 2.67	29.25 $\pm$ 1.03	47.44 $\pm$ 0.65	5.212	0.010
AST (U/L)	39.75 $\pm$ 3.80	24.13 $\pm$ 0.16	24.78 $\pm$ 0.76	7.653	0.033
TBIL ( $\mu$ mol/L)	14.63 $\pm$ 6.44	14.80 $\pm$ 0.49	13.28 $\pm$ 0.57	4.035	0.015
DBIL ( $\mu$ mol/L)	5.47 $\pm$ 2.46	6.23 $\pm$ 0.17	4.87 $\pm$ 0.75	5.278	0.044
IBIL ( $\mu$ mol/L)	8.99 $\pm$ 4.01	9.19 $\pm$ 0.58	8.40 $\pm$ 0.17	3.197	0.013
Kidney damage indicators					
BUN (mg/dL)	34.27 $\pm$ 0.32	22.15 $\pm$ 0.21	28.91 $\pm$ 8.12	12.845	0.001
CR ( $\mu$ mol/L)	69.76 $\pm$ 2.17	71.89 $\pm$ 5.77	67.60 $\pm$ 9.64	7.649	0.053
UA ( $\mu$ mol/L)	302.13 $\pm$ 19.61	337.00 $\pm$ 15.52	341.78 $\pm$ 10.89	5.611	0.014
CK-MB (ng/mL)	11.34 $\pm$ 1.18	8.12 $\pm$ 1.45	9.21 $\pm$ 5.87	12.089	0.020
6 months post-treatment					
Liver damage indicators					
ALT (U/L)	18.50 $\pm$ 0.61	14.33 $\pm$ 4.04	13.00 $\pm$ 2.46	4.442	0.015
AST (U/L)	18.00 $\pm$ 2.83	19.67 $\pm$ 0.66	26.50 $\pm$ 0.71	5.647	0.023
TBIL ( $\mu$ mol/L)	12.74 $\pm$ 1.43	18.43 $\pm$ 0.12	9.64 $\pm$ 3.23	3.228	0.019
DBIL ( $\mu$ mol/L)	4.42 $\pm$ 0.44	5.86 $\pm$ 1.49	1.95 $\pm$ 0.62	5.467	0.042
IBIL ( $\mu$ mol/L)	8.14 $\pm$ 1.24	12.57 $\pm$ 0.87	6.19 $\pm$ 1.73	6.758	0.003
Kidney damage indicators					
BUN (mg/dL)	30.12 $\pm$ 0.28	18.92 $\pm$ 0.18	25.34 $\pm$ 6.87	14.672	0.003
CR ( $\mu$ mol/L)	71.50 $\pm$ 6.58	75.30 $\pm$ 19.43	121.45 $\pm$ 13.09	4.635	0.012
UA ( $\mu$ mol/L)	392.50 $\pm$ 14.85	328.67 $\pm$ 17.23	486.00 $\pm$ 12.62	6.758	0.025
CK-MB (ng/mL)	9.34 $\pm$ 1.18	7.12 $\pm$ 1.45	8.21 $\pm$ 5.87	9.879	0.023

### 3.2. Analysis of lipid profile control in three patient groups

There were no significant differences in the various indicators (including ApoA, TC, TG, HDL-C, LDL-C, Lp(a), and ApoB) among the three patient groups before treatment ( $P > 0.05$ ). After one month, three months, and six months of treatment, the indicators in study group 1 and study group 2 showed significant improvements compared to the control group ( $P < 0.05$ ), with particularly notable improvements in study group 1 ( $P < 0.05$ ). (Table 2)

**Table 2.** Analysis of lipid profile control in three patient groups (mean  $\pm$  SD)

Grouping	Control group (n = 41)	Study group 1 (n = 32)	Study group 2 (n = 27)	t/ $\chi^2$ value	P value
Before treatment					
ApoA (mg/dL)	1.21 $\pm$ 0.15	1.22 $\pm$ 0.18	1.21 $\pm$ 0.16	0.128	0.887
TC (mmol/L)	4.92 $\pm$ 1.26	5.68 $\pm$ 1.21	5.76 $\pm$ 1.44	0.176	0.543
TG (mmol/L)	1.39 $\pm$ 0.82	1.93 $\pm$ 0.87	1.31 $\pm$ 0.87	0.267	0.843
HDL-C (mmol/L)	1.39 $\pm$ 0.80	1.54 $\pm$ 0.62	0.93 $\pm$ 0.21	0.609	0.415
LDL-C (mmol/L)	2.99 $\pm$ 1.03	3.54 $\pm$ 1.65	4.21 $\pm$ 1.13	0.743	0.516
Lp(a) (nmol/L)	25.89 $\pm$ 1.43	26.45 $\pm$ 1.98	25.58 $\pm$ 1.45	0.115	0.896
ApoB (mg/dL)	0.94 $\pm$ 0.12	0.92 $\pm$ 0.15	0.91 $\pm$ 0.11	0.125	0.487
1 month post-treatment					
ApoA (mg/dL)	1.25 $\pm$ 0.16	1.45 $\pm$ 0.20	1.30 $\pm$ 0.18	8.256	0.003
TC (mmol/L)	3.21 $\pm$ 0.87	2.74 $\pm$ 0.74	2.93 $\pm$ 0.34	4.389	0.054
TG (mmol/L)	1.77 $\pm$ 0.98	1.73 $\pm$ 0.93	1.70 $\pm$ 0.76	6.587	0.023
HDL-C (mmol/L)	1.10 $\pm$ 0.22	1.23 $\pm$ 0.14	1.05 $\pm$ 0.26	7.869	0.044
LDL-C (mmol/L)	1.93 $\pm$ 0.47	1.56 $\pm$ 0.64	1.69 $\pm$ 0.38	8.970	0.025
Lp(a) (nmol/L)	24.12 $\pm$ 1.58	20.05 $\pm$ 1.06	22.38 $\pm$ 1.24	12.371	0.014
ApoB (mg/dL)	0.85 $\pm$ 0.09	0.75 $\pm$ 0.08	0.80 $\pm$ 0.09	11.282	0.001
3 months post-treatment					
ApoA (mg/dL)	1.28 $\pm$ 0.17	1.52 $\pm$ 0.21	1.35 $\pm$ 0.19	9.142	0.001
TC (mmol/L)	3.15 $\pm$ 0.57	3.23 $\pm$ 1.21	3.13 $\pm$ 0.22	6.753	0.014
TG (mmol/L)	1.80 $\pm$ 0.97	2.05 $\pm$ 0.38	1.95 $\pm$ 0.89	5.473	0.025
HDL-C (mmol/L)	1.10 $\pm$ 0.17	1.10 $\pm$ 0.26	1.14 $\pm$ 0.28	6.776	0.047
LDL-C (mmol/L)	1.79 $\pm$ 0.33	1.74 $\pm$ 0.81	1.77 $\pm$ 0.92	9.034	0.011
Lp(a) (nmol/L)	22.45 $\pm$ 1.06	18.20 $\pm$ 0.87	20.15 $\pm$ 2.65	14.825	0.011
ApoB (mg/dL)	0.82 $\pm$ 0.08	0.68 $\pm$ 0.07	0.75 $\pm$ 0.08	16.333	0.008
6 months post-treatment					
ApoA (mg/dL)	1.30 $\pm$ 0.18	1.58 $\pm$ 0.22	1.40 $\pm$ 0.20	10.257	0.005
TC (mmol/L)	3.33 $\pm$ 0.23	3.88 $\pm$ 1.24	5.06 $\pm$ 0.04	12.434	0.034
TG (mmol/L)	2.20 $\pm$ 0.41	1.89 $\pm$ 0.75	3.15 $\pm$ 0.12	9.807	0.011
HDL-C (mmol/L)	1.11 $\pm$ 0.11	1.20 $\pm$ 0.17	0.87 $\pm$ 0.02	7.658	0.024
LDL-C (mmol/L)	2.06 $\pm$ 0.04	2.19 $\pm$ 0.44	3.30 $\pm$ 0.50	12.312	0.035
Lp(a) (nmol/L)	20.80 $\pm$ 2.13	16.50 $\pm$ 0.98	18.20 $\pm$ 0.78	18.326	0.012
ApoB (mg/dL)	0.78 $\pm$ 0.07	0.62 $\pm$ 0.06	0.70 $\pm$ 0.07	21.548	0.013

### 3.3. Incidence of cardiovascular adverse events in three patient groups

The overall incidence of cardiovascular adverse events was 25.00% in the control group, 5.00% in study group 1, and 15.00% in study group 2, with statistically significant differences among the groups ( $P < 0.05$ ), and the lowest

incidence observed in study group 1. (**Table 3**)

**Table 3.** Incidence of cardiovascular adverse events in three patient groups [n (%)]

Events	Control group (n = 20)	Study group 1 (n = 20)	Study group 2 (n = 20)
Acute myocardial infarction	1	0	1
Heart failure	1	0	1
Death	0	0	0
Rehospitalization	1	0	0
Total incidence (%)	5 (25.00)	1 (5.00)	3 (15.00)
t/ $\chi^2$ value		14.392	
P value		0.001	

## 4. Discussion

ACS is a critical type of cardiovascular disease, with PCI being the primary means of revascularization. However, even after successful PCI, patients still face a high risk of MACE, and lipid management is one of the core strategies for secondary prevention of ACS <sup>[7]</sup>. This study explored the impact of early initiation of intensive lipid-lowering therapy on the lipid profile control rate and MACE in patients with ACS undergoing PCI.

This study found that an intensive lipid-lowering regimen initiated early with PCSK9 inhibitors demonstrated optimal efficacy in improving liver and kidney function, aligning with the “lower is better” lipid-lowering strategy recommended by multiple international guidelines (e.g., ESC 2021, ACC/AHA 2018). The theoretical basis for early intervention lies in the fact that during the acute phase of ACS, inflammatory responses are heightened, and plaque vulnerability increases. Early reduction and improvement of liver and kidney function can reduce the volume of the lipid core and stabilize plaque structure. Additionally, early intensive lipid lowering may slow the progression of atherosclerosis by inhibiting oxidative stress and endothelial dysfunction.

Another significant finding of this study is that there were no significant differences in baseline indicators (including ApoA, TC, TG, HDL-C, LDL-C, Lp(a), and ApoB) among the three groups of patients before treatment ( $P > 0.05$ ). After one month, three months, and six months of treatment, all indicators in study group 1 and study group 2 showed significant improvements compared to the control group ( $P < 0.05$ ), with study group 1 demonstrating particularly pronounced improvements ( $P < 0.05$ ). Furthermore, the incidence of MACE was significantly lower in the early intensive lipid-lowering group. These results are consistent with the conclusions of large-scale clinical trials conducted by Hirai and Yoshikawa *et al.*, which suggest possible mechanisms including stabilizing vulnerable plaques and reducing the risk of plaque rupture; improving endothelial function and reducing the tendency for thrombosis; and inhibiting inflammatory responses to slow the progression of atherosclerosis <sup>[8,9]</sup>.

It is noteworthy that the early intensive lipid-lowering group included in this study received PCSK9 inhibitor treatment immediately after PCI, whereas the control group mostly adopted a stepwise adjustment strategy. This may lead to differences in lipid control between the two groups manifesting in the short term, thereby affecting the incidence of MACE. In recent years, the widespread application of PCSK9 inhibitors has further enhanced lipid-lowering efficacy without increasing the risk of muscle or liver toxicity associated with statins <sup>[10]</sup>. Therefore, for high-risk PCI patients with acute coronary syndrome, an early combined lipid-lowering strategy (e.g., statins + ezetimibe + PCSK9 inhibitors) may represent a safe and effective option.

## 5. Conclusion

In summary, early initiation of intensive lipid-lowering therapy can significantly improve the rate of achieving lipid targets in patients with ACS undergoing PCI and reduce the risk of MACE, while demonstrating good safety. This strategy aligns with the current guideline-recommended concept of “early intervention and intensive management,” holding significant clinical importance for improving the prognosis of ACS patients. In the future, it is necessary to further optimize individualized lipid-lowering regimens to enhance treatment accessibility and long-term efficacy.

## Disclosure statement

The authors declare no conflict of interest.

## References

- [1] Atwood J, 2022, Management of Acute Coronary Syndrome. *Emerg Med Clin North Am*, 40(4): 693–706.
- [2] Faro D, Laudani C, Agnello F, et al., 2023, Complete Percutaneous Coronary Revascularization in Acute Coronary Syndromes With Multivessel Coronary Disease: A Systematic Review. *JACC Cardiovasc Interv*, 16(19): 2347–2364.
- [3] Pogran E, Burger A, Zweiker D, et al., Lipid-Lowering Therapy after Acute Coronary Syndrome. *J Clin Med*, 13(7): 2043.
- [4] Wu X, Ye Y, Liu X, et al., 2024, Benefits of Intensive Lipid-Lowering Therapies in Patients with Acute Coronary Syndrome: A Systematic Review and Meta-Analysis. *Ann Med*, 56(1): 2389470.
- [5] Lewek J, Niedziela J, Desperak P, et al., 2023, Intensive Statin Therapy Versus Upfront Combination Therapy of Statin and Ezetimibe in Patients With Acute Coronary Syndrome: A Propensity Score Matching Analysis Based on the PL-ACS Data. *J Am Heart Assoc*, 12(18): e030414.
- [6] Okada K, Haze T, Kikuchi S, et al., 2024, Early, Intensive and Persistent Lipid-Lowering Therapy for Secondary Prevention of Acute Coronary Syndrome. *J Atheroscler Thromb*, 31(12): 1748–1762.
- [7] Iannuzzo G, Gentile M, Bresciani A, et al., 2021, Inhibitors of Protein Convertase Subtilisin/Kexin 9 (PCSK9) and Acute Coronary Syndrome (ACS): The State-of-the-Art. *J Clin Med*, 10(7): 1510.
- [8] Hirai K, Kawasaki T, Soejima T, et al., 2023, Impact of Intensive Low-Density Lipoprotein Cholesterol-Lowering Therapy on Coronary Artery Plaques in Acute Coronary Syndrome. *Am J Cardiol*, 2023(204): 84–91.
- [9] Yoshikawa M, Honda A, Arashi H, et al., 2024, Addition of Ezetimibe to Intensive Lipid-Lowering Therapy Is Associated With a Lower Incidence of Heart Failure in Patients With Acute Coronary Syndrome. *Circ J*, 88(11): 1819–1824.
- [10] Ferri N, Ruscica M, Lupo M, et al., 2022, Pharmacological Rationale for the Very Early Treatment of Acute Coronary Syndrome with Monoclonal Antibodies Anti-PCSK9. *Pharmacol Res*, 2022(184): 106439.

### Publisher's note

Bio-Byword Scientific Publishing remains neutral with regard to jurisdictional claims in published maps and institutional affiliations.



# The Clinical Effect of Xuesaitong in the Treatment of Coronary Heart Disease and its Influence on the Hemorheology of Patients

Dejia Hu, Jihai Fan, Wei Gui, Zhen Li, Peng Zhao, Xianlei Deng, Chenran Guo, Lingui Xu

Department of Cardiovascular Medicine, BOE Suzhou Hospital, Suzhou 215000, Jiangsu, China

*\*Author to whom correspondence should be addressed.*

**Copyright:** © 2025 Author(s). This is an open-access article distributed under the terms of the Creative Commons Attribution License (CC BY 4.0), permitting distribution and reproduction in any medium, provided the original work is cited.

**Abstract:** *Objective:* To explore the therapeutic effect of Xuesaitong on patients with coronary heart disease and its influence on their hemorheology. *Methods:* A total of 80 patients with coronary heart disease were included as observation samples. All of them received treatment in our hospital from January 2024 to January 2025. They were divided into the control group (n = 40, conventional treatment) and the observation group (n = 40, conventional treatment + Xuesaitong treatment) by lottery. The clinical efficacy was analyzed. *Result:* The therapeutic effect and the improvement of hemorheology in the observation group were both better than those in the control group, and the comparisons were statistically significant ( $P < 0.05$ ). *Conclusion:* The treatment effect of Xuesaitong on patients with coronary heart disease is remarkable, and it is worthy of clinical promotion and application.

**Keywords:** Xuesaitong; Coronary heart disease; Clinical effect; Hemorheology

**Online publication:** December 31, 2025

## 1. Introduction

Coronary heart disease is a common and frequently-occurring disease in the clinical cardiovascular system. Clinically, it is mainly characterized by angina pectoris, chest tightness, and shortness of breath after activity. Its pathological mechanism is related to vascular endothelial injury, lipid metabolism disorders, platelet aggregation, and abnormal hemorheology, etc. <sup>[1]</sup> For this disease, clinical treatment mainly focuses on symptomatic therapy. Although it can delay the progression of the disease to a certain extent, some patients have problems such as poor disease control and insignificant improvement in hemorheological indicators, which affect their prognosis <sup>[2]</sup>. Traditional Chinese medicine has unique insights in treating such diseases, and Xuesaitong is a commonly used Chinese patent medicine in clinical practice. Based on this, this study will conduct an in-depth analysis of the therapeutic effect of Xuesaitong on patients with coronary heart disease and its impact on their hemorheology.

## 2. Materials and methods

### 2.1. Research data

A total of 80 patients with coronary heart disease admitted to our hospital from January 2024 to January 2025 were included as observation samples. They were divided into two groups by lottery, with 40 cases in each group. In the control group, there were 22 males and 18 females. The age ranged from 45 to 75 years old, with an average of  $(62.34 \pm 5.18)$  years old. In the observation group, there were 23 males and 17 females. The age ranged from 46 to 74 years old, with an average of  $(61.82 \pm 6.01)$  years old. Comparison of general data between the two groups ( $P > 0.05$ ). This research does not violate national laws and regulations and complies with medical ethics principles.

The inclusion criteria are as follows:

- (1) Diagnosed with coronary heart disease through examinations such as CCTA and CAG;
- (2) Clear consciousness and normal cognitive function;
- (3) The patient and their family members are fully informed and voluntarily sign the informed consent form.

The exclusion criteria are as follows:

- (1) Complicated with severe cardiovascular complications such as acute myocardial infarction and severe heart failure;
- (2) Combined with serious underlying diseases such as malignant tumors and severe infections;
- (3) Patients with mental disorders or cognitive dysfunction.

### 2.2. Methods

#### 2.2.1. Control group

The control group received conventional treatment, mainly symptomatic treatment, such as lifestyle intervention, antiplatelet therapy, lipid regulation to stabilize plaques, and improvement of myocardial blood supply, etc.

#### 2.2.2. Observation group

The observation group was additionally treated with Xuesaitong (produced by: Bikang Pharmaceutical Xinyi Group Holding Co., LTD.; National Drug Approval Number: Z32020673). Xuesaitong injection was administered at a dose of 300 mg, diluted in 250 mL of 5% glucose solution. The diluted solution was delivered via intravenous infusion at a controlled rate of 40–60 drops per minute, once daily. Treatment was continued for a duration of two weeks in both groups.

### 2.3. Observation indicators

#### 2.3.1. Therapeutic effect

Clinical symptoms were significantly relieved or disappear, daily activity endurance was significantly enhanced, and the myocardial ischemia manifestations shown on the electrocardiogram are significantly improved or return to normal. Clinical symptoms have been alleviated, the frequency and severity of attacks have decreased, the endurance for daily activities has improved, and the electrocardiogram shows that the manifestations of myocardial ischemia have improved. Clinical symptoms do not improve or even worsen; daily activity endurance does not improve or decreases; electrocardiogram shows no improvement or deterioration in myocardial ischemia manifestations. The total effective rate = (number of markedly effective cases + number of effective cases)/total number of cases  $\times 100\%$ .

#### 2.3.2. Hemorheology



Changes in the high shear (high cut-off) whole blood viscosity, low shear (low cut-off) whole blood viscosity, and plasma viscosity ratio were analyzed.

## 2.4. Statistical methods

Data were processed using SPSS24.0 software. Measurement data were expressed as mean  $\pm$  SD and the t-test was applied. The comparison of count data rates was conducted using the  $\chi^2$  test. A  $P$  value  $< 0.05$  was considered statistically significant.

## 3. Results

### 3.1. Therapeutic effect

The therapeutic effect of the observation group was better than that of the control group ( $P < 0.05$ ) (Table 1).

**Table 1.** Therapeutic effect (n, %)

Group	n	Show effect	Effective	Invalid	Total effective rate
Observation group	40	28	11	1	97.50%
Control group	40	19	14	7	82.50%
$\chi^2$	-	-	-	-	5.000
P	-	-	-	-	0.025

### 3.2. Hemorheology

At the baseline period, the comparison of hemorheology between the two groups ( $P > 0.05$ ). After treatment, compared with the control group, the hemorheology of the observation group was better ( $P < 0.05$ ) (Table 2).

**Table 2.** Hemorheology (mean  $\pm$  SD, mPa·s)

Group	n	High cut-off value of whole blood viscosity		Low cut-off value of whole blood viscosity		Plasma viscosity ratio	
		Before treatment	After treatment	Before treatment	After treatment	Before treatment	After treatment
Observation group	40	6.85 $\pm$ 0.52	5.23 $\pm$ 0.41	9.76 $\pm$ 0.83	7.32 $\pm$ 0.65	1.92 $\pm$ 0.13	1.65 $\pm$ 0.09
Control group	40	6.82 $\pm$ 0.55	5.98 $\pm$ 0.43	9.73 $\pm$ 0.81	8.56 $\pm$ 0.72	1.91 $\pm$ 0.12	1.78 $\pm$ 0.10
t	-	0.251	7.984	0.164	8.085	0.357	6.111
P	-	0.803	0.000	0.871	0.000	0.722	0.000

## 4. Discussion

In traditional Chinese medicine, coronary heart disease is classified under the categories of “chest obstruction” and “heart pain”. The core of its onset lies in the obstruction of the heart meridian. Although the location of the disease is in the heart, it is closely related to the dysfunction of the liver, spleen and kidney [3]. The pathological essence of this disease is “deficiency at the root and excess at the symptoms”. Improper diet leading to the internal generation of phlegm and dampness, emotional imbalance causing Qi stagnation and blood stasis, internal invasion of cold

pathogenic factors blocking the heart meridian, and old age and physical weakness resulting in deficiency of the heart and kidneys can all cause obstruction of the heart meridian, leading to chest pain <sup>[4]</sup>. The core of traditional Chinese medicine in treating coronary heart disease emphasizes syndrome differentiation and treatment, as well as addressing both the symptoms and root causes. During the treatment process, it is necessary to focus on overall conditioning rather than merely addressing local symptoms. Personalized treatment plans should be formulated for patients by analyzing the differences in their syndrome types <sup>[5]</sup>. For instance, for “inherent deficiency”, it is necessary to tonify Qi, nourish Yin and warm Yang to support the body’s vital energy and restore the functions of the internal organs. For “symptomatic excess”, methods such as promoting blood circulation and removing blood stasis, resolving phlegm and dispersing nodules, regulating Qi and relieving pain, and warming Yang and dispelling cold are used to eliminate pathogenic factors and unblock the heart meridians <sup>[6]</sup>. At the same time, traditional Chinese medicine emphasizes supporting the body’s vital energy without assisting pathogenic factors and eliminating pathogenic factors without harming the body’s vital energy. It not only improves the operating environment of the heart meridian by regulating Qi and blood and balancing the internal organs, but also pays attention to avoiding the bias of a single treatment method <sup>[7]</sup>.

The Xuesaitong injection used in this study is a commonly used traditional Chinese medicine injection in clinical practice. Its core component is the total saponins of *Panax notoginseng* extracted and purified from the dried roots and rhizomes of *Panax notoginseng* from the Araliaceae family. The effective components include ginsenoside Rg1, ginsenoside Rb1, and *Panax notoside* R1, etc. <sup>[8]</sup> The research shows that the therapeutic effect of the observation group is better than that of the control group ( $P < 0.05$ ). The core component of Xuesaitong is total saponins from *Panax notoginseng*. It inherits the nature of *Panax notoginseng*, which is “sweet, warm, slightly bitter and enters the liver and heart meridians”. During the treatment process, it can closely focus on the core pathogenesis of coronary heart disease patients, which is characterized by blood stasis in the heart vessels and deficiency of the root and excess of the symptoms <sup>[9]</sup>. This medicine has the effect of promoting the circulation of Qi and blood and unblocking the blood vessels. It can directly disperse the stasis and turbidity in the coronary blood vessels, quickly relieve angina pectoris and chest tightness, and improve the problem of “pain due to obstruction” in patients <sup>[10]</sup>. At the same time, Xuesaitong also has the effect of tonifying Qi and nourishing the heart. It can replenish heart Yang, enrich heart blood, improve the deficiency of heart muscle nourishment and insufficient motility caused by heart Qi deficiency, and reduce shortness of breath and fatigue caused by “lack of nourishment leads to pain” <sup>[11]</sup>. From the perspective of Western medicine, the total saponins of *Panax notoginseng* in Xuesaitong can play a role from different angles. Among them, ginsenoside Rg1 can activate vascular endothelial nitric oxide synthase to promote the release of nitric oxide and dilate coronary arteries to increase myocardial blood supply <sup>[12]</sup>. Ginsenoside Rb1 can protect myocardial mitochondrial function, inhibit apoptosis to enhance myocardial hypoxia tolerance, and at the same time regulate sympathetic nerve balance to reduce myocardial oxygen consumption, thereby improving the clinical symptoms of patients and enhancing the therapeutic effect.

The research also showed that compared with the control group, the improvement degree of hemorheology in the observation group was better ( $P < 0.05$ ). Xuesaitong can regulate the rhythm of Qi and blood circulation in patients, change the vicious cycle of blood stagnation leading to blood stasis and stasis aggravating stagnation, improve the thick and viscous state of blood as a whole, and optimize hemorheological indicators <sup>[13]</sup>. During the treatment process, total saponins of *Panax notoginseng* inhibit the release of platelet-activating factors and their binding to receptors, reduce the expression of adhesion molecules on the platelet surface, significantly suppress

the platelet aggregation rate, decrease the risk of microthrombosis formation, and prevent the increase of blood “aggregation”<sup>[14]</sup>. At the same time, it can enhance the fluidity and deformability of red blood cell membranes, reduce hematocrit, and decrease the electrostatic adhesion between red blood cells, thereby improving the high and low shear viscosities of whole blood<sup>[15]</sup>. In addition, total saponins of *Panax notoginseng* can also regulate the metabolism of macromolecular substances such as fibrinogen and lipoprotein in plasma, reduce the colloid osmotic pressure of plasma, and decrease the viscosity of plasma.

## 5. Conclusion

In conclusion, the application of Xuesaitong in the treatment of coronary heart disease has a remarkable effect, can effectively improve the hemorheology of patients, and has clinical promotion and application value.

## Disclosure statement

The authors declare no conflict of interest.

## References

- [1] Wu J, Fu P, Wang Y, 2025, Clinical Study on Xuesaitong Soft Capsules Combined with Aspirin in the Treatment of Coronary Heart Disease in the Elderly. *Modern Medicine and Clinical Practice*, 40(7): 1711–1715.
- [2] Zhang R, 2023, Observation on the Therapeutic Effect of Xuesaitong Combined with Atorvastatin in the Treatment of Unstable Angina Pectoris of Coronary Heart Disease. *Smart Health*, 9(14): 251–254.
- [3] Dong Z, Han S, Lin L, et al. Comprehensive Evaluation Study of Xuesaitong Soft Capsules. *Chinese Journal of Clinical Pharmacology*, 37(12): 1612–1624.
- [4] Li X, Li H, Han L, et al., 2023, Research Progress on the Clinical Efficacy and Safety of Xuesaitong Injection. *China Prescription Drugs*, 21(11): 178–182.
- [5] Xu C, 2023, Therapeutic Effects of Xuesaitong Injection and Compound Danshen Drop Pills on Angina Pectoris of Coronary Heart Disease. *Electronic Journal of Cardiovascular Diseases in Integrated Traditional Chinese and Western Medicine*, 11(27): 25–27.
- [6] Zhang X, Ma X, Chen X, 2023, The Effect of Xuesaitong Freeze-Dried Powder Injection combined with Betaloc on the Frequency, Duration and Cardiac Function of Angina Pectoris Attacks in Emergency Patients with Coronary Heart Disease and Angina Pectoris. *Baotou Medical Journal*, 47(3): 19–21.
- [7] Jia M, Liang X, Fu G, et al., 2023, Prince Li Xian? Expert Consensus on the Clinical Application of Xuesaitong Soft Capsules. *Chinese Journal of Traditional Chinese Medicine*, 48 (20): 5668–5674.
- [8] Li G, 2021, Evaluation of the Clinical Effect of Xuesaitong Injection in the Treatment of Coronary Heart Disease. *Medical Frontiers*, 11(9): 41–42.
- [9] Chen J, 2021, Effects of Xuesaitong Combined with Dipyridamole on Hemorheological Index Levels and the Frequency of Angina pectoris Attacks in Patients with Coronary Heart Disease. *Chinese Journal of Minkang Medicine*, 33(6): 94-96.
- [10] Cai Y, 2023, The Effect of Xuesaitong as an Adjuvant Therapy on Patients with Coronary Heart Disease and its Influence on Hemorheology. *Electronic Journal of Integrated Traditional Chinese and Western Medicine on Cardiovascular Diseases*, 11(1): 40–42.

- [11] Li H, Wang N, Huang B, 2022, Observation on the Therapeutic Effect of Xuesaitong Soft Capsules in the Treatment of Exertional Angina Pectoris. *Chinese Journal of Modern Pharmaceutical Application*, 16(20): 6–9.
- [12] Liu K, Shen F, 2022, Evaluation of the Intervention Effect of Xuesaitong Soft Capsules in Coronary Atherosclerotic Plaques. *Chinese Journal of Modern Drug Application*, 16(16): 126–128.
- [13] Dong Y, Chen H, Liu Y, et al., 2020, Clinical Study on the Intervention of Xuesaitong Soft Capsules in the IncR CTB114C7.4-miR3656-BCL2A1 Regulatory Network in Patients with Coronary Heart Disease and Blood Stasis Syndrome. *World Science and Technology: Modernization of Traditional Chinese Medicine*, 22(11): 3846–3852.
- [14] Zhang C, Peng Y, Wu H, 2022, The Influence of Xuesaitong on Serum Homocysteine and other Substances in Patients with Angina Pectoris after Interventional Therapy. *Northwest Journal of Pharmacy*, 37(2): 154–158.
- [15] Liang M, 2021, The Efficacy of metoprolol Combined with Xuesaitong Injection in the Treatment of Coronary Heart Disease and Heart Failure and Its Impact on patients' Blood Rheology and Cardiac Function. *Smart Health*, 7(27): 169–171.

**Publisher's note**

Bio-Byword Scientific Publishing remains neutral with regard to jurisdictional claims in published maps and institutional affiliations.

# Clinical Application of PCSK9 Inhibitor in Tumor Therapy

Wenjie Lu<sup>1</sup>, Lusha E<sup>2\*</sup>

<sup>1</sup>Baotou Medical College, Inner Mongolia University of Science & Technology, Baotou 014000, Inner Mongolia Autonomous Region, China

<sup>2</sup>Inner Mongolia Clinical Medical College, Hohhot 010000, Inner Mongolia Autonomous Region, China

*\*Corresponding author: Lusha E, elusha2008@126.com*

**Copyright:** © 2025 Author(s). This is an open-access article distributed under the terms of the Creative Commons Attribution License (CC BY 4.0), permitting distribution and reproduction in any medium, provided the original work is cited.

**Abstract:** Proprotein Convertase Subtilisin/Kexin Type 9 (PCSK9), a key protein secreted by the liver, initially emerged as a research focus in the cardiovascular field due to its central role in regulating lipid metabolism. With the deepening of research, the functional scope of PCSK9 and its inhibitors has continued to expand. They not only demonstrate remarkable efficacy in lipid management and the prevention/treatment of atherosclerotic cardiovascular disease (ASCVD) but also show enormous potential value in cancer prevention and control. Beyond indirectly regulating tumor progression by modulating lipid and inflammatory metabolism, PCSK9 may also exert direct effects on tumorigenesis and progression by participating in tumor cell proliferation, apoptosis signaling pathways, and immune regulation (e.g., influencing the expression of LDLR-related molecules on the surface of immune cells). However, no unified consensus has been reached in existing mechanistic studies. Regarding clinical evidence, there is heterogeneity among the results of multiple cohort studies and clinical trials. Some studies indicate that PCSK9 inhibitors do not significantly increase cancer risk or cancer-related mortality, and even some data suggest potential protective effects against specific types of tumors. Conversely, a small number of studies imply that long-term use may be associated with a slight elevation in the risk of certain cancers. Such discrepancies may stem from heterogeneity in sample size, follow-up duration, tumor types, and baseline characteristics of the study populations. Based on a review of numerous relevant studies, this article concludes that PCSK9 inhibitors may become a key therapeutic agent for cancer treatment in the future.

**Keywords:** PCSK9 inhibitors; Blood lipids; Tumors; Targeted therapy

**Online publication:** December 31, 2025

## 1. Introduction

Cancer has become a global health crisis. Despite continuous medical advancements, it remains the second leading cause of death worldwide, but is projected to become the primary cause by 2060 (with approximately 18.63 million deaths). The disease continues to rise globally, exacerbating the healthcare burden. In countries at the top quintile of socioeconomic development, cancer has surpassed cardiovascular diseases as the second leading cause



of death <sup>[1]</sup>. It is also a major contributor to disability-adjusted life years (DALYs). PCSK9 has evolved from a cholesterol-regulating factor into a pivotal node bridging metabolism and immunity, demonstrating significant research and clinical potential in oncology. PCSK9 regulates multiple proteins and signaling pathways in cancer, including JNK, NF-κB, and mitochondria-mediated apoptosis. Current evidence supports PCSK9 inhibitors as a potential strategy to reduce tumor risk and enhance immunotherapy efficacy, particularly in specific cancers such as breast, gastric and pancreatic cancers.

## **2. Exploring the role and mechanism of PCSK9 inhibitors in tumor prevention and control**

### **2.1. Targeted regulation of digestive tract tumors**

#### **2.1.1. Stomach cancer, esophageal cancer**

PCSK9 is closely associated with lipid levels, and its relationship with gastric cancer is equally significant. HDL-C serves as an independent risk factor for gastric cancer <sup>[2]</sup>. The study by Ghahremanfard *et al.* explicitly states that “serum lipid profile testing holds significant value in cancer progression,” emphasizing that lipid profiles are not merely indicators of cardiovascular health but are also associated with the development of cancer <sup>[3]</sup>. Furthermore, basic research has demonstrated that PCSK9 gene and protein expression levels in gastric cancer tissues are significantly higher than in adjacent normal tissues, with expression increasing as the tumor progresses. These findings further confirm the association between PCSK9 and gastric cancer pathogenesis. Zoltan *et al.* demonstrated that assessing PCSK9 levels in elderly cancer patients enables risk stratification, where those with elevated expression may require intensified therapies (e.g., enhanced chemotherapy or immunotherapy) and closer survival monitoring <sup>[4]</sup>.

Moreover, PCSK9 could serve as a cross-disease therapeutic target, targeting elderly patients with high PCSK9 levels, PCSK9 inhibitors may simultaneously improve lipid profiles, reduce inflammation, and indirectly enhance survival outcomes. Innovative Mendelian randomization (MR) studies targeting drug targets by Ding *et al.* have demonstrated a significant association between PCSK9 inhibitors and protective effects against gastric cancer (GC) <sup>[5]</sup>. Genetically, this evidence confirms that long-term use of statins, PCSK9 inhibitors, and other mainstream lipid-lowering drugs does not increase overall or specific cancer risks. It alleviates concerns among clinicians and patients about ‘carcinogenicity of lipid-lowering drugs,’ providing safety evidence for long-term lipid-lowering therapy in high-risk populations, such as cardiovascular disease patients.

Xu *et al.*’s fundamental mechanism study, validated by cell experiments and animal models, elucidates the core molecular mechanism of GC development: “PCSK9 activates the MAPK signaling pathway by upregulating HSP70 (heat shock protein 70), thereby promoting GC cell metastasis and inhibiting apoptosis” <sup>[6]</sup>. This discovery provides a novel potential target for targeted therapy of GC. Simultaneously, esophageal cancer research has never stopped progressing. Researchers have for the first time revealed a close association between serum anti-PCSK9 antibody levels and postoperative prognosis in esophageal cancer patients. Specifically, higher antibody levels correlate with longer patient survival. This discovery provides a new research direction for clinical prognostic stratification and individualized management <sup>[7]</sup>.

As mentioned above, the authors suggest that PCSK9 is directly involved in the progression of gastric cancer and may also indirectly influence it by regulating lipid metabolism. Therefore, PCSK9 inhibitors could suppress gastric cancer development through these dual mechanisms. However, the current understanding of its role in esophageal cancer remains unclear and requires further investigation to confirm.



### 2.1.2. Hepatocellular carcinoma

The mechanism of PCSK9 in hepatocellular carcinoma (HCC) has been preliminarily elucidated, where PCSK9 expression levels in HCC tissues are significantly lower than in adjacent normal tissues. *In vitro* experiments demonstrated that PCSK9 inhibits the Jun N-terminus kinase (JNK) signaling pathway by binding to glutathione S-transferase Pi1 (GSTP1), thereby suppressing HCC cell growth<sup>[8]</sup>. This discovery reveals the anticancer role of PCSK9 in HCC, providing a new molecular mechanism basis for targeted therapy of HCC. Alannan *et al.*'s data analysis reveals that PCSK9 serves as a cross-regulatory node between lipid metabolism and tumor immunity in HCC, suggesting it may function as a potential prognostic biomarker and therapeutic target<sup>[9]</sup>. This finding was reported by Jin *et al.*, the groundbreaking foundational research on drug repositioning and combination therapy for HCC has been successfully completed<sup>[10]</sup>. The core findings demonstrate that the established drug Flubendazole can significantly inhibit HCC progression through PCSK9-dependent inhibition, while enhancing the efficacy of first-line targeted therapy Lenvatinib and reducing its toxic side effects.

This provides a cost-effective and easily translatable new strategy for HCC treatment. For patients with HCC, particularly those intolerant to Lenvatinib, it offers a “cost-effective, low-toxicity, and highly efficient” combination therapy regimen. Moreover, Flubendazole's oral administration ensures high patient compliance. Additionally, in Xu *et al.*'s innovative basic research on enhancing immunotherapy sensitivity in liver cancer, PCSK9 was found to mediate immune evasion through dual mechanisms: inhibiting T cell function and upregulating PD-L1<sup>[11]</sup>. Inhibition of PCSK9 blocks both pathways simultaneously. Directly blocking PCSK9 prevents T cell binding, restoring T cell cytotoxicity, while indirectly downregulating PD-L1 enhances antibody efficacy, creating a ‘dual sensitization’ effect. Thus, the absence of PCSK9 is not entirely beneficial to the organism, as noted by Ioannou *et al.* the PCSK9 gene knockout (KO) mouse model demonstrates that PCSK9 deficiency exacerbates non-alcoholic steatohepatitis (NASH) by promoting hepatic cholesterol accumulation and accelerates HCC development<sup>[12]</sup>.

This finding overturns the previous notion that “PCSK9 inhibition is exclusively beneficial” and provides critical safety evidence for clinical use of PCSK9 inhibitors. The study reveals PCSK9's dual role in liver diseases, while prior research focused on its lipid-lowering and cardiovascular protective effects, this investigation confirms that “in metabolic disorders (e.g., NASH), PCSK9 deficiency/inhibition may promote hepatic lesions through cholesterol accumulation.” This paradigm shift challenges the single-benefit hypothesis and offers essential guidance for clinical application: Patients with concurrent NASH or high hepatic cholesterol risk should undergo regular monitoring of liver cholesterol levels and NASH progression to avoid indiscriminate use of PCSK9 inhibitors.

### 2.1.3. PDAC: Proprotein convertase

PCSK9 is primarily synthesized and secreted by hepatocytes, with minor production and release from the kidneys, pancreas, intestines, and adipose tissue. Its core mechanism involves binding to low-density lipoprotein (LDL) receptors, thereby blocking their recycling process and ultimately leading to elevated blood LDL-C levels, which induces dyslipidemia<sup>[13]</sup>. It indicates a positive correlation between PCSK9 levels and the severity of HTGP. PCSK9 serves as a biomarker for predicting liver and lung colonization. Elevated PCSK9 levels direct liver-preferring cells toward lung colonization, whereas PCSK9 knockout redirects lung-preferring cells to liver colonization, thereby establishing PCSK9's necessity and sufficiency for secondary organ site preference<sup>[14]</sup>.

#### 2.1.4. Control and management of colorectal tumors

APC and KRAS are the two most critical driver mutations in colorectal cancer (CRC). They often work in concert, with APC driving the initiation phase and KRAS the progression phase, jointly driving tumor development, proliferation, drug resistance, and metastasis. These mutations are key targets for molecular subtyping and clinical treatment decisions in this disease. In a cohort of CRC patients, researchers studied isogenic cell lines and transgenic mice <sup>[15]</sup>. We established that APC/KRAS mutant CRC induces de novo cholesterol biosynthesis, accompanied by elevated geranylgeranyl-1,2-diphosphate (GGPP), a metabolite essential for KRAS activation. PCSK9, a top-upregulated cholesterol-related gene, demonstrates that depletion of PCSK9 inhibits APC/KRAS mutant CRC cell growth *in vitro* and *in vivo*, whereas overexpression of PCSK9 induces tumorigenesis. Here, the results indicate that PCSK9 promotes APC/KRAS mutant CRC and is a therapeutic target <sup>[15]</sup>. Our data collectively demonstrate that PCSK9 is a carcinogen in APC/KRAS mutant CRC. PCSK9 inhibitors inhibit the growth of APC/KRAS mutant CRC *in vitro* and *in vivo*.

Multidimensional translational studies combining cell experiments, animal models, and human colon cancer samples by Porcheron *et al.* conclusively demonstrate that either single or combined silencing of PCSK7/PCSK9 (proprotein convertase family members) significantly inhibits colon cancer metastasis by enhancing T cell cytotoxicity <sup>[16]</sup>. The dual-silencing approach outperforms single-silencing, providing a novel strategy for immunotherapy targeting advanced metastatic colon cancer. In conclusion, PCSK9 inhibitors can not only directly inhibit colorectal tumors through signaling pathways but also enhance the efficacy of PD-1 inhibitors as adjuvant therapy.

#### 2.2. Exploration of the correlation of breast cancer

Research data confirms that metabolic syndrome is a key risk factor for breast cancer, with lipid levels showing a significant correlation to disease risk <sup>[17–19]</sup>. Cholesterol and its metabolites not only provide “energy or raw materials” for tumor cells, but also actively participate in breast cancer pathophysiology by activating oncogenic signaling pathways and modulating hormone receptor activity. These compounds thus function as “active regulatory factors” in cancer progression, rather than mere “passive nutrients.” Kitahara *et al.*’s study has found that high total cholesterol ( $\geq 240$  mg/dl) is significantly positively associated with the risk of prostate cancer in men (HR = 1.24, 95% CI: 1.07–1.44), colon cancer (HR = 1.12, 95% CI: 1.00–1.25), and breast cancer in women (HR = 1.17, 95% CI: 1.03–1.33), with a clear dose-response trend <sup>[20]</sup>. Clinical testing has revealed that serum PCSK9 levels in breast cancer patients are significantly higher than in healthy individuals, and patients have elevated TC and LDL-C levels, as well as reduced HDL-C levels <sup>[21]</sup>. This correlation suggests that PCSK9 may influence breast cancer development by regulating lipid metabolism or directly modulating the tumor microenvironment. Although direct evidence for PCSK9 inhibitors in breast cancer treatment remains limited, the combined measurement of serum PCSK9 and lipid profiles has been validated as a valuable tool for early screening, diagnosis, and precision therapy and lay the foundation for follow-up intervention studies <sup>[21]</sup>.

A study published by Wenbin *et al.* revealed that a common lineage mutation in the PCSK9 gene (rs562556, V474I) promotes breast cancer metastasis by targeting low-density lipoprotein receptor-related protein 1 (LRP1) <sup>[22]</sup>. This provides the first direct evidence of genetic susceptibility to breast cancer metastasis and suggests that anti-PCSK9 therapies could become a novel strategy for prevention. By integrating human genetics, functional experiments, and mechanism analysis, the study elucidated the molecular mechanism by which PCSK9 V474I mutation promotes metastasis through LRP1 degradation and validated the preclinical

efficacy of anti-PCSK9 therapies. These findings not only offer a new genetic explanation for breast cancer metastasis but also pave the way for developing precision therapies to “prevent metastatic cancer.” Future large-scale clinical trials are needed to verify the safety and effectiveness of this strategy, as well as to explore synergistic effects with other targeted drugs (such as EMT inhibitors)<sup>[23]</sup>. A chimeric virus-like particle (cVLP) vaccine targeting PCSK9 was developed and validated in a preclinical HER2-positive breast cancer model for its efficacy when combined with the cVLP-HER2 vaccine. The results demonstrated that this combination strategy significantly enhanced anti-tumor immune responses, inhibited tumor growth, and prolonged survival. The core mechanism involves improving the tumor immune microenvironment through PCSK9 targeting, providing a novel combination approach for HER2-positive breast cancer immunotherapy. This highlights the pivotal role of PCSK9 inhibitors in breast cancer treatment, underscoring the continued importance of advancing research in this field.

### **3. The effect of PCSK9 on tumor**

Foreign research studies confirm that PCSK9 mediates tumor cell proliferation, invasion, and migration by regulating EMT (epithelial-mesenchymal transition) and the PI3K/Akt signaling pathway<sup>[24]</sup>. Indirectly, PCSK9 inhibitors, novel lipid-lowering agents, may influence tumors through lipid metabolism. Hyperlipidemia accelerates tumor development by promoting inflammation, oxidative stress, and angiogenesis, while tumor cells elevate lipid levels by remodeling lipid metabolism to meet their energy demands<sup>[25]</sup>. The efficacy of lipid-lowering drugs in tumor prevention and control varies. PCSK9 inhibitors demonstrate non-lipid-lowering anticancer effects (e.g., in GC prevention), overcoming the limitations of conventional lipid-lowering drugs and providing a new research direction for the interdisciplinary field of ‘blood lipids-tumor’<sup>[25]</sup>.

### **4. Conclusion**

PCSK9 inhibitors are currently primarily used to lower blood lipids, though their efficacy in treating various cancers remains under investigation. Most of their mechanisms are still unclear, necessitating further data collection to elucidate these pathways and enhance cancer treatment strategies. This development offers a promising approach for patients undergoing prolonged radiotherapy, chemotherapy, or surgery. However, due to the relatively short market availability of PCSK9 inhibitors, adverse reaction data remain limited. Clinical evidence for their use in pregnant women, nursing mothers, and patients with severe hepatic or renal impairment is insufficient and requires further validation. In other disease treatments involving inflammation and lipid management, PCSK9 inhibitors show significant relevance to conditions like osteoarthritis and organ transplantation. For our rapidly evolving society, whether PCSK9 inhibitors will bring benefits or challenges to cancer patients remains to be seen. Future research should focus on large-scale, multicenter clinical studies to thoroughly explore the mechanisms and long-term effects of PCSK9 inhibitors across multiple therapeutic areas, facilitating their transition from basic research to clinical application and providing comprehensive solutions for multidisciplinary disease management.

### **Disclosure statement**

The authors declare no conflict of interest.

## References

- [1] Collaboration GBODC, Kocarnik J, Compton K, et al., 2022, Cancer Incidence, Mortality, Years of Life Lost, Years Lived With Disability, and Disability-Adjusted Life Years for 29 Cancer Groups From 2010 to 2019: A Systematic Analysis for the Global Burden of Disease Study 2019. *JAMA Oncology*, 8(3): 420–444.
- [2] Mokmeli S, Tehrani G, Zamiri R, et al., 2016, Investigating the Frequency of the ERCC1 Gene C8092A Polymorphism in Iranian Patients with Advanced Gastric Cancer Receiving Platinum-based Chemotherapy. *Asian Pacific Journal of Cancer Prevention: APJCP*, 17(3): 1369–1372.
- [3] Ghahremanfard F, Mirmohammadkhani M, Shahnazari B, et al., 2015, The Valuable Role of Measuring Serum Lipid Profile in Cancer Progression. *Oman Medical Journal*, 30(5): 353–357.
- [4] Ungvari Z, Menyhart O, Lehoczi A, et al., 2025, PCSK9 Expression and Cancer Survival: A Prognostic Biomarker at the Intersection of Oncology and Geroscience. *GeroScience*.
- [5] Ding W, Chen L, Xia J, et al., 2024, Causal Association between Lipid-lowering Drugs and Cancers: A Drug Target Mendelian Randomization Study. *Medicine*, 103(18): e38010.
- [6] Xu B, Li S, Fang Y, et al., 2020, Proprotein Convertase Subtilisin/Kexin Type 9 Promotes Gastric Cancer Metastasis and Suppresses Apoptosis by Facilitating MAPK Signaling Pathway Through HSP70 Up-Regulation. *Frontiers in Oncology*, 2020(10): 609663.
- [7] Ito M, Hiwasa T, Oshima Y, et al., 2021, Association of Serum Anti-PCSK9 Antibody Levels with Favorable Postoperative Prognosis in Esophageal Cancer. *Frontiers in Oncology*, 2021(11): 708039.
- [8] He M, Hu J, Fang T, et al., 2021, Protein Convertase Subtilisin/Kexin Type 9 Inhibits Hepatocellular Carcinoma Growth by Interacting with GSTP1 and Suppressing the JNK Signaling Pathway. *Cancer Biology & Medicine*, 19(1): 90–103.
- [9] Alannan M, Seidah N, Merched A, 2022, PCSK9 in Liver Cancers at the Crossroads between Lipid Metabolism and Immunity. *Cells*, 11(24): 4132.
- [10] Jin W, Yu J, Su Y, et al., 2023, Drug Repurposing Flubendazole to Suppress Tumorigenicity via PCSK9-Dependent Inhibition and Potentiate Lenvatinib Therapy for Hepatocellular Carcinoma. *International Journal of Biological Sciences*, 19(7): 2270–2288.
- [11] Xu W, Hu M, Lu X, et al., 2024, Inhibition of PCSK9 Enhances the Anti-Hepatocellular Carcinoma Effects of TCR-T Cells and Anti-PD-1 Immunotherapy. *International Journal of Biological Sciences*, 20(10): 3942–3955.
- [12] Ioannou G, Lee S, Linsley P, et al., 2022, Pcsk9 Deletion Promotes Murine Nonalcoholic Steatohepatitis and Hepatic Carcinogenesis: Role of Cholesterol. *Hepatology Communications*, 6(4): 780–794.
- [13] Guo S, Xia X, Gu H, et al., 2020, Proprotein Convertase Subtilisin/Kexin-Type 9 and Lipid Metabolism. *Advances in Experimental Medicine and Biology*, 2020(1276): 137–156.
- [14] Rademaker G, Hernandez G, Seo Y, et al., 2025, PCSK9 Drives Sterol-Dependent Metastatic Organ Choice in Pancreatic Cancer. *Nature*, 643(8074): 1381–1390.
- [15] Wong C, Wu J, Ji F, et al., 2022, The Cholesterol Uptake Regulator PCSK9 Promotes and is a Therapeutic Target in APC/KRAS-Mutant Colorectal Cancer. *Nature Communications*, 13(1): 3971.
- [16] Porcheron C, Le Devehat M, Roubtsova A, 2025, Blockade of Colon Cancer Metastasis via Single and Double Silencing of PCSK7/PCSK9: Enhanced T Cells Cytotoxicity in Mouse and Human. *Journal for Immunotherapy of Cancer*, 13(6): e011364.
- [17] Baek A, Nelson E, 2016, The Contribution of Cholesterol and Its Metabolites to the Pathophysiology of Breast Cancer. *Hormones & Cancer*, 7(4): 219–228.

- [18] Garcia-Estevez L, Moreno-Bueno G, 2019, Updating the Role of Obesity and Cholesterol in Breast Cancer. *Breast Cancer Research: BCR*, 21(1): 35.
- [19] Leignadier J, Dalenc F, Poirot M, et al., 2017, Improving the Efficacy of Hormone Therapy in Breast Cancer: The Role of Cholesterol Metabolism in SERM-Mediated Autophagy, Cell Differentiation and Death. *Biochemical Pharmacology*, 2017(144): 18–28.
- [20] Kitahara C, González A, Freedman N, et al., 2011, Total Cholesterol and Cancer Risk in a Large Prospective Study in Korea. *Journal of Clinical Oncology: Official Journal of the American Society of Clinical Oncology*, 29(12): 1592–1598.
- [21] Mu Y, Hao N, 2021, Detection and Clinical Significance of Serum PCSK9 and Blood Lipids Levels in Breast Cancer Patients. *Journal of Modern Oncology*, 29(15): 2633–2635.
- [22] Mei W, Tabrizi S, Godina C, et al., 2025, A Commonly Inherited Human PCSK9 Germline Variant Drives Breast Cancer Metastasis via LRP1 Receptor. *Cell*, 188(2): 371–389.
- [23] Scalambra L, Ruzzi F, Pittino O, et al., 2025, Targeting PCSK9, through an Innovative cVLP-based Vaccine, Enhanced the Therapeutic Activity of a cVLP-HER2 Vaccine in a Preclinical Model of HER2-Positive Mammary Carcinoma. *Journal of Translational Medicine*, 23(1): 136.
- [24] Wang L, Li S, Luo H, et al., 2022, PCSK9 Promotes the Progression and Metastasis of Colon Cancer Cells through Regulation of EMT and PI3K/AKT Signaling in Tumor Cells and Phenotypic Polarization of Macrophages. *Journal of Experimental & Clinical Cancer Research: CR*, 41(1): 303.
- [25] Zhang F, Shi Z, 2022, Progress in the Research of Hyperlipidemia and Lipid-Lowering Therapy in Malignant Tumors. *Beijing Medical Journal*, 44(11): 1027–1030.

**Publisher's note**

Bio-Byword Scientific Publishing remains neutral with regard to jurisdictional claims in published maps and institutional affiliations.



# Prediction of Rapidly Progressing Coronary Plaques Using a 3D Convolutional Neural Network Model Based on Coronary CT Angiography

Wentao Zhang<sup>1</sup>, Bingcang Huang<sup>2</sup>, Weiping Lu<sup>2</sup>, Ying Wang<sup>2</sup>, Guangjie Sun<sup>1</sup>, Jiahong Xu<sup>3</sup>, Zhiru Ge<sup>3\*</sup>

<sup>1</sup>School of Gongli Hospital Medical Technology, University of Shanghai for Science and Technology, Shanghai 200093, China

<sup>2</sup>Department of Radiology, Gongli Hospital of Shanghai Pudong New Area, Shanghai 200135, China

<sup>3</sup>Department of Cardiology, Gongli Hospital of Shanghai Pudong New Area, Shanghai 200135, China

\*Author to whom correspondence should be addressed.

**Copyright:** © 2025 Author(s). This is an open-access article distributed under the terms of the Creative Commons Attribution License (CC BY 4.0), permitting distribution and reproduction in any medium, provided the original work is cited.

**Abstract:** *Objective:* To develop a three-dimensional convolutional neural network (3D-CNN) model based on coronary computed tomography angiography (CCTA) for predicting rapid plaque progression (RPP), and to compare its performance against traditional machine learning models and existing advanced methodologies. *Methods:* This retrospective study analyzed 150 patients who underwent serial CCTA examinations. Following strict alignment of CTA volume data with plaque masks, traditional machine learning models (LASSO, Elastic Net, Random Forest, XGBoost) and a lightweight 3D-CNN model were constructed. RPP was defined as an annualized plaque burden (PB) increase  $\geq 1.0\%$ . Model performance was primarily evaluated using the area under the receiver operating characteristic curve (AUC), with SHAP (SHapley Additive exPlanations) employed for model interpretation. *Results:* Traditional models demonstrated limited discriminatory ability, with AUCs ranging from 0.32 to 0.51. The developed 3D-CNN model achieved an AUC of 0.75 on the independent test set, with a sensitivity of 0.64 and a specificity of 0.88. SHAP analysis revealed that the 3D-CNN focused on internal plaque texture and Hounsfield Unit (HU) distribution patterns, whereas traditional models relied on limited features such as plaque volume. *Conclusion:* The 3D-CNN model can directly learn deep features associated with RPP from CCTA images. Its performance is significantly superior to traditional models and demonstrates potential comparable to current advanced radiomics and machine learning methods, offering a novel tool for non-invasive identification of high-risk plaques using a single time-point baseline scan.

**Keywords:** Coronary CT angiography; Plaque progression; Machine learning; Deep learning; Radiomics; Neural networks; Explainable artificial intelligence

**Online publication:** December 31, 2025



# 1. Introduction

Rapid plaque progression (RPP) is a significant predictor of acute coronary events<sup>[1,2]</sup>. Serial invasive angiographic studies have confirmed that non-obstructive lesions can progress rapidly, constituting a key mechanism for subsequent acute events<sup>[3,4]</sup>. Compared to slowly progressing plaques, RPP is significantly associated with an increased risk of future major adverse cardiovascular events<sup>[5,6]</sup>. Therefore, early identification of plaques at risk for rapid progression is crucial for preventing acute coronary syndromes. Coronary CT angiography (CCTA) is a preferred non-invasive imaging modality for evaluating coronary artery disease<sup>[7]</sup>. Recently, quantitative plaque analysis based on CCTA has emerged as a new direction for risk assessment<sup>[8]</sup>. However, traditional methods often rely on manually extracted morphological features (e.g., plaque burden, component volumes), which may inadequately capture the internal heterogeneity, microenvironment, and complex spatiotemporal dynamics of plaques<sup>[9,10]</sup>.

Radiomics enables precise disease phenotyping beyond visual assessment by extracting high-dimensional quantitative features from medical images<sup>[11]</sup>. Recent studies suggest that CCTA-based radiomics aids in identifying high-risk plaques and predicting their progression<sup>[12,13]</sup>. Furthermore, machine learning (ML) frameworks can integrate clinical, laboratory, qualitative, and quantitative CCTA features to effectively identify individuals at risk of RPP<sup>[14,15]</sup>. Despite advances in radiomics and ML, these methods predominantly rely on pre-defined, handcrafted features, potentially failing to capture all spatial contextual information inherent in the raw 3D image data. Three-dimensional convolutional neural networks (3D-CNNs) can learn hierarchical feature representations end-to-end from raw image data, offering a new avenue for more fully leveraging information within CCTA images<sup>[16,17]</sup>. Based on this rationale, this study aimed to develop a lightweight 3D-CNN model for predicting RPP and to systematically compare and validate its performance against traditional ML models and advanced radiomics methods reported in the literature.

## 2. Materials and methods

### 2.1. Study population

This retrospective study was approved by the Institutional Review Board, with a waiver for informed consent. We consecutively screened patients who underwent at least two CCTA examinations at Gongli Hospital of Shanghai Pudong New Area between January 2017 and November 2024.

The inclusion criteria were as follows:

- (1) An interval of  $\geq 1$  year between the two CCTA scans;
- (2) Presence of at least one atherosclerotic plaque (diameter  $> 2$  mm) on the baseline CCTA.

The exclusion criteria were as follows:

- (1) Poor image quality precluding plaque analysis;
- (2) Coronary revascularization performed between the two CCTA examinations;
- (3) Missing clinical data.

A total of 150 patients were finally enrolled and randomly split into a training set (105 patients, 70%) and a test set (45 patients, 30%). Based on an annualized PB increase  $\geq 1.0\%$ , patients were categorized into a progression group ( $n = 64$ ) and a non-progression group ( $n = 86$ ). Baseline characteristics are shown in **Table 1**.

**Table 1. Baseline patient characteristics**

Variable	Overall (n = 150)	Progression group (n = 64)	Non-progression group (n = 86)	P-value
Demographics				
Age, years	61.2 ± 8.9	63.5 ± 8.7	59.4 ± 8.8	0.721
Male, n (%)	85 (56.7)	40 (62.5)	45 (52.3)	0.205
Body mass index, kg/m <sup>2</sup>	25.4 ± 3.3	25.9 ± 3.5	25.0 ± 3.1	0.087
Cardiovascular risk factors, n (%)				
Hypertension	82 (54.7)	42 (65.6)	40 (46.5)	0.019
Diabetes mellitus	33 (22.0)	20 (31.3)	13 (15.1)	0.016
Dyslipidemia	56 (37.3)	26 (40.6)	30 (34.9)	0.471
Smoking history	45 (30.0)	25 (39.1)	20 (23.3)	0.132
Laboratory findings				
Total Cholesterol, mmol/L	4.70 ± 1.18	4.65 ± 1.22	4.74 ± 1.15	0.642
LDL-C, mmol/L	2.88 ± 0.87	2.92 ± 0.91	2.85 ± 0.84	0.618
HDL-C, mmol/L	1.23 ± 0.30	1.18 ± 0.28	1.27 ± 0.31	0.046
Triglycerides, mmol/L	1.66 ± 0.98	1.72 ± 1.05	1.61 ± 0.92	0.482
Morphological analysis				
Plaque length, mm	15.8 ± 8.3	18.9 ± 8.7	13.4 ± 7.2	< 0.001
Total plaque volume, mm <sup>3</sup>	185.6 ± 128.4	258.3 ± 142.7	130.5 ± 88.6	< 0.001
Stenosis degree, %	38.7 ± 18.2	46.3 ± 18.9	32.9 ± 15.4	< 0.001
Minimal lumen area, mm <sup>2</sup>	4.0 ± 2.2	3.2 ± 1.9	4.6 ± 2.3	< 0.001
Plaque composition analysis				
Calcified volume, mm <sup>3</sup>	38.9 ± 47.2	52.4 ± 53.8	28.7 ± 38.5	0.002
Calcified volume ratio, %	20.9 ± 15.8	20.3 ± 15.2	21.4 ± 16.3	0.659
Non-calcified volume, mm <sup>3</sup>	146.7 ± 102.3	205.9 ± 118.6	101.8 ± 72.4	< 0.001
Non-calcified volume ratio, %	79.1 ± 15.8	79.7 ± 15.2	78.6 ± 16.3	0.659
Low-attenuation plaque volume, mm <sup>3</sup>	9.8 ± 13.6	15.3 ± 16.8	5.6 ± 8.9	< 0.001
Low-attenuation plaque ratio, %	5.3 ± 6.8	5.9 ± 7.1	4.8 ± 6.5	0.325
Mean CT value of LAP, HU	27.8 ± 17.9	24.6 ± 15.8	30.2 ± 19.1	0.038
Fat attenuation index (FAI), HU	-69.8 ± 7.6	-67.2 ± 7.1	-71.8 ± 7.4	< 0.001
Plaque burden, %	52.3 ± 11.8	58.7 ± 10.9	47.4 ± 10.2	0.005
Annualized ΔPB, %/year	0.8 ± 2.3	2.1 ± 1.5	-0.3 ± 0.8	< 0.001
High-risk plaque features, n (%)				
Positive remodeling	92 (61.3)	48 (75.0)	44 (51.2)	0.003
Low-density plaque	28 (18.7)	18 (28.1)	10 (11.6)	0.009
Spotty calcification	25 (16.7)	14 (21.9)	11 (12.8)	0.128
Napkin-ring sign	3 (2.0)	2 (3.1)	1 (1.2)	0.381

LDL-C: Low-density lipoprotein cholesterol; HDL-C: High-density lipoprotein cholesterol; LAP: Low-attenuation plaque; HU: Hounsfield units; PB: Plaque burden; ΔPB: Change in plaque burden.

## 2.2. CCTA image acquisition and preprocessing

All CCTA examinations were performed using a Siemens dual-source CT scanner (Somatom Definition Flash, Siemens Healthineers, Forchheim, Germany). Image acquisition and reconstruction parameters were as follows: tube voltage 120 kVp, tube current modulated automatically based on patient body mass index (range 350–600 mA), and collimation width  $64 \times 0.6$  mm. All original DICOM data underwent strict quality control. Prior to scanning, all patients received sublingual nitroglycerin (0.5 mg). Beta-blockers were administered for heart rate control if the pre-scan heart rate was  $> 65$  beats per minute. Plaque quantification was performed using the United Imaging Intelligence CTA Coronary AI Analysis System ([www.uui-ai.com](http://www.uui-ai.com)). Plaque segmentation and annotation were conducted using ITK-SNAP (version 4.0).

Custom Python scripts (`analyze_alignment.py`) were used to perform slice-by-slice verification of spatial coordinates, slice thickness, and pixel spacing between the CTA volume data and corresponding plaque masks for each case. Alignment reports were generated to exclude mismatched samples.

Following previous studies, plaque volume subtypes were measured based on Hounsfield Unit (HU) thresholds: low-attenuation plaque ( $< 30$  HU), non-calcified plaque (30–130 HU), and calcified plaque ( $> 130$  HU). RPP was defined as an annualized plaque burden (PB) increase  $\geq 1.0\%$  [8,18]. PB was calculated as  $(\text{Plaque Volume} / \text{Vessel Volume}) \times 100\%$ . The annualized PB progression ( $\Delta\text{PB}/\text{year}$ ) was calculated as  $(\text{Follow-up PB} - \text{Baseline PB}) / \text{Scan interval time (years)}$ .

## 2.3. Feature extraction and model construction

### 2.3.1. Traditional machine learning models

The model was implemented using the `make_features_and_models.py` script. A set of features was extracted from each plaque region of interest (ROI), including geometric features (volume, aspect ratio), HU statistical features (mean, standard deviation, etc.), and calcification ratio, among other radiomics features. These were merged with plaque attributes (type, stenosis degree) from clinical follow-up sheets and patient risk factors to form a structured feature table. LASSO, Elastic Net, Random Forest, and XGBoost models were constructed. Hyperparameter optimization was performed using case-stratified 5-fold cross-validation. Model performance was evaluated on the fixed independent test set.

### 2.3.2. 3D-CNN model

The model was implemented using the `train_cnn_min.py` script.

The input data are as follows:

- (1) Image input: A  $96 \times 96 \times 96$  voxel 3D image patch was cropped from the aligned CTA volume data, centered on the plaque centroid. HU values were windowed ( $-100$  to  $500$  HU) and normalized;
- (2) Tabular features: 26-dimensional clinical and plaque tabular features were concatenated.

A lightweight 3D-CNN served as the backbone, incorporating Squeeze-and-Excitation (SE) attention modules to enhance feature representation. The final fully connected layers fused the imaging and tabular features to output a risk probability.

Data augmentation and regularization techniques included label smoothing (smoothing = 0.1), MixUp ( $\alpha = 0.4$ ), and CutMix ( $\alpha = 0.1$ ). The model was trained using the AdamW optimizer with cosine annealing learning rate decay, and early stopping was implemented to prevent overfitting.

## 2.4. Statistical analysis and model interpretation

Statistical analyses were performed using SPSS (version 26.0, IBM, Armonk, NY, USA) and R software (version 4.1.2, R Foundation, Vienna, Austria). Continuous variables were compared using the independent samples t-test or Mann-Whitney U test, as appropriate. Categorical variables are presented as frequencies and percentages, and compared using the chi-square test. The AUC, sensitivity, specificity, accuracy, and F1-score were calculated for all models. The DeLong test was used to compare differences in ROC curves. SHAP analysis was applied to the 3D-CNN model to quantify the contribution of each feature to the model predictions and identify key predictors.

## 3. Results

### 3.1. Model performance comparison

As shown in **Table 2**, the four traditional machine learning models demonstrated poor discriminatory ability on the test set (AUC range: 0.32–0.51). In contrast, the proposed 3D-CNN model achieved the best performance, with an AUC of 0.75 (95% CI: 0.69–0.81), a sensitivity of 0.64, and a specificity of 0.88.

**Table 2.** Performance comparison of different models on the test set

Model	AUC (95% CI)	Sensitivity	Specificity	F1-Score
LASSO	0.32 (0.25–0.39)	0.21	0.80	0.18
Elastic Net	0.35 (0.28–0.42)	0.24	0.82	0.21
Random Forest	0.48 (0.41–0.55)	0.38	0.79	0.35
XGBoost	0.51 (0.44–0.58)	0.42	0.81	0.39
3D-CNN	0.75 (0.69–0.81)	0.64	0.88	0.68

### 3.2. ROC curve analysis

The ROC curves for the traditional ML models were close to the diagonal, indicating limited discriminatory ability (**Figure 1**). In contrast, the ROC curve for the 3D-CNN model demonstrated superior classification performance, with an AUC of 0.75 (95% CI: 0.69–0.81) on the test set, which was significantly higher than all traditional models (DeLong test,  $P < 0.01$ ). This result visually underscores the advantage of the 3D-CNN in identifying rapid plaque progression (**Figure 2**).

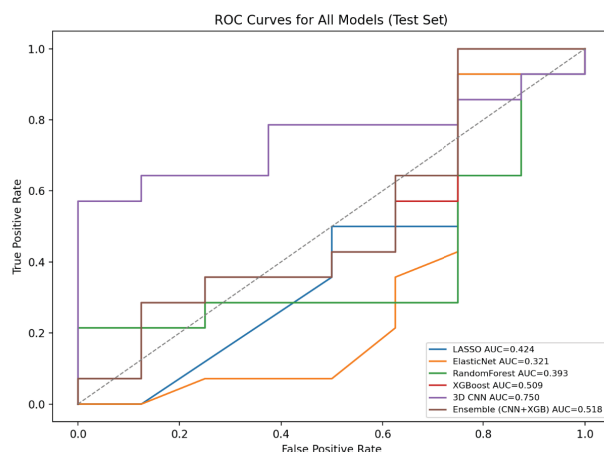


**Figure 1.** ROC curves for all models (test set).

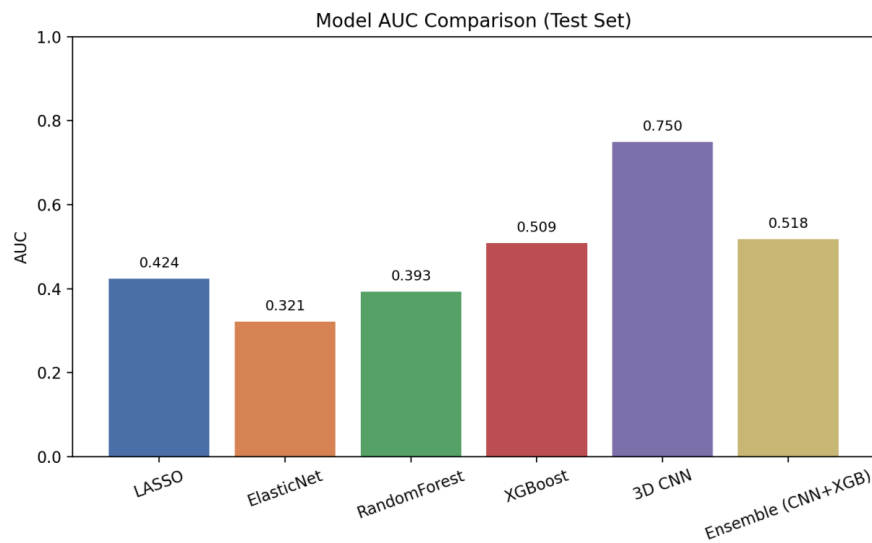


**Figure 2.** Model AUC comparison(test set).

### 3.3. Model interpretability analysis

To understand the models' decision-making basis, SHAP analysis was applied. For the best-performing traditional model (XGBoost), SHAP analysis indicated that its decisions primarily relied on traditional radiomics features such as plaque volume and the standard deviation of HU values (**Figure 3**). For the 3D-CNN model, SHAP analysis revealed that its decisions depended on a different set of feature patterns, corresponding to activations in the network's intermediate layers, which reflect local textural heterogeneity and complex HU distributions within the plaque (**Figure 4** and **Figure 5**).

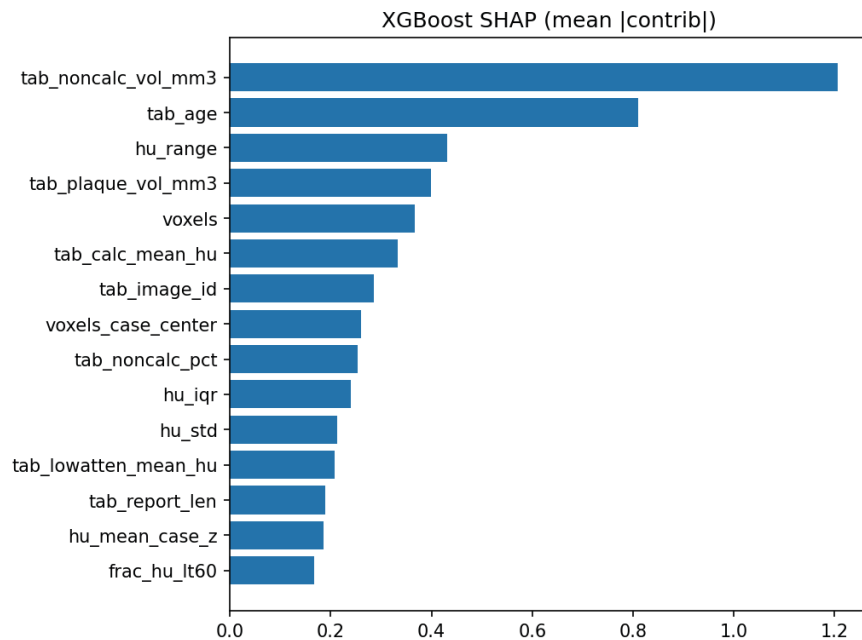


**Figure 3.** SHAP summary plot for the XGBoost model.

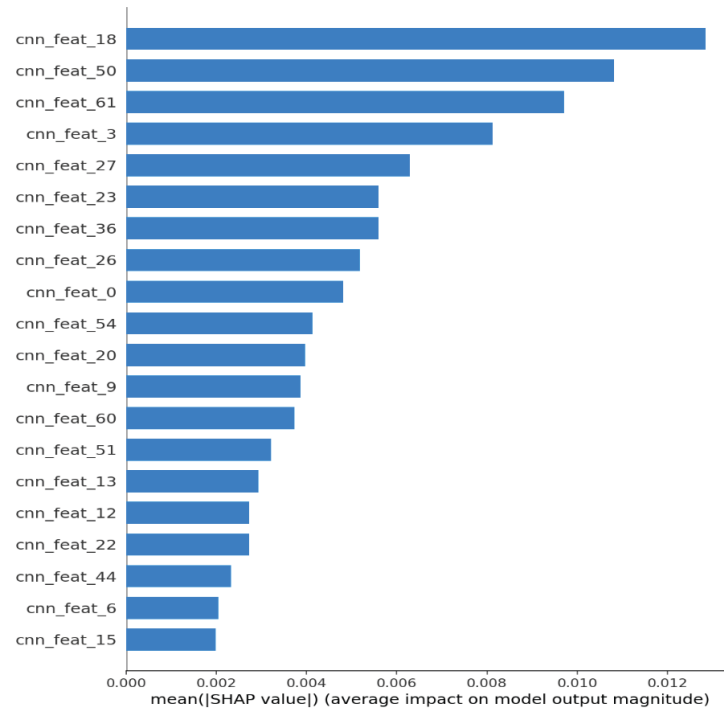


**Figure 4.** SHAP summary plot for the 3D-CNN model.

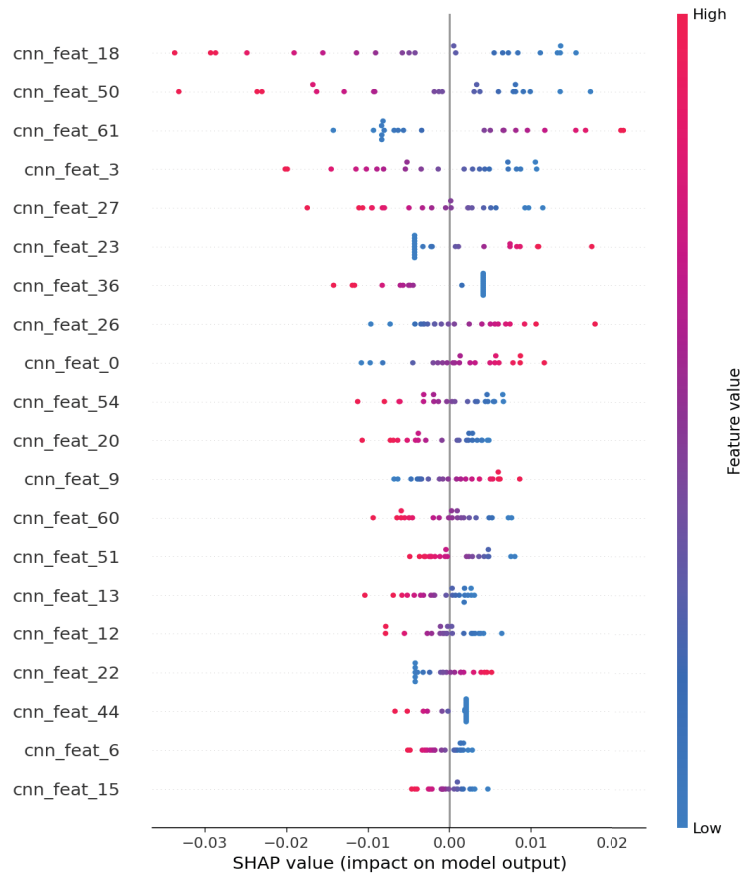


**Figure 5.** Representative intermediate-layer activations of the 3D-CNN model.



## 4. Discussion

### 4.1. Cross-method performance comparison and paradigm shift

The poor performance of traditional ML models (AUC: 0.32–0.51) aligns with findings by Feng *et al.*, who also reported limited performance using traditional plaque parameters, underscoring the constraints of relying solely on morphological features for predicting plaque progression<sup>[19]</sup>. In contrast, our 3D-CNN model demonstrated significantly superior performance (AUC = 0.75). This AUC is comparable to models built on radiomics signatures by Chen *et al.* (AUC 0.81–0.82) and deep learning frameworks reported by Lin *et al.*, indicating the potential of 3D-CNNs to compete with current state-of-the-art prediction tools<sup>[12,16]</sup>. SHAP analysis further elucidated the reason for this performance gap: traditional models relied on limited features like plaque volume, consistent with studies emphasizing the importance of plaque burden, whereas the 3D-CNN automatically focused on internal plaque texture and HU distribution patterns<sup>[20]</sup>. This finding resonates with radiomics studies by Chen *et al.* and Feng *et al.*, which identified features related to textural heterogeneity (e.g., wavelet-based gray-level non-uniformity) as highly predictive<sup>[13,19]</sup>. This signifies an important paradigm shift, where plaque risk assessment is evolving from a morphology-based “how big is it” approach towards a qualitative and heterogeneity-based “what does it look like inside” analysis.

### 4.2. Biological interpretation of features and methodological complementarity

The “texture” features emphasized by our 3D-CNN may be biologically congruent with the heterogeneity features extracted via pre-defined filters in radiomics studies. Both point towards the spatial complexity and compositional instability of plaque as the intrinsic driver of rapid progression. This aligns with the pathological mechanisms revealed by natural history studies using intravascular ultrasound (IVUS), where intra-plaque heterogeneity and microenvironmental changes are key markers of active progression<sup>[2,18]</sup>. Methodologically, this study highlights the contrast and complementarity between deep learning and radiomics. Radiomics offers good interpretability through pre-defined features, while 3D-CNNs can automatically learn more complex spatial patterns. Both approaches converge on the core concept of “image heterogeneity,” providing a rationale for future hybrid models that leverage the strengths of both.

### 4.3. Clinical translation and precision prevention

Current ESC guidelines emphasize risk stratification and precise preventive strategies for patients with chronic coronary syndromes<sup>[7,21]</sup>. Clinical decision-making often relies on periodic CCTA re-evaluation to detect plaque progression, potentially leading to delayed intervention. The primary clinical value of our 3D-CNN model lies in its potential to identify plaques with a high-risk “trajectory” for rapid progression using only a single baseline CCTA scan, even if they appear stable at the time of imaging. This could serve as a decision-support tool, enabling intensification of lipid-lowering therapy or other targeted interventions for high-risk patients (e.g., those with hypertension, diabetes, or lower HDL-C levels, as suggested by our data) at an earlier stage. This facilitates a shift from reactive treatment to proactive prevention, aligning perfectly with evidence-based precision medicine principles<sup>[22]</sup>.

### 4.4. Limitations and future directions

This study has several following limitations:

- (1) As a single-center retrospective study, selection bias is inevitable, and the sample size, while reasonable, could be larger for a deep learning model;

- (2) Although widely used, the definition of RPP based on annualized PB change requires validation against hard clinical endpoints (e.g., myocardial infarction) in long-term follow-up studies.

Future research should focus on as follows:

- (1) External validation: Prospective, multi-center, large-scale validation to assess the model's generalizability and robustness;
- (2) Association with clinical endpoints: Long-term follow-up to directly link model predictions to hard endpoints like acute coronary events, establishing its definitive prognostic value;
- (3) Technical integration: Exploring hybrid prediction models that more deeply integrate deep learning, radiomics, and clinical risk factors;
- (4) Workflow integration: Developing automated, integrated analysis pipelines incorporating image segmentation and prediction into clinical workstations to enhance practicality.

## 5. Conclusion

This study successfully developed a model for predicting coronary plaque progression based on a single baseline CCTA scan. The results demonstrate that a 3D convolutional neural network, incorporating concepts from radiomics, significantly outperforms traditional machine learning models. Its performance is comparable to current advanced radiomics and deep learning methods reported internationally. This confirms the substantial application potential and clinical translation value of advanced image analysis techniques for the precise risk assessment of coronary plaques.

## Disclosure statement

The authors declare no conflict of interest.

## References

- [1] Stone G, Maehara A, Lansky A, et al., 2011, A Prospective Natural-History Study of Coronary Atherosclerosis. *New England Journal of Medicine*, 364(3): 226–35.
- [2] Erlinge D, Maehara A, Ben-Yehuda O, et al., 2021, Identification of Vulnerable Plaques and Patients by Intracoronary Near-Infrared Spectroscopy and Ultrasound (PROSPECT II): A Prospective Natural History Study. *The Lancet*, 397(10278): 985–995.
- [3] Yokoya K, Takatsu H, Suzuki T, et al., 1999, Process of Progression of Coronary Artery Lesions from Mild or Moderate Stenosis to Moderate or Severe Stenosis: A Study based on Four Serial Coronary Arteriograms per Year. *Circulation*, 100(9): 903–909.
- [4] Ojio S, Takatsu H, Tanaka T, et al., 2000, Considerable Time from the Onset of Plaque Rupture and/or Thrombi until the Onset of Acute Myocardial Infarction in Humans: Coronary Angiographic Findings within 1 Week Before the Onset of Infarction. *Circulation*, 102(17): 2063–2069.
- [5] Ahmadi A, Leipsic J, Blankstein R, et al., 2015, Do Plaques Rapidly Progress Prior to Myocardial Infarction? The Interplay between Plaque Vulnerability and Progression. *Circulation Research*, 117(5): 450–458.
- [6] Jernberg T, Hasvold P, Henriksson M, et al., 2015, Cardiovascular Risk in Post-Myocardial Infarction Patients: Nationwide Real World Data Demonstrate the Importance of a Long-Term Perspective. *European Heart Journal*,

36(19): 1163–70.

- [7] Knuuti J, Wijns W, Saraste A, et al., 2019, ESC Guidelines for the Diagnosis and Management of Chronic Coronary Syndromes. *European Heart Journal*, 41(3): 407–477.
- [8] Serruys P, Hara H, Garg S, et al., 2021, Coronary Computed Tomographic Angiography for Complete Assessment of Coronary Artery Disease: JACC State-of-the-Art Review. *Journal of the American College of Cardiology*, 78(7): 713–736.
- [9] Van Assen M, Varga-Szemes A, Schoepf U, et al., 2020, Automated Plaque Analysis for the Prognostication of Major Adverse Cardiac Events. *European Journal of Radiology*, 2020(116): 76–83.
- [10] Lee S, Sung J, Rizvi A, et al., 2018, Quantification of Coronary Atherosclerosis in the Assessment of Coronary Artery Disease. *Circulation: Cardiovascular Imaging*, 11(7): e007562.
- [11] Gillies R, Kinahan P, Hricak H, 2016, Radiomics: Images are More than Pictures, They are Data. *Radiology*, 278(2), 563–577.
- [12] Chen Q, Xie G, Tang C, et al., 2023, Development and Validation of CCTA-based Radiomics Signature for Predicting Coronary Plaques With Rapid Progression. *Circulation: Cardiovascular Imaging*, 16(2): e014711.
- [13] Chen Q, Pan T, Wang Y, et al., 2023, A Coronary CT Angiography Radiomics Model to Identify Vulnerable Plaque and Predict Cardiovascular Events. *Radiology*, 307(2): e221693.
- [14] Han D, Kolli K, Al'Aref S, et al., 2020, Machine Learning Framework to Identify Individuals at Risk of Rapid Progression of Coronary Atherosclerosis: From the PARADIGM Registry. *Journal of the American Heart Association*, 9(5): e013958.
- [15] Motwani M, Dey D, Berman D, et al., 2017, Machine Learning for Prediction of All-Cause Mortality in Patients with Suspected Coronary Artery Disease: A 5-year Multicentre Prospective Registry Analysis. *European Heart Journal*, 38(6): 500–507.
- [16] Lin A, Manral N, McElhinney P, et al., 2022, Deep Learning-Enabled Coronary CT Angiography for Plaque and Stenosis Quantification and Cardiac Risk Prediction: An International Multicentre Study. *The Lancet Digital Health*, 4(4): e256–e265.
- [17] Sehly A, He A, Jaltotage B, et al., 2024, Coronary Artery Stenosis and Vulnerable Plaque Quantification on CCTA by Deep Learning Methods. *European Heart Journal*, 43(Supplement\_1): ehad655.187.
- [18] Nicholls S, Hsu A, Wolski K, et al., 2010, Intravascular Ultrasound-Derived Measures of Coronary Atherosclerotic Plaque Burden and Clinical Outcome. *Journal of the American College of Cardiology*, 55(21): 2399–2407.
- [19] Feng C, Chen R, Dong S, et al., 2023, Predicting Coronary Plaque Progression with Conventional Plaque Parameters and Radiomics Features Derived from Coronary CT Angiography. *European Radiology*, 33(5): 3132–3143.
- [20] Mortensen M, Dzaye O, Steffensen F, et al., 2020, Impact of Plaque Burden Versus Stenosis on Ischemic Events in Patients With Coronary Atherosclerosis. *Journal of the American College of Cardiology*, 76(19): 2213–2222.
- [21] Byrne R, Rossello X, Coughlan J, et al., 2023, ESC Guidelines for the Management of Acute Coronary Syndromes. *European Heart Journal*, 44(38): 3720–3826.
- [22] Williams M, Kwiecinski J, Doris M, et al., 2020, Low-Attenuation Noncalcified Plaque on Coronary Computed Tomography Angiography Predicts Myocardial Infarction: Results From the Multicenter SCOT-HEART Trial (Scottish Computed Tomography of the HEART). *Circulation*, 141(18): 1452–1462.

**Publisher's note**

Bio-Byword Scientific Publishing remains neutral with regard to jurisdictional claims in published maps and institutional affiliations.

# Exploration of the Relationship Between Aldehyde Dehydrogenase 2 Gene Polymorphisms and Venous Thromboembolism in Critically Ill Patients

Chunlei Xia†, Wentao Zhang†, Kun Zhang, Zhao Lin, Siyu Xu\*

Department of Intensive Medicine, Jiangning Clinical Medical College, Kangda College of Nanjing Medical University, Nanjing 211100, Jiangsu, China

† These authors contributed equally to this work and share the first authorship.

\*Author to whom correspondence should be addressed.

**Copyright:** © 2025 Author(s). This is an open-access article distributed under the terms of the Creative Commons Attribution License (CC BY 4.0), permitting distribution and reproduction in any medium, provided the original work is cited.

**Abstract:** *Objective:* Whether patients with venous thromboembolism (VTE) receive targeted treatment or not, their mortality rates remain relatively high. Common risk factors for VTE include tumors, trauma, obesity, infection, and gene mutations related to the coagulation/anticoagulation system. However, research on the relationship between non-coagulation/anticoagulation system gene mutations and VTE is currently insufficient. *Methods:* This study retrospectively collected clinical data from 123 patients in the Department of Critical Care Medicine at Nanjing Jiangning Hospital from June 1, 2023, to December 31, 2024. Through univariate and multivariate analyses, risk factors for VTE in critically ill patients were identified, and a risk prediction model was constructed. *Results:* The proportion of patients carrying the ALDH2\*2 genotype was higher in the VTE group than in those with the ALDH2\*1 genotype (21.3% vs 7.9%,  $P = 0.032$ ). Patients carrying the ALDH2\*2 genotype had a 6.553-fold increased risk of developing VTE compared to those with the ALDH2\*1 genotype. Patients with a history of diabetes had an 11.491-fold increased risk of VTE compared to those without diabetes, while patients with a history of smoking had a 39.302-fold increased risk compared to non-smokers. For each additional year of age, the risk of VTE increased by 12.5%. For each one-unit increase in left ventricular shortening fraction, the risk of VTE decreased by 37.4%. *Conclusion:* Mutation of the mitochondrial metabolic enzyme ALDH2 is a risk factor for VTE in critically ill patients and may represent a novel pathway for VTE prevention in this population.

**Keywords:** Acetaldehyde dehydrogenase 2; Intensive medicine; Venous thromboembolism; Risk prediction

**Online publication:** December 31, 2025

## 1. Introduction

Venous thromboembolism (VTE), encompassing deep vein thrombosis and pulmonary thromboembolism, carries

an approximate mortality rate of 25% in untreated cases, while the short-term mortality rate among treated VTE patients ranges from 15 to 30%. Risk factors for VTE include malignancy, antiphospholipid antibody syndrome, prolonged immobilization, trauma, obesity, estrogen therapy, infection, and others <sup>[1]</sup>. Several studies have identified anticoagulant-related factors (protein S, protein C, antithrombin) and procoagulant-related factors (coagulation factors I/II/V/VIII/IX/XI, vWF) as hereditary risk factors for VTE <sup>[2–5]</sup>. Lindström reported 16 genetic loci predisposing to VTE in European and African American populations <sup>[6]</sup>. Research focusing on the Chinese population has revealed that mutations in gene loci related to the protein C anticoagulant system increase the risk of VTE by 2.5 to 6.4 times <sup>[7,8]</sup>. However, research on non-coagulation/anticoagulation system genes and VTE remains insufficient.

Acetaldehyde dehydrogenase (ALDH) is one of the key enzymes involved in ethanol metabolism, encompassing ALDH1 and ALDH2. The enzyme encoded by ALDH2\*1/\*1 exhibits normal activity and is generally denoted as ALDH2\*1, whereas the mutant form of ALDH2 is labeled as ALDH2\*2, which includes genotypes ALDH2\*1/\*2 and ALDH2\*2/\*2. The enzyme encoded by ALDH2\*1/\*2 retains only 30–40% of the normal enzymatic activity, while the enzyme encoded by ALDH2\*2/\*2 exhibits almost no activity <sup>[9]</sup>. The mutation frequency of ALDH2 in the Asian population ranges from 30–50%, significantly higher than that in Western populations. ALDH2 can prevent the accumulation of reactive oxygen species that damage tissues and organs, and mice with the ALDH2 gene knocked out exhibit pronounced vascular endothelial injury and vascular dysfunction <sup>[10]</sup>. ALDH2 activation can alleviate lung injury by inhibiting oxidative stress and reversing alveolar epithelial cell dysfunction <sup>[11]</sup>. Critically ill patients often present with vascular endothelial injury and an inflammatory state, which triggers the coagulation cascade and promotes thrombus formation. The thrombus, in turn, activates immune cells and exacerbates inflammation <sup>[12]</sup>. ALDH2 may serve as an effective intervention target for the vicious cycle of “coagulation-inflammation”.

This study preliminarily explores the association between ALDH2 gene polymorphisms, which are not part of the coagulation/anticoagulation system, and VTE in critically ill patients. The aim is to enhance healthcare professionals’ understanding of VTE, facilitate effective screening of VTE patients, and improve the standardized prevention rate of VTE.

## 2. Methodology

### 2.1. Study design and participants

This study is a cross-sectional study that retrospectively collected clinical data from patients in the Intensive Care Unit of Jiangning Hospital Affiliated to Nanjing Medical University from June 1, 2023, to December 31, 2024. Ultimately, 123 critically ill patients were included.

The inclusion criteria are as follows:

- (1) Age  $\geq$  18 years old;
- (2) No prior history of VTE.

The exclusion criteria are as follows:

- (1) Patients with tumors, antiphospholipid antibody syndrome, major trauma or fractures, surgical patients, or pregnant women;
- (2) Patients who refuse ALDH2 genotyping;
- (3) Patients who refuse to sign the informed consent form.



## 2.2. Clinical diagnosis of VTE

All enrolled patients underwent duplex ultrasound examination of both lower extremities on the second day of admission to check for deep vein thrombosis (DVT) or spiral CT pulmonary angiography during hospitalization to detect pulmonary embolism (PE). The collected ultrasound or spiral CT pulmonary angiography images underwent quality control by the Ultrasound Department and Imaging Department of Jiangning Hospital Affiliated to Nanjing Medical University.

## 2.3. Laboratory examination

DNA was extracted and amplified from the patients' venous blood using a DNA extraction kit (Takara Bio). Subsequently, the ALDH2 genotype was determined using an ALDH2 gene polymorphism detection kit (HybriBio).

## 2.4. Statistical analysis

This study employed SPSS software (IBM SPSS Statistics, IBM Corp.) for statistical analysis. The distribution of continuous variables was assessed using the Kolmogorov-Smirnov test. Variables conforming to a normal distribution were expressed as mean  $\pm$  standard deviation (SD), and inter-group comparisons were conducted using the t-test. Variables with a non-normal distribution were represented by median (interquartile range), and inter-group comparisons were performed using the Wilcoxon rank-sum test. Categorical variables were presented as frequencies and percentages, and differences between groups were compared using the  $\chi^2$  test or Fisher's exact test. A  $P$ -value  $< 0.05$  was considered statistically significant.

Variables that showed statistical significance in the univariate analysis were included in the multivariate analysis. A forward stepwise regression strategy was adopted to screen for variables that still exhibited statistical significance. Using these variables as independent variables and the occurrence of VTE as the dependent variable, a binary logistic regression was employed to establish a risk prediction model.

## 3. Results

### 3.1. Analysis of clinical characteristics of patients with Non-VTE and VTE

In this study, clinical data from 123 critically ill patients were collected. Statistically significant differences in ALDH2 genotypes were observed between the VTE group and the non-VTE group, with the ALDH2\*2 genotype being more prevalent in the VTE group than the ALDH2\*1 genotype (**Table 1**, 21.3% vs 7.9%). Diabetes and a history of cerebral infarction also showed statistically significant differences between the two groups. The proportion of patients with a history of diabetes was higher in the VTE group (**Table 1**, 17.7% vs 4.5%), as was the proportion of patients with a history of cerebral infarction (**Table 1**, 28.6% vs 8.4%). The proportion of patients with a history of alcohol consumption was lower in the VTE group (17.2% vs 0%), which may be related to the weak alcohol metabolism capacity and restricted alcohol consumption in patients with the ALDH2\*2 genotype. The creatinine level in the VTE group was higher than that in the non-VTE group, while the fractional shortening was lower in the VTE group compared to the non-VTE group, with both differences being statistically significant (**Table 1**).



**Table 1.** Clinical characteristics of patients with non-VTE and VTE

Variable	Category	Non-VTE <sup>a</sup> (n=107)	VTE <sup>a</sup> (n = 16)	P-value	Correlation coefficient (r)
ALDH2	ALDH2*1	70 (92.1)	6 (7.9)	0.032	0.190
	ALDH2*2	37 (78.7)	10 (21.3)		
Gender	Male	72 (88.9)	9 (11.1)	0.385	0.078
	Female	35 (83.3)	7 (16.7)		
Coronary heart disease	No	31 (88.6)	4 (11.4)	0.975	0.03
	Yes	76 (86.4)	12 (13.6)		
Diabetes	No	42 (95.5)	2 (4.5)	0.037	0.185
	Yes	65 (82.3)	14 (17.7)		
Hypertension	No	25 (92.6)	2 (7.4)	0.512	0.088
	Yes	82 (85.4)	14 (14.6)		
Atrial fibrillation	No	90 (88.2)	12 (11.8)	0.584	0.081
	Yes	17 (81.0)	4 (19.0)		
Cerebral infarction	No	87 (91.6)	8 (8.4)	0.014	0.244
	Yes	20 (71.4)	8 (28.6)		
Smoking history	No	42 (97.7)	1 (2.3)	0.010	0.227
	Yes	65 (81.3)	15 (18.8)		
Drinking history	No	77 (82.8)	16 (17.2)	0.034	0.215
	Yes	30 (100.0)	0 (0.0)		
Age		66.3 ± 11.7	75.7 ± 9.2	0.003	0.267
BMI		24.97 (23.44, 27.01)	24.50 (21.57, 25.36)	0.180	-0.122
White blood		6.68 (5.15, 8.03)	5.70 (4.09, 6.41)	0.009	-0.236
Hemoglobin		133.55 ± 16.82	122.69 ± 22.19	0.023	-0.205
Sodium		141.0 (139.4, 143.0)	142.1 (139.7, 143.1)	0.357	0.083
Chloride		103.5 (101.3, 105.3)	104.9 (101.8, 105.9)	0.196	0.117
Creatinine		74 (65, 88)	83 (74, 112)	0.026	0.202
ALT		23 (15, 33)	16 (13, 21)	0.076	-0.160
AST		21 (17, 27)	20 (17, 26)	0.447	-0.069
PASP		39 (38, 44)	41 (39, 43)	0.494	0.062
EF		65 (62, 66)	63 (61, 65)	0.075	-0.161
FS		35 (34, 36)	34 (33, 35)	0.049	-0.178

a: Continuous variables are presented as mean ± standard deviation or median (interquartile range), and categorical variables are presented as frequency (percentage); ALDH2: Aldehyde dehydrogenase 2; VTE: Venous thromboembolism; BMI: Body mass index; ALT: Alanine aminotransferase; AST: Aspartate aminotransferase; PASP: Pulmonary artery pressure; EF: Left ventricular ejection fraction; FS: Left ventricular fractional shortening

### 3.2. Multifactorial logistic regression analysis of the risk of VTE occurrence

Variables with a *P*-value less than 0.05 in the univariate analysis, including age, ALDH2 genotype, history of diabetes, history of cerebral infarction, history of smoking, history of alcohol consumption, total white blood cell count, hemoglobin content, creatinine, and fractional shortening, were included in the multifactorial logistic regression analysis. The multifactorial analysis revealed statistically significant differences in age, ALDH2 genotype, history of diabetes, history of smoking, and fractional shortening (**Table 2**).

For each additional year of age, the risk of VTE occurrence increased by 12.5% (**Table 2**, OR = 1.125, 95% CI: 1.034–1.223, *P* = 0.006); patients with the ALDH2\*2 genotype had a 6.553-fold higher risk of VTE compared to those with the ALDH2\*1 genotype (**Table 2**, 95% CI: 1.521–28.226, *P* = 0.012); patients with a history of diabetes had an 11.491-fold higher risk of VTE compared to those without a history of diabetes (**Table 2**, 95% CI: 1.667–93.620, *P* = 0.014); patients with a history of smoking had a 39.302-fold higher risk of VTE compared to those without a history of smoking (**Table 2**, OR = 39.302, 95% CI: 1.930–800.402, *P* = 0.017); for each unit increase in fractional shortening, the risk of VTE occurrence decreased by 37.4% (**Table 2**, OR = 0.626, 95% CI: 0.457–0.859, *P* = 0.004).

**Table 2.** Results of multifactorial regression analysis

Variable	B	S.E.	Wald	P	Exp (B) [OR]	95% CI	
ALDH2	1.880	0.745	6.366	0.012	6.553	1.521	28.226
Diabetes	2.525	1.028	6.037	0.014	12.491	1.667	93.620
Smoking	3.671	1.538	5.700	0.017	39.302	1.930	800.402
Age	0.118	0.043	7.574	0.006	1.125	1.034	1.223
FS	-0.468	0.161	8.415	0.004	0.626	0.457	0.859
Constant	-0.472	4.162	0.013	0.910	0.624	-	

ALDH2: Aldehyde Dehydrogenase 2; FS: Left Ventricular Fractional Shortening

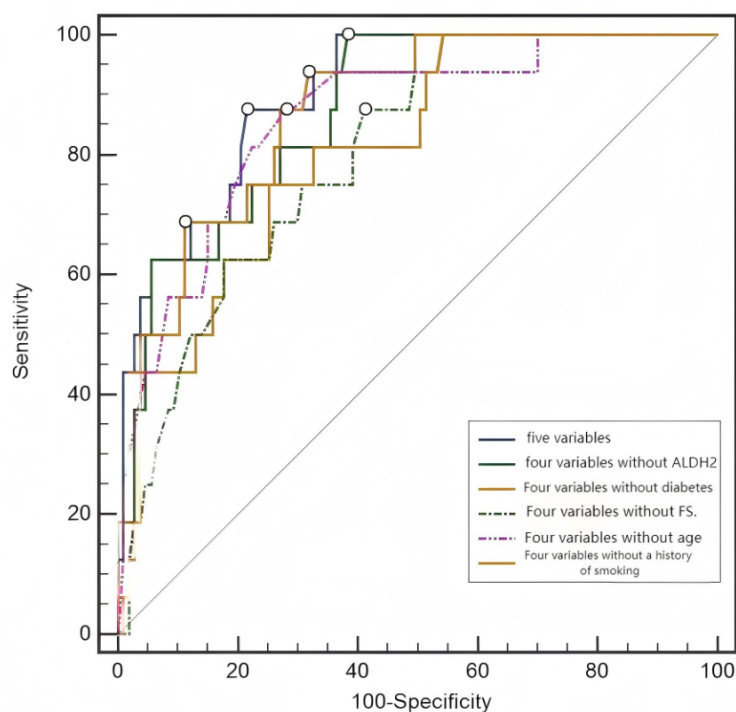
### 3.3. ROC curve analysis of VTE risk prediction model

A VTE risk prediction model for critically ill patients was constructed using variables selected through multivariate analysis, and the theoretical probability of VTE occurrence in enrolled patients was calculated. The ROC curve was plotted using MedCalc software. The five-variable model, which included age, ALDH2 genotype, history of diabetes, history of smoking, and fractional shortening, had an area under the curve (AUC) of 0.901, indicating good discriminatory power of the model. Each of the aforementioned variables was removed separately to reconstruct four-variable models. After DeLong testing, it was found that removing the fractional shortening or diabetes variables resulted in a decrease in the model's AUC to 0.802 and 0.851, respectively, with statistically significant differences. This suggests that fractional shortening and history of diabetes make relatively important contributions to the model's predictive ability (**Table 3**, **Figure 1**). The model's AUC decreased from 0.901 to 0.872 after removing the ALDH2 genotype, but this difference did not reach statistical significance.

**Table 3.** Comparison of VTE risk assessment models in critically Ill patients

Model	AUC	S.E.	95% CI	Z	P
Five-Variable Model	0.901	0.0347	0.834–0.947		
Four-Variable Model (excluding ALDH2)	0.872	0.0404	0.800–0.925	1.121	0.262
Four-Variable Model (excluding Diabetes)	0.851	0.0429	0.775–0.909	2.132	0.033
Four-Variable Model (excluding FS)	0.802	0.0505	0.721–0.868	2.579	0.010
Four-Variable Model (excluding Age)	0.860	0.0488	0.786–0.916	1.103	0.270
Four-Variable Model (excluding Smoking)	0.833	0.0525	0.755–0.894	1.508	0.132

ALDH2: Aldehyde dehydrogenase 2; FS: Left ventricular fractional shortening

**Figure 1.** ROC curve of VTE risk assessment model in critically Ill patients.

## 4. Discussion

ALDH2, a metabolic enzyme localized in mitochondria, plays a crucial role in clearing toxic lipid peroxides. Critically ill patients often experience stress and inflammatory activation, leading to an increase in reactive oxygen species (ROS). This, in turn, triggers lipid peroxidation in organelles, resulting in vascular endothelial cell dysfunction and promoting thrombosis. Our research has found that patients with ALDH2 gene mutations are more prone to developing VTE. Previous studies have revealed that ALDH2 activity in coronary atherosclerotic tissues is lower than that in normal tissues<sup>[13]</sup>. The application of the ALDH2 agonist Alda-1 can reverse LPS-induced cardiac dysfunction, suggesting that targeted intervention of ALDH2 may prevent the occurrence and progression of VTE<sup>[14]</sup>.

Hyperglycemia can trigger multiple signaling pathways that damage vascular endothelium, and diabetic patients often exhibit a hypercoagulable state, increasing the risk of VTE. Research by Heit *et al.* indicates that

fasting blood glucose levels  $\geq 140$  mg/dL or the presence of diabetes complications are associated with VTE, highlighting the importance of blood glucose regulation in critically ill patients to reduce the risk of VTE <sup>[15]</sup>. A meta-analysis has shown that smoking is associated with an increased risk of VTE, with a risk ratio of 1.38 <sup>[16]</sup>. Harmful substances such as nicotine can promote platelet aggregation and increase blood viscosity, leading to thrombosis. Previous studies have demonstrated that the incidence of VTE remains constant among males across all age groups, but the incidence of VTE in females over 60 years old increases compared to females under 55 years old <sup>[17]</sup>. Our study is limited by the sample size and lacks subgroup analysis stratified by age. However, the results indicate that patients in the VTE group are significantly older than those in the non-VTE group, suggesting that endothelial dysfunction caused by aging is a crucial factor in VTE formation <sup>[18]</sup>. Pastori's research has demonstrated that heart failure, atrial fibrillation, and myocardial infarction events within three months prior to admission are strong risk factors for VTE <sup>[19]</sup>. This study reveals a significant decrease in the left ventricular fractional shortening in patients in the VTE group. This association can be explained by cardiac pump failure and slow venous return in patients.

This study preliminarily reveals the relationship between ALDH2 gene polymorphism and VTE in critically ill patients and constructs a VTE risk assessment model for such patients. Incorporating ALDH2 gene polymorphism, an indicator with regional distribution differences, will further enrich the domestic VTE risk assessment system and provide data and theoretical support for the early detection and intervention of VTE. Due to the relatively small sample size of the study, some potential influencing factors may not have been effectively identified. Subsequent research should involve multi-center collaboration to further expand the sample size, optimize the predictive model, conduct external data validation, and enhance the stability and generalizability of the model.

## 5. Conclusion

The mutation of the mitochondrial metabolic enzyme ALDH2 constitutes a risk factor for the development of VTE in critically ill patients. This finding highlights a potential novel pathway for VTE prevention in this vulnerable population.

## Funding

Science Foundation of Kangda College of Nanjing Medical University (Project No.: KD2023KYJJ250); Education Foundation of Kangda College of Nanjing Medical University (Project No.: KDJYYJYB202332)

## Disclosure statement

The authors declare no conflict of interest.

## References

- [1] Khan F, Tritschler T, Kahn S, et al., 2021, Venous Thromboembolism. *Lancet*, 398(10294): 64–77.
- [2] Sanson B, Simioni P, Tormene D, et al., 1999, Incidence of Venous Thromboembolism in Asymptomatic Carriers of Antithrombin, Protein C, or Protein S Deficiency: A Prospective Cohort Study. *Blood*, 94(11): 3702–3706.
- [3] Heit J, Sobell J, Li H, et al., 2005, Incidence of Venous Thromboembolism among Factor V Leiden Carriers: A

Community-Based Cohort Study. *Journal of Thrombosis and Haemostasis*, 3(2): 305–311.

- [4] Folsom A, Cushman M, Tsai M, et al., 2002, Prospective Study of the G20210A Polymorphism in the Prothrombin Gene, Plasma Prothrombin Concentration, and Incidence of Venous Thromboembolism. *American Journal of Hematology*, 71(4): 285–290.
- [5] Tang W, Teichert M, Chasman D, et al., A Genome-Wide Association Study for Venous Thromboembolism: The Extended Cohorts for Heart and Aging Research in Genomic Epidemiology (CHARGE) Consortium. *Genetic Epidemiology*, 37(5): 512–521.
- [6] Lindstrom S, Wang L, Smith E, et al., 2019, Genomic and Transcriptomic Association Studies Identify 16 Novel Susceptibility Loci for Venous Thromboembolism. *Blood*, 134(19): 1645–1657.
- [7] Tang L, Lu X, Yu J, et al., 2012, The PROC c.574\_576del Polymorphism: A Prevalent Genetic Risk Factor for Venous Thrombosis in the Chinese Population. *Journal of Thrombosis and Haemostasis*, 10(10): 2019–2026.
- [8] Tang L, Wang H, Lu X, et al., 2013, Common Genetic Risk Factors for Venous Thrombosis in the Chinese Population. *American Journal of Human Genetics*, 92(2): 177–187.
- [9] Zhang R, Wang J, Xue M, et al., 2017, ALDH2 - Genetic Polymorphism and Regulation of Enzymatic Activity: Their Epidemiological and Clinical Implications. *Current Drug Targets*, 18(15): 1810–1816.
- [10] Pan G, Roy B, Palaniyandi S, 2021, Diabetic Aldehyde Dehydrogenase 2 Mutant (ALDH2\*2) Mice Exhibit Increased Susceptibility to Cardiac Ischemic-Reperfusion Injury Due to 4-Hydroxy-2-Nonenal-Induced Damage to Coronary Endothelial Cells. *Journal of the American Heart Association*, 10(18): e021140.
- [11] Tsai H, Hsu Y, Lu C, et al., 2021, Pharmacological Activation of Aldehyde Dehydrogenase 2 Confers Protection Against Heatstroke-Induced Acute Lung Injury by Modulating Oxidative Stress and Endothelial Dysfunction. *Frontiers in Immunology*, 2021(12): 740562.
- [12] Engelmann B, Massberg S, 2013. Thrombosis as an Intravascular Effector of Innate Immunity. *Nature Reviews Immunology*, 13(1): 34–45.
- [13] Pan C, Xing J, Zhang C, et al., 2016, Aldehyde Dehydrogenase 2 Inhibits Inflammatory Response and Regulates Atherosclerotic Plaque. *Oncotarget*, 7(24): 35562–35576.
- [14] Liu H, Hu Q, Ren K, et al., 2023, ALDH2 Mitigates LPS-Induced Cardiac Dysfunction, Inflammation, and Apoptosis Through the cGAS/STING Pathway. *Molecular Medicine*, 29(1): 171.
- [15] Heit A, Leibson C, Ashrani A, et al., 2009, Is Diabetes Mellitus an Independent Risk Factor for Venous Thromboembolism? A Population-Based Case-Control Study. *Arteriosclerosis, Thrombosis, and Vascular Biology*, 29(9): 1399–1405.
- [16] Gregson J, Kaptoge S, Bolton T, et al., 2019, Cardiovascular Risk Factors Associated With Venous Thromboembolism. *JAMA Cardiology*, 4(2): 163–173.
- [17] Silverstein M, Heit J, Mohr D, et al., 1998, Trends in the Incidence of Deep Vein Thrombosis and Pulmonary Embolism: A 25-Year Population-Based Study. *Archives of Internal Medicine*, 158(6): 585–593.
- [18] Bochenek M, Schutz E, Schafer K, 2016, Endothelial Cell Senescence and Thrombosis: Ageing Clots. *Thrombosis Research*, 2016(147): 36–45.
- [19] Pastori D, Cormaci V, Marucci S, et al., 2023, A Comprehensive Review of Risk Factors for Venous Thromboembolism: From Epidemiology to Pathophysiology. *International Journal of Molecular Sciences*, 24(4): 3169.

**Publisher's note**

Bio-Byword Scientific Publishing remains neutral with regard to jurisdictional claims in published maps and institutional affiliations.

# Clinical Diagnostic Value of Serum Low-Density Lipoprotein Cholesterol Combined with Carotid Artery Ultrasound Parameters in Patients with Coronary Heart Disease

Hongping Lu<sup>1</sup>, Qilong Chen<sup>2\*</sup>

<sup>1</sup>Helie Street Community Health Service Center, Wuxi 214100, Jiangsu, China

<sup>2</sup>Department of Medical Imaging, Wuxi No. 9 People's Hospital, Wuxi 214100, Jiangsu, China

\*Author to whom correspondence should be addressed.

**Copyright:** © 2025 Author(s). This is an open-access article distributed under the terms of the Creative Commons Attribution License (CC BY 4.0), permitting distribution and reproduction in any medium, provided the original work is cited.

**Abstract:** *Objective:* To analyze and study the results of carotid artery ultrasound examination and serum low-density lipoprotein cholesterol (LDL-C) detection in patients with coronary heart disease, aiming to explore their application effectiveness and value in the clinical diagnosis of coronary heart disease. *Methods:* A retrospective analysis was conducted on the diagnostic conditions of suspected coronary heart disease patients who visited our hospital from May 2023 to June 2025. Using coronary angiography results as the gold standard, 60 patients diagnosed with coronary heart disease were selected as the study group, and 60 patients without coronary heart disease were selected as the control group. LDL-C levels and carotid artery ultrasound parameters were compared between the two groups to evaluate their diagnostic value. *Results:* The IMT and plaque semi-quantitative scores in the study group were higher than those in the control group ( $P < 0.05$ ); carotid artery plaques were detected in 47 patients in the study group, with a total of 103 plaques. The proportion of patients with  $\geq 2$  types of plaques was 66.67%, mainly consisting of heterogeneous plaques (34.95%) and soft plaques (56.31%), which were significantly higher than those in the control group ( $P < 0.05$ ); LDL-C and TC levels in the study group were significantly higher than those in the control group ( $P < 0.05$ ). *Conclusion:* The detection of serum LDL-C and carotid artery ultrasound parameters holds significant application value in the diagnosis of coronary heart disease (CHD). A combined detection approach can serve as an important reference for screening coronary artery lesions and provide a reference basis for formulating clinical diagnosis and treatment strategies.

**Keywords:** Serum low-density lipoprotein cholesterol; Carotid artery ultrasound parameters; Coronary heart disease; Diagnostic value

**Online publication:** December 31, 2025



## 1. Introduction

Coronary heart disease, as the most prevalent type of atherosclerotic cardiovascular disease, exhibits a high incidence rate among middle-aged and elderly populations. It is primarily characterized by cardiac circulatory disturbances and myocardial ischemia and hypoxia, with clinical manifestations including dyspnea, palpitations, chest pain, arrhythmia, decreased physical strength, and easy fatigue, posing a severe threat to patient health and safety. Early diagnosis and effective intervention are thus imperative. However, due to the disease's strong concealment and lack of specific symptoms in the early stages, early diagnosis presents certain difficulties<sup>[1]</sup>.

Currently, although coronary angiography is widely recognized as the “gold standard” for diagnosing CHD, this examination faces issues such as high technical thresholds, exorbitant costs, and significant invasiveness to patients, making it challenging to popularize in clinical practice. Relevant studies have indicated that carotid artery ultrasound parameters and certain serum markers hold potential application value in the diagnosis of cardiovascular diseases. Among them, serum low-density lipoprotein cholesterol (LDL-C) is a commonly used assessment indicator. Elevated LDL-C levels can induce coronary atherosclerosis, and the occurrence and development of cardiovascular diseases are closely related to arteriosclerosis. Therefore, LDL-C is considered an independent risk factor for CHD and holds a significant reference value in its diagnosis<sup>[2,3]</sup>.

In addition, due to its advantages of being safe, non-invasive, cost-effective, and efficient, ultrasound examination is increasingly widely used in clinical practice. Studies have confirmed that intima-media thickness (IMT) of the carotid artery is a reliable non-invasive assessment indicator for the early diagnosis of coronary heart disease<sup>[4]</sup>. Based on this, this study selected 120 patients with suspected coronary heart disease as the research subjects and further explored the application value of carotid artery ultrasound and LDL-C detection in the diagnosis of coronary heart disease by conducting these two tests.

## 2. Materials and methods

### 2.1. General information

The study selected patients with suspected coronary heart disease who visited our hospital from May 2023 to June 2025 as the sample selection period. Using coronary angiography results as the gold standard, 60 patients diagnosed with coronary heart disease were selected as the study group, and 60 patients without coronary heart disease were selected as the control group.

In the control group, there were 27 female patients and 33 male patients; the age range was 46-78 years, with an average age of  $(62.43 \pm 4.77)$  years; the body mass index (BMI) range was 22.1-27.6 kg/m<sup>2</sup>, with an average BMI of  $(25.28 \pm 1.30)$  kg/m<sup>2</sup>. In the study group, there were 28 female patients and 32 male patients; the age range was 48-77 years, with an average age of  $(63.08 \pm 4.91)$  years; the BMI range was 22.6-27.3, with an average BMI of  $(25.35 \pm 1.02)$  kg/m<sup>2</sup>. There were no statistically significant differences in baseline data between the two groups ( $P > 0.05$ ), meeting the basic requirements for comparative studies.

### 2.2. Inclusion and exclusion criteria

The inclusion criteria are as follows: The diagnostic gold standard was based on the results of coronary angiography. Patients in the study group were confirmed to have coronary heart disease and met the relevant diagnostic criteria outlined in the “Guidelines for the Diagnosis and Treatment of Stable Coronary Artery Disease”<sup>[5]</sup>. For all suspected coronary heart disease patients included in the study, carotid ultrasound examination and serum indicator testing had to be completed on the same day, with the interval between

coronary angiography and these tests not exceeding three days. Patients who had not received coronary heart disease-related treatment within the past six months and had complete medical records were also included.

The exclusion criteria are as listed:

- (1) Patients with concurrent immunodeficiency diseases or hematological system disorders;
- (2) Patients with impaired liver or kidney function;
- (3) Patients with confirmed malignant tumors;
- (4) Patients with a history of allergy to iodine contrast agents or those unable to tolerate relevant imaging examinations.

## **2.3. Methods**

The methodology is as follows:

- (1) Carotid ultrasound examination: The examinee was placed in a supine position, with the neck area fully exposed. A color ultrasound diagnostic instrument was used, with the probe frequency set at 7.5 MHz. During the examination, the examinee was instructed to turn their head 45° away from the side being examined, and the probe was used to scan both carotid arteries. The detected indicators included carotid IMT, plaque types, plaque characteristics, and plaque semi-quantitative scores;
- (2) Serum indicator testing: Five milliliters of fasting blood was collected from the examinee's elbow vein in the morning, and the serum was separated through centrifugation and stored for testing;
- (3) Coronary angiography: A digital flat-panel angiography machine was used for the examination, with its results serving as the diagnostic gold standard. The examinee was placed in a supine position, and local disinfection was performed, followed by the placement of a surgical drape according to standard operating procedures. A puncture site was selected approximately 2 cm above the transverse crease of the right wrist, at a location with a palpable radial artery pulse. After administering local anesthesia to the puncture area with 1% lidocaine, the right radial artery was punctured, and a sheath was inserted. Subsequently, iopromide contrast agent was injected. Two experienced interventional physicians independently evaluated the coronary artery lesions using a blinded method. If their opinions were consistent, the results could be directly recorded. In cases of discrepancies, they should jointly review the angiographic video, each explaining their rationale for judgment until a consensus was reached. If consensus could not be reached after discussion, a chief physician with SCAI coronary imaging certification who had not participated in the initial discussion should be brought in for review to reach a final conclusion. When at least one of the following vessels (the right coronary artery or its major branches, the left main coronary artery, the left circumflex artery, or the left anterior descending artery) exhibited a diameter stenosis exceeding 50%, combined with the overall condition of the patient, a diagnosis of coronary heart disease could be made.

## **2.4. Observation indicators**

The observation indicators are as follows:

- (1) Carotid artery ultrasound parameters: Ultrasound examination data from all patients were summarized and analyzed, with plaque scores, IMT, and specific types and categories of plaques recorded. Comparative studies were then conducted after data organization. The specific criteria for judgment are as follows:

- (i) Semi-quantitative scoring of plaques: A score of 0 is assigned when there is no intimal thickening; a score of 1 is given when there is localized intimal thickening, but the IMT value does not exceed 1.5 mm; a score of 2 is recorded when a plaque has formed but has not caused significant vascular stenosis; a score of 3 is assigned for mild stenosis with a lumen stenosis rate below 50%; a score of 4 is given for moderate to severe stenosis, where the lumen stenosis rate exceeds 50% but is not completely occluded; and a score of 5 is recorded for complete vascular occlusion;
  - (ii) IMT measurement and determination: The measurement locations are selected at the bilateral carotid artery bifurcations and 1.0 cm proximal to them. Continuous monitoring is performed over three cardiac cycles, and the average value is calculated. An IMT < 1.0 mm indicates normal intima; an IMT between 1.0–1.5 mm is determined as intimal thickening; and an IMT ≥ 1.5 mm is judged as plaque formation;
  - (iii) Plaque classification: Plaques are classified into three types: hard plaques, soft plaques, and heterogeneous plaques. In terms of the number of types, 0 types represent no plaques, 1 type represents the presence of only one of the hard, soft, or heterogeneous plaques, and ≥ 2 types represent the simultaneous presence of two or three of the aforementioned plaque types;
- (2) Serum index detection. After collecting and processing the patient's venous blood, serum index levels are measured within 0.5–2.0 hours using a fully automated biochemical analyzer. These include LDL-C, high-density lipoprotein cholesterol (HDL-C), total cholesterol (TC), and triglycerides (TG).

## 2.5. Data processing

This study utilized SPSS 22.0 statistical software for analysis. Count data were analyzed using the  $\chi^2$  test and presented as rates (%). Measurement data were tested using the *t*-value and presented as mean ± standard deviation (SD). A *P*-value less than 0.05 was considered the baseline for statistical significance.

## 3. Results

### 3.1. Ultrasonic examination results

The IMT and semi-quantitative plaque score in the study group were higher than those in the control group. In the study group, carotid artery plaques were detected in 47 patients, totaling 103 plaques, while in the control group, carotid artery plaques were detected in 9 patients, totaling 10 plaques. The proportion of patients with two or more types of plaques in the study group was 66.67%, significantly higher than that in the control group (*P* < 0.05), as shown in **Table 1** and **Table 2**.

**Table 1.** Comparison of IMT and semi-quantitative plaque scores (mean ± SD)

Group	Number of cases (n)	Plaque score (points)	IMT (mm)
Research group	60	2.35 ± 0.91	1.42 ± 0.23
Control group	60	0.92 ± 0.26	0.68 ± 0.19
<i>t</i> -value	-	11.704	19.214
<i>P</i> -value	-	< 0.001	< 0.001

**Table 2.** Comparison of plaque types and varieties [n (%)]

Group	Number of cases (n)	Plaque number diversity			Plaque echogenicity type		
		0 type	1 type	≥ 2 types	Hard plaque	Heterogeneous plaque	Soft plaque
Research group	60	13 (21.67)	7 (11.67)	40 (66.67)	9 (8.74)	36 (34.95)	58 (56.31)
Control group	60	51 (85.00)	9 (15.00)	0 (0.00)	3 (30.00)	7 (70.00)	0 (0.00)
$\chi^2$ -value	-	48.348	0.289	60.000	1.543	4.750	11.569
<i>P</i> -value	-	< 0.001	0.591	< 0.001	0.214	0.029	0.001

### 3.2. Serum indicators

There were no significant differences in the levels of TG and HDL-C between the two groups ( $P > 0.05$ ). The levels of LDL-C and TC in the study group were significantly higher than those in the control group ( $P < 0.05$ ), as shown in **Table 3**.

**Table 3.** Comparison of serum indicators (mean  $\pm$  SD, mmol/L)

Group	Number of cases (n)	LDL-C	HDL-C	TC	TG
Research group	60	4.97 $\pm$ 1.67	1.71 $\pm$ 0.48	5.88 $\pm$ 1.53	3.59 $\pm$ 1.20
Control group	60	3.13 $\pm$ 1.60	1.68 $\pm$ 0.36	4.05 $\pm$ 1.42	3.61 $\pm$ 1.09
<i>t</i> -value	-	6.163	0.387	6.791	0.096
<i>P</i> -value	-	< 0.001	0.699	< 0.001	0.924

## 4. Discussion

As the most prevalent clinical cardiac disease, CHD arises when the endothelial cells of the coronary arteries are damaged, allowing lipid components to infiltrate and deposit on the coronary artery walls. This triggers the proliferation of fibroblasts, monocytes, and smooth muscle cells, accompanied by platelet adhesion and aggregation, forming atherosclerotic plaques that protrude into the lumen. These plaques can narrow the coronary lumen, obstruct blood flow, and result in myocardial ischemia and hypoxia, leading to myocardial dysfunction and subsequent organic lesions. Hence, it is also known as ischemic heart disease. Currently, CHD has emerged as one of the leading causes of mortality worldwide.

According to relevant survey data, the number of CHD patients in China exceeds ten million, with the death toll ranking second globally and still on the rise<sup>[6,7]</sup>. Therefore, early identification of CHD and timely and effective prevention and treatment hold significant public health implications. In the diagnosis of CHD, coronary angiography is internationally recognized as the gold standard. However, its clinical application is somewhat limited due to its invasive nature, high examination costs, the need for hospitalization, and the risk of surgical complications. At this stage, the search for more accurate, cost-effective, and early diagnostic measures has become a focal point of clinical research, with ultrasound examination consistently playing a pivotal role. Coronary arteries and carotid arteries share similar characteristics, both exhibiting slow blood flow phenomena and a high risk of atherosclerosis<sup>[8]</sup>.

Ultrasound examination offers the advantages of being simple to operate and highly reproducible, making it a widely utilized clinical examination method. Carotid artery ultrasound demonstrates high sensitivity in detecting plaques, facilitating easier identification of carotid artery plaque conditions in patients and providing a basis for formulating treatment plans. IMT serves as a hallmark indicator of early atherosclerosis, with each 0.1mm increase in IMT in patients with coronary heart disease elevating the risk of concurrent acute myocardial infarction by 11% <sup>[9]</sup>. Moreover, the occurrence of atherosclerosis is frequently associated with abnormal lipid metabolism, which constitutes the pathological foundation for various cardiovascular diseases. Specifically, the extensive deposition of lipid particles such as LDL-C on the arterial intima promotes plaque formation and continuous enlargement, eventually leading to rupture, thrombus formation, lumen occlusion, or even complete blockage, thereby triggering adverse cardiovascular events. Therefore, LDL-C level detection can be employed to assess the degree of atherosclerosis and holds significant guiding value for the prevention and treatment of cardiovascular diseases <sup>[10]</sup>.

According to the findings of this study, LDL-C levels in patients with coronary heart disease were  $(4.97 \pm 1.67)$  mmol/L, and TC levels were  $(5.88 \pm 1.53)$  mmol/L, both significantly higher than those in patients without coronary heart disease. Cholesterol indicators are among the important metrics for assessing cardiovascular disease risk. After undergoing oxidative modification, LDL-C leads to extensive cholesterol deposition within the arterial wall, precipitating arteriosclerosis. Consequently, its detection level can serve as an effective basis for diagnosing cardiovascular diseases. In addition to cholesterol, IMT also holds significant reference value in the diagnosis of CHD. It can, to a certain extent, reflect the severity of coronary artery lesions and can be considered as an independent risk factor for CHD. Observing the morphological changes in IMT through carotid artery ultrasound examination can effectively predict the progression trend of CHD at a stage before arterial plaque formation.

Moreover, plaque formation is a typical characteristic of atherosclerosis, providing a visual reflection of the severity of arteriosclerosis <sup>[11,12]</sup>. In this study, patients with CHD had a plaque score of  $2.35 \pm 0.91$  points and an IMT of  $1.42 \pm 0.23$  mm, both of which were higher than those in patients without CHD. Furthermore, the proportion of patients with  $\geq 2$  types of plaques (66.67%) was higher than that in patients without CHD, indicating that carotid artery ultrasound parameters can effectively reflect the extent of coronary artery lesions in patients, thereby clarifying the occurrence and progression of CHD.

## 5. Conclusion

In summary, both carotid artery ultrasound parameters and LDL-C levels are closely associated with the degree of coronary artery stenosis in patients with CHD. Combining these two factors can significantly improve the accuracy of predicting the risk of CHD occurrence. Therefore, when dealing with patients suspected of having CHD, joint detection of these two indicators can enhance diagnostic accuracy and facilitate the timely formulation and implementation of targeted intervention plans.

## Disclosure statement

The authors declare no conflict of interest.



## References

- [1] Qian C, Wang L, Xiong X, et al., 2025, The Value of Serum Low-Density Lipoprotein Cholesterol and High-Sensitivity C-Reactive Protein Combined with Carotid Artery Ultrasound Parameters in Diagnosing Suspected Coronary Heart Disease Patients. *Journal of Practical Medicine*, 41(9): 1401–1406.
- [2] Fu Y, Zhang Y, Nie Y, et al., 2023, Application Value of Serum hs-CRP, Hcy Combined with Carotid Ultrasound Parameters in Assessing the Severity of Coronary Artery Stenosis in Patients with Coronary Heart Disease. *Guangxi Medical Journal*, 45(19): 2301–2304.
- [3] Wang L, Wang C, Li Y, 2024, The Application Value of Small, Dense Low-Density Lipoprotein Cholesterol in the Diagnosis of Coronary Heart Disease and Stroke. *Chinese Community Doctors*, 40(32): 107–109.
- [4] Liu T, Huang S, 2024, Detection Results of Serum Hcy and Carotid Artery Ultrasound Parameters in Patients with Coronary Heart Disease and their Predictive Value for the Degree of Coronary Artery Stenosis. *Knowledge of Prevention and Treatment of Cardiovascular Diseases*, 14(21): 26–30.
- [5] Interventional Cardiology Group, Cardiovascular Disease Branch of the Chinese Medical Association; Atherosclerosis and Coronary Heart Disease Group, Cardiovascular Disease Branch of the Chinese Medical Association, et al., 2018, Guidelines for the Diagnosis and Treatment of Stable Coronary Heart Disease. *Chinese Journal of Cardiology*, 46(9): 680–694.
- [6] Zhang M, 2024, The Application Value of Combined Detection of Small Dense Low-Density Lipoprotein Cholesterol and High-Sensitivity C-Reactive Protein in the Diagnosis of Coronary Atherosclerotic Heart Disease. *Systems Medicine*, 9(22): 78–81.
- [7] Xie C, Yan L, Xu X, 2023, Research on the Application Value of Combined Detection of Small Dense Low-Density Lipoprotein Cholesterol and Low-Density Lipoprotein Cholesterol in the Diagnosis and Treatment of Cardiovascular Diseases. *Medical Information*, 36(6): 97–100.
- [8] Zhu L, 2023, Research on the Value of Combined Cardiac Color Doppler Ultrasound and Carotid Artery Ultrasound Examination in the Diagnosis of Coronary Heart Disease. *Journal of Practical Medical Imaging*, 24(6): 466–470.
- [9] Liu C, Sun W, Ma D, et al., 2023, Clinical Significance of Combined Carotid Artery and Middle Cerebral Artery Ultrasound Examination in Predicting Coronary Artery Lesions. *Journal of Electrocardiology & Circulation*, 42(6): 536–540.
- [10] Fan P, 2023, Analysis of the Correlation between Serum Small Dense Low-Density Lipoprotein and Coronary Heart Disease. *Forum on Primary Medical Care*, 27(19): 94–96.
- [10] Zhou R, Pang H, Zong L, 2022, Analysis of the Diagnostic Effect of Carotid Artery Ultrasound Examination of Atherosclerotic Plaque Parameters on Coronary Heart Disease in Elderly Hypertensive Patients. *Modern Health Preservation*, 22(20): 1744–1746.
- [11] Huang J, 2021, Diagnostic Value of Carotid Atherosclerotic Plaque Ultrasound in Patients with Coronary Heart Disease. *Chinese and Foreign Medical Treatment*, 40(17): 1–3.
- [12] Ding Y, 2022, Application Effect of Combined Serum Bilirubin and Low-Density Lipoprotein Cholesterol Test in the Early Diagnosis of Coronary Heart Disease. *Journal of Clinical Rational Drug Use*, 13(27): 19–20.

### Publisher's note

Bio-Byword Scientific Publishing remains neutral with regard to jurisdictional claims in published maps and institutional affiliations.





## Integrated Services Platform of International Scientific Cooperation

Innoscience Research (Malaysia), which is global market oriented, was founded in 2016. Innoscience Research focuses on services based on scientific research. By cooperating with universities and scientific institutes all over the world, it performs medical researches to benefit human beings and promotes the interdisciplinary and international exchanges among researchers.

Innoscience Research covers biology, chemistry, physics and many other disciplines. It mainly focuses on the improvement of human health. It aims to promote the cooperation, exploration and exchange among researchers from different countries. By establishing platforms, Innoscience integrates the demands from different fields to realize the combination of clinical research and basic research and to accelerate and deepen the international scientific cooperation.

### Cooperation Mode



Clinical Workers



In-service Doctors



Foreign Researchers



Hospital



University



Scientific institutions

# OUR JOURNALS



The *Journal of Architectural Research and Development* is an international peer-reviewed and open access journal which is devoted to establish a bridge between theory and practice in the fields of architectural and design research, urban planning and built environment research.

Topics covered but not limited to:

- Architectural design
- Architectural technology, including new technologies and energy saving technologies
- Architectural practice
- Urban planning
- Impacts of architecture on environment

*Journal of Clinical and Nursing Research (JCNR)* is an international, peer reviewed and open access journal that seeks to promote the development and exchange of knowledge which is directly relevant to all clinical and nursing research and practice. Articles which explore the meaning, prevention, treatment, outcome and impact of a high standard clinical and nursing practice and discipline are encouraged to be submitted as original article, review, case report, short communication and letters.

Topics covered by not limited to:

- Development of clinical and nursing research, evaluation, evidence-based practice and scientific enquiry
- Patients and family experiences of health care
- Clinical and nursing research to enhance patient safety and reduce harm to patients
- Ethics
- Clinical and Nursing history
- Medicine



*Journal of Electronic Research and Application* is an international, peer-reviewed and open access journal which publishes original articles, reviews, short communications, case studies and letters in the field of electronic research and application.

Topics covered but not limited to:

- Automation
- Circuit Analysis and Application
- Electric and Electronic Measurement Systems
- Electrical Engineering
- Electronic Materials
- Electronics and Communications Engineering
- Power Systems and Power Electronics
- Signal Processing
- Telecommunications Engineering
- Wireless and Mobile Communication

